PROXIMAL FEMORAL REPLACEMENT FOR THE TREATMENT OF ONCOLOGIC DISORDERS IN THE HIP

C Gusho BS[1], B Clayton MD[1], N Mehta MD[1], P Escobedo BS[1], M Colman MD[1], S Gitelis MD[1], A Blank, MD, MS[1]

[1]RUSH UNIVERSITY MEDICAL CENTER

Disclosures: Please see AAOS/MSTS list of disclosures.

INTRODUCTION

Proximal femoral bone tumors are often treated with proximal femoral replacement (PFR).

Uncertainty remains regarding the rates of survivorship and complications in PFR.[1-4]

This study evaluated a single institutional experience with PFR and analyzed complications and implant survival over a 15-year period.

METHODS

Thirty-eight procedures (37 patients) were identified and retrospectively reviewed from years 2005-2019.

	Frequency	Percent
Chondrosarcoma	8	21.1
Ewing sarcoma	1	2.6
Lymphoma	1	2.6
Metastatic bone disease	20	52.6
Myxofibrosarcoma	1	2.6
Osteosarcoma	4	10.5
Pathological fracture	2	5.3
Soft tissue sarcoma	1	2.6
Total	38	100.0

Table 1. Preoperative diagnoses.

	Frequency*	Percent
Guardian®/ELEOS™	14	35.8
Stryker GMRS	10	25.6
LINK®	9	23.1
Zimmer Segmental	3	7.7
Stanmore Custom	1	2.6
Hemiarthroplasty	33	86.8
Single Bearing	2	5.3
Dual mobility	1	2.6
Constrained Liner	2	5.3

Table 11. Surgery characteristics. *missing data omitted.

RESULTS

- The rate of revision was 5.1% (2 cases).
- Both were cemented Stryker implants - infected dislocation, periprosthetic fracture.
- Median implant survival was 115 months.
- 10-year survival probability was 93.3%.

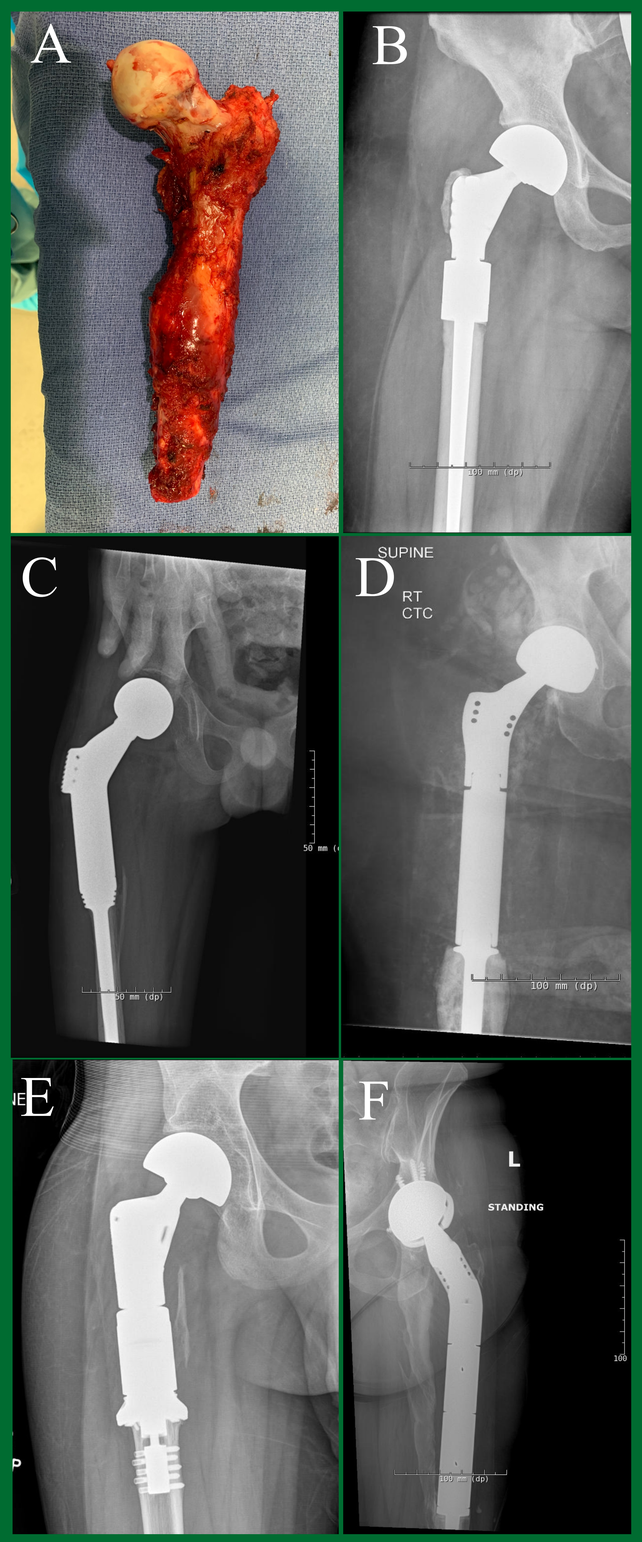

Figure 1. Following proximal femoral removal (A), an endoprosthesis was implanted: LINK® (B), custom Stanmore (C), Styrker GMRS (D), Zimmer compress (E), Guardian®/ELEOS™ (F).

RESULTS (continued)

OVERALL IMPLANT SURVIVAL

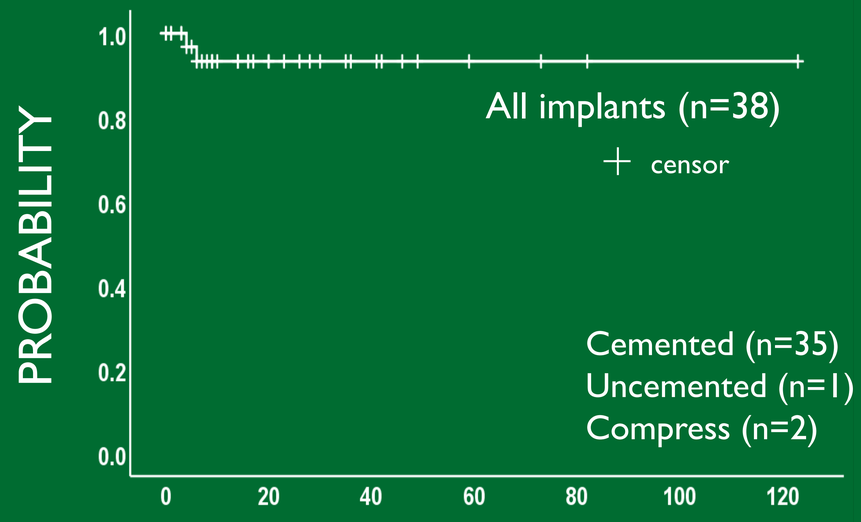

Figure 2. Proximal femoral implant survivorship (n=38).

CONCLUSIONS

For oncologic disorders of the proximal femur, modular endoprosthetic replacement is safe and reliable.

We believe our low revision rates are due to combination of improved surgical technique over time as well as postoperative use of a brace.

REFERENCES

1. Ahlmann ER, Menendez LR, Kermani C, Gotha H. Survivorship and clinical outcome of modular endoprosthetic reconstruction for neoplastic disease of the lower limb. *J Bone Joint Surg Br*. 2006;88(6):790-795. doi:10.1302/0301-620X.88B6.17519
2. Bernthal NM, Greenberg M, Heberer K, Eckardt JJ, Fowler EG. What are the functional outcomes of endoprosthestic reconstructions after tumor resection? *Clin Orthop Relat Res*. 2015;473(3):812-819. doi:10.1007/s11999-014-3655-1
3. Cannon CP, Mirza AN, Lin PP, Lewis VO, Yasko AW. Proximal Femoral Endoprosthesis for the Treatment of Metastatic. *ORTHOPEDICS*. 2008;31(4):361-361. doi:10.3928/01477447-20080401-03
4. Chandrasekar CR, Grimer RJ, Carter SR, Tillman RM, Abudu AT. Modular endoprosthetic replacement for metastatic tumours of the proximal femur. *J Orthop Surg Res*. 2008;3:50. doi:10.1186/1749-799X-3-50

Single Institution Analysis of Ablations versus Partial Nephrectomies for Small Renal Masses

Fionna Sun BA[1], Zachary Dreyer BA[1], Pranav Moudgil MD[2], Diane Studzinski BS[3], Stephen A. Vartanian MD[3], Frank Burks MD[4]

[1]Oakland University William Beaumont School of Medicine, [2]Beaumont Health, Department of Interventional Radiology,
[3]Beaumont Health, Department of General Surgery, [4]Beaumont Health, Department of Urology

OAKLAND UNIVERSITY WILLIAM BEAUMONT — School of MEDICINE

Beaumont

Introduction

Renal Cell Carcinoma (RCC) accounts for roughly 3% of adult malignancies and 95% of primary kidney neoplasms [1,2]. With the more widespread use of various imaging modalities there has been an increase in early diagnosis of the disease, specifically in the case of small renal masses (<4cm)(SRMs). In 2019, there is an estimate of 74,000 new cases of RCC in the US. Treatment options for SRM patients range from active surveillance to nephron-sparing ablative therapy or partial nephrectomies to non-sparing radical nephrectomies with varying standard guidelines recommendations depending on patient comorbidities and disease staging [3,4]. Evaluation of SRM treatment, specifically T1a RCC, is becoming increasingly important, including not only the modality itself but follow-up guidelines as well.

Objective

The purpose of this study is to evaluate the experience of a large, suburban hospital in treatment of RCC from initial workup through follow-up. Evaluation of different treatment modalities, partial nephrectomy vs ablation types, will help to characterize the best management course for SRM.

Methods

- Performed a retrospective chart review of 295 patients at Beaumont Royal Oak hospital in Royal Oak, MI. Cost data available for 189 patients.
- Included partial nephrectomy or ablation index procedures from 2010-2019 with renal masses <4cm on preoperative imaging.
- Data collected included demographics, comorbidities, imaging workup, intraoperative and postoperative complications, 30 day readmission, and hospital billed costs and charges.
- Statistical analysis utilized the Mann-Whitney test, Kruskal-Wallis Test, Fisher's Exact test, and student's unpaired t-test.

Results

Ablations

- Minimally invasive approach. Success is dependent on size of tumor and probe accessibility.
- 133 patients with Abl (6 lap-cryo, 73 cryo-, 44 microwave and 10 radiofrequency ablation) were included with a mean tumor size of 2.34cm.

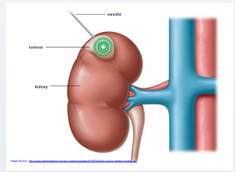

Partial Nephrectomies

- Also considered nephron-sparing. 56 partial nephrectomies were included with a mean tumor size of 2.48cm.
- Radical or complete nephrectomies (n=23) were excluded for their non-nephron sparing approach.

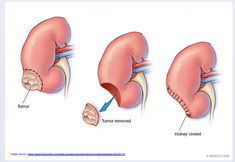

Demographics

	Overall		Ablations (Composite)		Partial Nephrectomy		p-value
	Patients	Percentage	Patients	Percentage	Patients	Percentage	
Age	66.3 years		69.6 years		58.6 years		**<0.001**
Sex	131 male, 58 female		93 male, 40 female		38 male, 18 female		
Hypertension	138	73.0%	100	75.2%	38	67.9%	0.303
Diabetes Type II	46	24.3%	32	24.1%	14	25.0%	0.896
Obesity	38	20.1%	23	17.3%	15	26.8%	0.138
Peripheral Vascular Disease	28	14.8%	22	16.5%	6	10.7%	0.005
Chronic Kidney Disease	40	21.2%	28	21.1%	12	21.4%	0.963
Acute Kidney Injury History	15	7.9%	11	8.3%	4	7.1%	0.781
Dyslipidemia	88	46.6%	61	45.9%	27	48.2%	0.773
Cardiovascular Disease	78	41.3%	58	43.6%	20	35.7%	0.315
Congestive Heart Failure	8	4.2%	5	3.8%	3	5.4%	0.620
Coronary Artery Disease	39	20.6%	27	20.3%	12	21.4%	0.865
Cancer (Overall)	52	27.5%	35	26.3%	17	30.4%	0.565
Genitourinary Cancer	21	11.1%	13	9.8%	8	14.3%	0.370
Smoking History	111	58.7%	81	60.9%	30	53.6%	0.373
Alcohol History	89	47.1%	63	47.4%	26	46.4%	0.900
Family History Kidney Disease	2	1.1%	0	0.0%	2	3.6%	**0.028**
Family History Kidney Cancer	2	1.1%	2	1.5%	0	0.0%	0.358

Table 1. Demographics and comorbidities of partial nephrectomy patients v. combined ablation patients. Overall, demographics and comorbidities including relevant past medical history and social history were similar between patients undergoing a partial nephrectomy vs ablation. Patients undergoing partial nephrectomies were lower in age and had a lower incidence of family history for kidney disease in comparison to those undergoing an ablation.

Follow-up

Recurrence

- Overall, 16 patients of the 189 observed a recurrence (8.5%).
- 4 partial nephrectomy patients had a recurrence (7.1%). All 4 of these patients underwent an ablative procedure following the diagnosis.
- 12 patients who had undergone an ablation required an additional procedure (9.0%). Cryoablations were most frequently recorded as the index procedure but were responsible for 15 of the necessary 17 re-interventions.
- There was no significant difference in the rate of recurrence between nephrectomy and ablation procedures.
- The average follow-up time was 4.95 years for PN and 2.78 years for Abl.

Complications

		Pyelonephritis	Renal Insufficiency	Urine Leakage	Hematuria	Epididymitis	UTI	Hemorrhage	Hematoma
Overall	Number	1	2	1	1	0	2	3	4
	Percentage	0.70%	1.40%	0.70%	0.70%	0.00%	1.40%	2.10%	2.80%
Partial Nephrectomy	Number	0	0	1	0	0	0	0	1
	Percentage	0.00%	0.00%	2.50%	0.00%	0.00%	0.00%	0.00%	2.50%
Ablation	Number	1	2	0	1	0	2	3	3
	Percentage	0.97%	1.94%	0.00%	0.97%	0.00%	1.94%	2.91%	2.91%
P-value		1.000	1.000	0.280	1.000	0.000	1.000	0.560	1.000

Table 2: Renal-specific complication rates of Partial Nephrectomies vs Ablations. Various renal function measures and pathologies are shown. There were no significant differences between any of the recorded complications with low occurrence rates.

- There were 43 overall intraoperative and immediate post-op complications recorded. 36 from ablations and 7 from nephrectomies.
- There were no observed significant differences between individual complications but a composite complication rate including all of those listed below showed a lower rate for nephrectomies (p=0.044).
- The rates of CKD was not different between nephrectomy at 9.0% (5 patients) and ablation at 13.5% (18 patients) (p=0.389). Rates of an AKI history in patients were also similar (p=0.780).
- Post-operative renal-related pathology shown in Table 2 demonstrates low occurrences of renal insufficiency and infection with the highest rates reported with hemorrhage and hematoma formation.

30 Day ED Visits

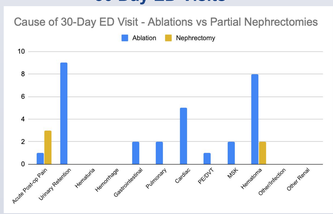

Figure 1: Causes of 30 Day ED Visits - Ablations vs Partial Nephrectomies. Of the 189 total patients included in follow-up, 20 presented to the ED within 1 month of their procedure. 8 of these followed a partial nephrectomy (14%) and 12 following an ablation procedure (9%)(p=0.31). 3 patients presented more than once within the first 30 days and 6 of the 8 that presented were readmitted for management of urine leakage, hematuria or a hematoma. Patients undergoing an ablation were more likely to present for urinary retention or non-renal related causes.

Charges and Costs

Table 3: Relative Total Charge and Cost to Payer Comparison. 129 of 189 patients had available charge and cost data. PN had significantly higher hospital charges and cost to payer rates in comparison to a composite of all ablations.

	All Ablations n= 81	Partial Nephrectomies n=48	P-Value
Total Charge	1x	1.57x	p=0.0016
Total Cost to Payer	1x	2.79x	p<0.0001
Mann whitney test			

	PCRYO (n=62)	PMV (n=6)	PRF (n=7)	LCRYO (n=6)
Total Charge	1x	0.67x	1.47x	1.67x
Total Cost to Payer	1x	2.67x	0.79x	3.52x

PCRYO- Percutaneous Cryoablation
PMV- Percutaneous Microwave Ablation
PRF- Percutaneous Radiofrequency Ablation
LCRYO- Laparoscopic Cryoablation

Table 4: Relative Total Charge and Cost to Payer Comparison Between Percutaneous Cryoablation and Other Ablation techniques. Amongst ablation techniques, PMV demonstrated the lowest total hospital charge. LCRYO had the highest hospital charges and total cost to payer, over three times as costly to payers than PCRYO. Of note, the number of patients with available data for PMV, PRF, and LCRYO was much lower than for PCRYO.

Conclusion

Our study found that patients undergoing either partial nephrectomies or ablations for their SRM RCC had comparable demographics and comorbidities. The exception was for a higher age in ablation procedures, as expected given the selection bias for higher risk patients not being candidates for major surgery. Despite differing initial treatments used for SRM RCC, these comparable populations had similar outcomes with no overall differences in 30-day ED visits or recurrence rates observed within the 5 year follow-up time for PN or nearly 3 years for Abl. Rates of renal-specific postoperative complications demonstrated no preference for specific complications between the two modalities but overall rates showed slightly higher rates for ablation procedures. PN demonstrated 50% higher total hospital charge in comparison to all Abl procedures and a cost to payer rate over 2.5 times the Abl rate. Further breakdown of the individual Abl techniques offers further consideration for the most cost-effective treatment modalities.

As the timing and rates of detection of RCC continues to improve, more consideration will be given to the inclusion of patient populations, follow-up protocols and long-term outcomes when choosing a treatment modality. Specifically, ablative techniques that can accommodate higher risk patients at a lower charge/cost and similar complication rates need to be weighed against the long-term outcomes seen with partial nephrectomy interventions in the treatment of SRM.

Future Steps

Future steps include the expansion of this study to capture a larger patient population and to complete more robust statistics on differentiating ablation subtypes in comparison to partial nephrectomies. Analysis will consist of examining study parameters to determine complication, comorbidity, and recurrence rates between different nephron-sparing and non-nephron sparing approaches for those diagnosed with SRMs.

References

1. Murai, M., & Oya, M. (2004). Renal cell carcinoma: etiology, incidence and epidemiology. Current opinion in urology, 14(4), 229-233.
2. Lam, J. S., Leppert, J. T., Belldegrun, A. S., & Figlin, R. A. (2005). Novel approaches in the therapy of metastatic renal cell carcinoma. World journal of urology, 23(3), 202-212.
3.Staff, A. U. A. Guideline for Management of the Clinical Stage 1 Renal Mass.
4. Klinghoffer, Z., Tarride, J. E., Novara, G., Ficarra, V., Kapoor, A., Shayegan, B., & Braga, L. H. (2013). Cost-utility analysis of radical nephrectomy versus partial nephrectomy in the management of small renal masses: Adjusting for the burden of ensuing chronic kidney disease. Canadian Urological Association Journal, 7(3-4), 108.
5. Chehab, M., Friedlander, J. A., Handel, J., Vartanian, S., Krishnan, A., Wong, C. Y. O., ... & Ciacci, J. (2016). Percutaneous cryoablation vs partial nephrectomy: cost comparison of T1a tumors. Journal of endourology, 30(2), 170-176.

Safety of Sequential Bland Embolization-PRRT in Patients with Metastatic Neuroendocrine Tumors

[1]Dhiraj Sikaria MD, [1]Jose Jesurajan MD, [2]Jonathan Strosberg, MD, [3]Ghassan El-Haddad MD

[1]University of South Florida Morsani College of Medicine,
[2]Gastrointestinal Oncology, Moffitt Cancer Center, Tampa, FL, USA
[3]Interventional Radiology, Moffitt Cancer Center, Tampa, FL, USA

Background

- Peptide receptor radionuclide therapy (PRRT) with Lutathera (^{177}Lu-DOTATATE) was approved for somatostatin expressing metastatic neuroendocrine tumors (mNETs) by the US Food and Drug Administration in January 2018
- Approved based on data from NETTER-1 trial and ERASMUS
- Hepatic artery bland embolization (TAE) is one of the embolotherapies used for NET liver metastases with high rates of radiographic and symptomatic response
- The purpose of this study was to evaluate the hepatotoxicity of TAE followed by Lutathera PRRT in patients with mNETs

Methods

- Single institution retrospective cohort study of mNET patients with liver metastases who completed 4 cycles of PRRT for progressive disease between 08/2017 and 10/2019
- Patients who had undergone prior TAE were compared to patients who were embolization naïve
- Clinical and laboratory data findings, including liver function tests and follow up appointments were graded using the Common Terminology Criteria for Adverse Events (CTCAE) v5.0 grading system

Results

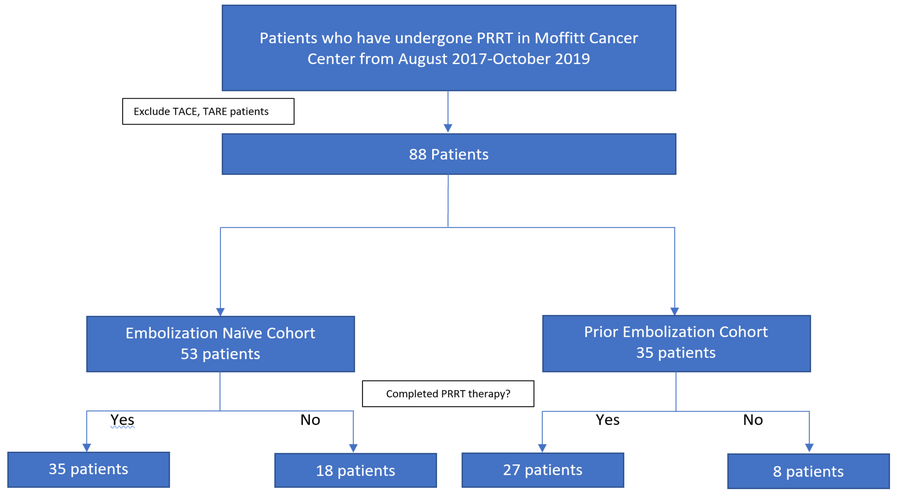

Table 1: CTCAE v5.0 toxicity information for patients with prior history of TAE vs those who were embolization naïve. P-value only significant ($p < 0.05$) for a statistically significant increase in rate of G1 Alkaline Phosphatase in patents with prior TAE.

Events	Prior TAE, %	Embolization naïve, %	Pearson-Chisquare	Likelihood ratio	Fisher exact 2 sided	Fisher exact 1 sided
G1AST	7.4	0	0.102	0.065	0.186	0.186
G2AST	0	0	x	x	x	x
G3AST	0	0	x	x	x	x
G1ALT	3.7	0	0.251	0.194	0.435	0.435
G2ALT	0	0	x	x	x	x
G3ALT	3.7	0	0.251	0.194	0.435	0.435
G1ALP	18.5	2.9	0.039	0.035	0.077	0.051
G2ALP	0	2.9	0.376	0.282	1	0.565
G3ALP	0	0	x	x	x	x
G1ALB	0	5.7	0.207	0.126	0.5	0.315
G2ALB	0	0	x	x	x	x
G3ALB	0	0	x	x	x	x
G1BILI	3.7	0	0.251	0.194	0.435	0.435
G2BILI	0	0	x	x	x	x
G3BILI	0	0	x	x	x	x
G1THROMB	33.3	40	0.59	0.589	0.609	0.393
G2THROMB	0	2.9	0.376	0.282	1	0.565
G3THROMB	0	0	x	x	x	x
G1CREAT	14.8	2.9	0.086	0.082	0.158	0.107
G2CREAT	0	2.9	0.376	0.282	1	0.565
G3CREAT	0	0	x	x	x	x
G1HYPERNA	0	0	x	x	x	x
G2HYPERNA	0	0	x	x	x	x
G3HYPERNA	0	0	x	x	x	x
G1HYPONA	3.7	0	0.251	0.194	0.435	0.435
G2HYPONA	0	0	x	x	x	x
G3HYPONA	0	0	x	x	x	x

Results

- 26 total patients did not complete 4 cycles of PRRT
  - -18 in the naïve cohort and 8 in the prior embolization cohort
- Majority discontinued therapy due to non-liver related side effects
- Only a statistically significant higher incidence of Grade 1 alkaline phosphatase increase in the prior TAE cohort ($p = .039$)
- Otherwise no increase in hepatotoxicity in completed therapy patients who received prior TAE
- Among patients who did not complete PRRT, there was only a statistically significant higher incidence of G1 creatinine elevation in the prior TAE group ($p = .037$)

Conclusion

- Performing bland TAE prior to treatment with 177Lu-DOTATATE PRRT does not appear to increase the risk of clinically significant hepatotoxicity in mNET patients
- This study adds to previous evidence supporting the safety of PRRT in the setting of previous embolization techniques
- Future studies needed to study long term effect of TAE-PRRT on liver toxicity

Transarterial Chemoembolization Combined With Durvalumab ± Bevacizumab in Patients With Locoregional HCC (EMERALD-1)

Riccardo Lencioni,[1] Masatoshi Kudo,[2] Shukui Qin,[3] Zhenggang Ren,[4] Stephen Chan,[5] Joseph Erinjeri,[6] Yasuaki Arai,[7] Philip He,[8] Shethah Morgan,[9] Gordon Cohen,[8] Bruno Sangro[10]

[1]University of Pisa School of Medicine, Pisa, Italy; [2]Kindai University, Osaka, Japan; [3]Cancer Center of Nanjing, Jinling Hospital, Nanjing, China; [4]Zhongshan Hospital, Fudan University, Shanghai, China; [5]Department of Clinical Oncology, The Chinese University of Hong Kong, Hong Kong; [6]Memorial Sloan Kettering Cancer Center, New York, NY, USA; [7]National Cancer Center, Tokyo, Japan; [8]AstraZeneca, Gaithersburg, MD, USA; [9]AstraZeneca, Cambridge, United Kingdom; [10]Liver Unit, Clínica Universidad de Navarra and CIBEREHD, Pamplona, Spain

Summary

- The EMERALD-1 study will expand our understanding of the potential clinical benefits of adding durvalumab or durvalumab with bevacizumab to TACE for patients with locoregional HCC who are not candidates for curative therapy.

Introduction

- Curative therapy is not always an option for patients with intermediate-stage HCC and a **standard approach for treatment is locoregional therapy such as TACE**.
- TACE therapy achieves tumor responses, **but progression and recurrence are common and often occur within 1 year**.[1]
- **Immune checkpoint inhibitors have shown promising efficacy with durable response as treatment for advanced HCC when combined with TACE**.[2,3]
- The immune checkpoint inhibitor atezolizumab combined with the VEGF inhibitor bevacizumab have been approved in HCC.[4,5]
- **Combining durvalumab with the VEGF inhibitor bevacizumab and TACE therapies warrants evaluation in patients with locoregional HCC**.

Methods

- **EMERALD-1 (NCT03778957)** is a randomized, double-blind, placebo-controlled, multicenter Phase 3 study assessing efficacy and safety for durvalumab when given concurrently with either DEB-TACE or conventional TACE followed by durvalumab ± bevacizumab in patients with locoregional HCC not amenable to curative therapy.
- 600 patients will be randomized 1:1:1 to Arms A, B, or C (**Figure 1**).
- Durvalumab (or its matched placebo) will begin at least 7 days following the initial TACE procedure.
- Bevacizumab (or its matched placebo) will be added to durvalumab (or its matched placebo) at least 14 days after the last TACE procedure.

Figure 1. EMERALD-1 study design

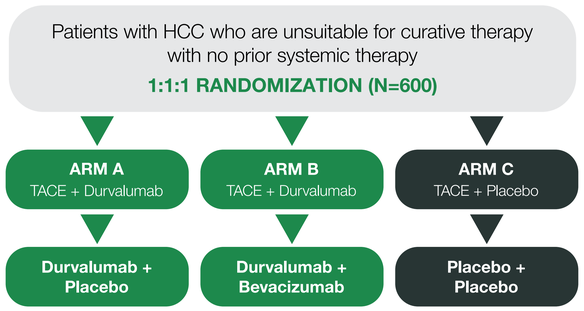

Figure 2. EMERALD-1 participating regions

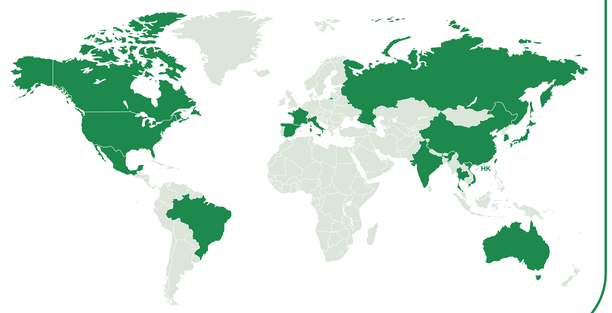

Key Inclusion Criteria

- Aged ≥18 years
- Histologically or radiologically confirmed HCC not amenable to curative therapy
- No prior systemic therapy for HCC
- Child-Pugh Score A to B7
- ECOG PS of 0 or 1 at enrollment

- Patients with HBV or HCV may be enrolled, but patients who are HBV+ must have adequately controlled viral suppression prior to enrollment and HBV/HCV replication will be monitored during the study and treated if appropriate.
- Patients are required to have an upper endoscopy performed to evaluate varices and risk of bleeding within 6 months of randomization.

Key Exclusion Criteria

- A history of nephrotic or nephritic syndrome
- Clinically significant cardiovascular disease
- Extrahepatic disease
- Evidence of main portal vein thrombosis (Vp3/Vp4)
- Prior or current evidence of bleeding diathesis, within 28 days following surgery, or GI perforation or active GI bleeding within 6 months of enrollment

- A tumor tissue sample is mandatory and may either be taken during the first TACE procedure or taken ≤3 months prior to randomization.
- There are currently 17 countries and regions participating in the EMERALD-1 study (**Figure 2**).

Study Endpoints

1
- Assess PFS for Arm B vs Arm C (by BICR using RECIST v 1:1)

2
- Evaluate PFS for all arms using modified RECIST (by BICR)
- Evaluate overall survival for all arms
- Investigate the relationship between baseline PD-L1 expression and efficacy outcomes
- Measure time to progression for all arms
- Evaluate objective response, duration of response, and disease control rate
- Assess disease-related symptoms, impacts, and HRQoL for all arms
- Evaluate safety and tolerability profile of all arms

Key exploratory objectives
- Investigate the association of candidate biomarkers with efficacy measures using blood and tissue samples
- Explore the impact of treatment and disease state on health care utility and resources

References

1. Lencioni R, et al. *Hepatology.* 2016;64(1):106-116.
2. Kelley RK, et al. *J Clin Oncol.* 2017;35(abstr 4073).
3. Duffy AG, et al. *J Hepatol*. 2017;66(3):545-551.
4. Finn RS, et al. *N Engl J Med*. 2020;382:1894-1905.
5. https://www.fda.gov/drugs/drug-approvals-and-databases/fda-approves-atezolizumab-plus-bevacizumab-unresectable-hepatocellular-carcinoma.

Abbreviations

BICR, blinded independent central review; DEB, drug-eluting bead; ECOG PS, Eastern Cooperative Oncology Group performance status; GI, gastrointestinal; HBV, hepatitis B virus; HCC, hepatocellular carcinoma; HCV, hepatitis C virus; HRQoL, health-related quality of life; PD-L1, programmed death ligand-1; PFS, progression-free survival; RECIST, Response Evaluation Criteria In Solid Tumors; TACE, transarterial chemoembolization; VEGF, vascular endothelial growth factor.

Acknowledgments

This study was funded by AstraZeneca. The authors would like to thank the patients, their families and caregivers, and all investigators involved in this study. Medical writing support, which was in accordance with Good Publication Practice (GPP3) guidelines, was provided by Anne-Marie Manwaring of Parexel (Littlehampton, UK) and was funded by AstraZeneca.

Contact Information

gordon.cohen@astrazeneca.com

Presented at the Symposium on Clinical Interventional Oncology I Virtual Meeting I October 2020

Conventional Transarterial Chemoembolisation and Drug-Eluting Bead Transarterial Chemoembolisation in HCC: a Comparison of Periprocedural Outcomes and Mortality in a Single Centre

Dr. Supun W. Abeyratne MBBS/BSc[1]
Dr. Denver Khoo MBBS/BSc (Hons)[2]
Dr. Shanalie Dias MBBS/BSc (Hons)[3]
Dr. Nigel Mott MBBS, FRANZCR[4]

Introduction

- Prior studies demonstrate drug-eluting bead transarterial chemoembolization (DEB-TACE) to have favourable short-term disease response and lower periprocedural complication rates compared to conventional transarterial chemoembolization (cTACE)
- Mortality and overall survival appear to be similar between the two modalities in the treatment of HCC
- No previous data exists comparing DEB-TACE to cTACE in an Australian population

Methods

- 92 patients undergoing TACE for treatment of HCC between October 2015 to October 2019 were included in this single centre retrospective study conducted at the Royal Brisbane and Women's Hospital
- Comparison of demographic and clinical variables between the DEB-TACE and cTACE groups was conducted using the Mann-Whitney U test for continuous variables, and Fisher's exact test or the Pearson Chi-square test for categorical variables
- The association between treatment modality and outcomes including 6-month mortality, 6-month radiological recurrence, and periprocedural complications (post-embolisation syndrome, cholecystitis, bleeding, nausea, and abdominal pain) was examined using logistic regression
- Confounding variables that were adjusted for included sex, age, number of lesions, lesion size (maximum diameter), number of treatments, and Child Pugh score.

Results

- 68 patients underwent DEB-TACE, and 24 underwent cTACE
- Statistically significant ($p<0.05$) differences were noted for sex and lesion number, other demographic and clinical background parameters demonstrated no significant difference between modalities
- No statistically significant difference was demonstrated between DEB-TACE and cTACE for 6-month mortality, 6-month radiological recurrence, or LOS
- No significant differences were demonstrated for periprocedural complications

Discussion

- Our study did not demonstrate any significant difference between cTACE and DEB-TACE for 6-month mortality, periprocedural complications, radiological recurrence, or LOS

	cTACE (, %)	DEB-TACE	p-value
LOS (days, mean)	1.13	1.57	0.25
6-month mortality (n, %)	1 (4.2)	6 (8.8)	0.81
Radiological recurrence at 6 months (n, %)	11 (45.8)	40 (59.7)	0.68

	cTACE	DEB-TACE	p-value
Post-embolisation syndrome (n, %)	0 (0)	5 (7.5)	1.00
Cholecystitis (n, %)	0 (0)	2 (2.9)	1.00
Bleeding (n, %)	0 (0)	3 (4.4)	1.00
Nausea (n, %)	2 (8.3)	3 (4.4)	0.939
Abdominal pain (n, %)	2 (8.3)	15 (22.4)	0.259

- Limitations of the study included limited external generalisability as single centre, degree of crossover as some patients had undergone TACE treatment corresponding to other group, and scope – only included immediate complications as inpatient

AN UPDATE ON LYMPH NODE METASTASES IN HIGH RISK EXTREMITY SOFT TISSUE SARCOMA AND PROGNOSTIC FACTORS INFLUENCING SURVIVAL

C Gusho BS[1], M Fice MD[1], C O'Donoghue MD, MPH[1], S Gitelis MD[1], A Blank, MD, MS[1]

[1]RUSH UNIVERSITY MEDICAL CENTER

Disclosures: the authors report no receipt of financial support for this study.

INTRODUCTION

Soft tissue sarcomas (STS) are a rare heterogeneous tumor group.

While metastases to lungs is more common, nodal metastases are rare.

Recent studies have classified rates of nodal metastases by subtype, though few have characterized nodal metastasis by anatomical location.[1-5]

This study queried a national database to describe the survival and prognostic factors of historically high-risk STS.

METHODS

Using the Surveillance, Epidemiology and End Results (SEER) database, 547 cases of extremity STS with nodal metastasis were identified from 2004 to 2015.

Rates were stratified by high or low-risk subtype and disease-free survival in high-risk STS was assessed.

Overall: 3.7%	PRN	Rate
Rhabdomyosarcoma*	105 of 393	26.7
Clear Cell*	24 of 128	18.8
Epithelioid*	32 of 221	14.5
Angiosarcoma*	19 of 235	8.1
Synovial*	31 of 959	3.2
Sarcoma, unspecified	59 of 894	17.6
UPS	35 of 1506	10.4
Spindle Cell	26 of 519	7.7
Leiomyosarcoma	22 of 1548	6.5
Ewing Sarcoma	12 of 118	3.6

Table 1. Nodal metastases by subtype. PRN, positive regional nodes. UPS, undifferentiated pleomorphic sarcoma. *high-risk.

RESULTS

- Nodal metastasis for all extremity STS was 3.7%
- Nodal metastasis in high-risk subtypes was 10.9%.
- Nodal metastasis in low-risk STS was 2.9% (p<0.001)
- Median survival of isolated nodal metastasis is 70.3 months.

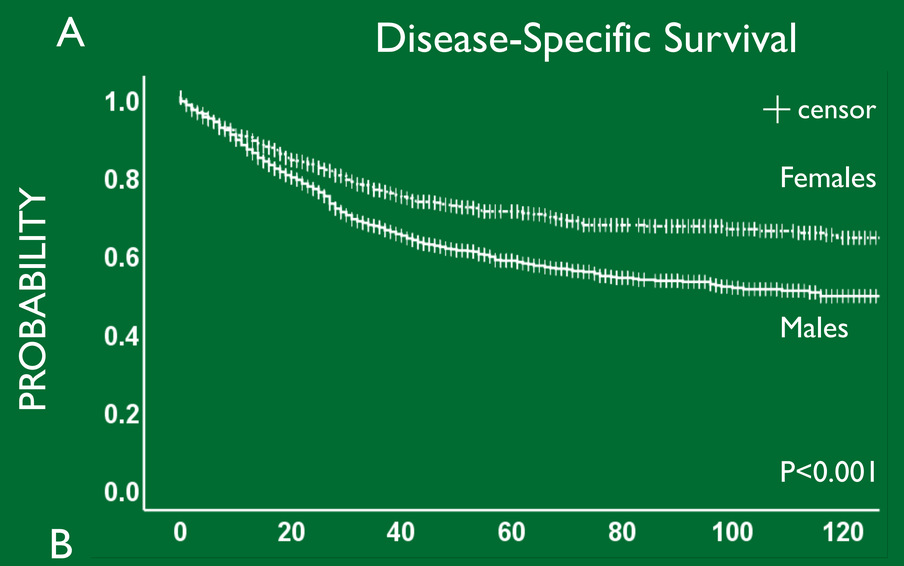

Figure 1. Survival for all high-risk extremity subtypes by sex and site, (A-B) and by nodal evaluation in isolated regional nodes only (no distant nodes) (C).

RESULTS (continued)

After controlling for confounding variables in disease-free survival of high-risk extremity STS, only age, Grade III or IV tumors, distant metastases, and positive regional nodes were significant negative predictors.

For isolated nodal metastasis, only age was a significant negative predictor.

Figure 2. Cross-sectioned lymph node (A) with fibrotic remnants on histology (B) after nodal metastasis from peripheral nerve sheath tumor.

CONCLUSIONS

Additionally, certain low-risk subtypes such as leiomyosarcoma and UPS have higher rates of nodal metastases contrary to previous understanding.

Patients with isolated nodal metastasis only had a poorer prognosis, but positive survival trend with nodal evaluation.

As previously studied, synovial sarcoma, historically considered high-risk, has a relatively low risk of nodal metastasis.

REFERENCES

1. Behranwala KA, A'Hern R, Omar A-M, Thomas JM. Prognosis of lymph node metastasis in soft tissue sarcoma. *Ann Surg Oncol*. 2004;11(7):714-719. doi:10.1245/ASO.2004.04.027
2. Daigeler A, Kuhnen C, Moritz R, et al. Lymph node metastases in soft tissue sarcomas: a single center analysis of 1,597 patients. *Langenbecks Arch Surg*. 2009;394(2):321-329. doi:10.1007/s00423-008-0371-x
3. Fong Y, Coit DG, Woodruff JM, Brennan MF. Lymph node metastasis from soft tissue sarcoma in adults. Analysis of data from a prospective database of 1772 sarcoma patients. *Ann Surg*. 1993;217(1):72-77. doi:10.1097/00000658-199301000-00012
4. Gaakeer HA, Albus-Lutter CE, Gortzak E, Zoetmulder FA. Regional lymph node metastases in patients with soft tissue sarcomas of the extremities, what are the therapeutic consequences? *Eur J Surg Oncol*. 1988;14(2):151-156.
5. Jacobs AJ, Morris CD, Levin AS. Synovial Sarcoma Is Not Associated With a Higher Risk of Lymph Node Metastasis Compared With Other Soft Tissue Sarcomas. *Clin Orthop Relat Res*. 2018;476(3):589-598. doi:10.1007/s11999.0000000000000057

Lymphatic Embolization for Post-Surgical Cancer Patients

Lynsey Maciolek, M.D.[1], Brandon Golant, B.S.[2], Steven Yevich, M.D., M.P.H.[1],
Department of Interventional Radiology, [2] Department of Diagnostic Radiology, Section of Neuroradiology,
The University of Texas MD Anderson Cancer Center, Houston, TX

THE UNIVERSITY OF TEXAS MD Anderson Cancer Center
Making Cancer History®

Introduction

Despite the best technique, surgery in cancer patients can result in significant damage to the lymphatic system that is manifested by development of a lymphocele or lymphatic leakage into the surgical bed or through the incision site. These complications typically occur after resection/dissection of lymph nodes or during resection of tumors located near a lymphatic chain or the cysterna chyli and thoracic duct. In the setting of thoracic surgery, the lymphatic leakage can accumulate in the pleura and result in a tension chylothorax. Lymphocyles and chylothorax not only cause symptoms from mass effect and potentially infection, but also can lead to severe electrolyte imbalances and malnutrition that can be life threatening.

Interventional radiology treatments provide a minimally invasive means to definitively treat these complications. Improvements in imaging and techniques to access the lymphatic system have advanced lymphatic embolization success rates and decreased the need for surgical re-intervention.

We provide examples of percutaneous treatment for post-surgical lymphatic complications in cancer patients.

Material and Methods

Three cases of therapeutic IR intervention for lymphatic leakage are presented. All patients are cancer patients, who developed post-surgical lymphoceles or lymphatic leakage that was not corrected by at least 4 weeks of diet modification. The multi-disciplinary decision to intervene by IR was made for symptomatic relief and to stop the significant loss of electrolytes and fluid.

Case 1: 62 year old woman with ovarian cancer status post resection of painful bilateral inguinal metastases. High volume chylous leakage developed through the bilateral incision sites with >1 liter leakage per day.

Case 2: 73 year old man with renal cell carcinoma status post left nephrectomy and retroperitoneal lymph node dissection. High volume chylous ascites developed, for which a peritoneal drain was placed for therapeutic relief. Peritoneal drainage was greater than 1 liter per day.

Case 3: 76 year old man with malignant neoplasm of the lower third of esophagus who underwent Ivor-Lewis esophagectomy. High volume tension chylothorax developed, for which a chest tube was placed for immediate therapeutic relief. Chest tube drainage was greater than 1 liter per day.

Results

In all three cases, diagnostic lymphangiograms were performed using the same technique in a hybrid CT-Fluoroscopy unit (Siemens). Bilateral inguinal lymph nodes were accessed by ultrasound guided direct puncture using a 25 gauge needle. Through this access, a total of 10-25 mL lipiodol was injected under slow manual pressure (approximately 10 mL per hour).

Intermittent fluoroscopy was performed to track the passage of lipiodol up the lymphatic chain, and identify the source(s) of leakage into the surgical bed, peritoneum, or pleural respectively by both fluoroscopy and CT. Once the leakage was identified, the leaking lymphatic channel was accessed using a 21 or 22 gauge needle under fluoroscopic and/or CT guidance. Goal was to secure needle access approximately 1 cm before from the leak point.

Once access was confirmed on imaging and by lymphatic fluid visualized at the hub, then embolization was performed by injection of approximately 0.5 mL of a 1:1 solution of histoacryl glue:lipiodol. Lipiodol was added to this solution to visualize the final location of glue on fluoroscopy or CT. For larger channels, 2-4 microcoils were placed across the lymphatic channel to form a metallic scaffold, which was subsequently definitively occluded by injection of approximately 0.5 mL of a 1:1 solution of histoacryl glue:lipiodol. After waiting 10 seconds for glue to set, the needle(s) were removed. In all cases, embolization was successful.

Conclusion

Percutaneous lymphangriograms and lymphatic embolizations provide a minimally invasive and effective treatment option for persistent high volume lymphatic leakage from surgical complications. While the methods are tedious and require a fine attention to detail and precision, these treatments can prove valuable particularly as alternative treatment can require a more invasive surgical lymphatic ligation. The use of combination CT-Fluoroscopy hybrid units allow the IR physician access to both types of imaging to improve successful outcome.

References

1.Inoue M, Nakatsuka S, Yashiro H, et al. Lymphatic Intervention for Various Types of Lymphorrhea: Access and Treatment. *Radiographics.* 2016;36(7):2199-2211.
2. Majdalany BS, El-Haddad G. Contemporary lymphatic interventions for post-operative lymphatic leaks. *Transl Androl Urol.* 2020;9(Suppl 1):S104-S113.
3. Weniger M, D'Haese JG, Angele MK, Kleespies A, Werner J, Hartwig W. Treatment options for chylous ascites after major abdominal surgery: a systematic review. *Am J Surg.* 2016;211(1):206-213.
4. Itkin M, Nadolski GJ. Modern Techniques of Lymphangiography and Interventions: Current Status and Future Development. *Cardiovasc Intervent Radiol.* 2018;41(3):366-376.
5. Lee EW, Shin JH, Ko HK, Park J, Kim SH, Sung KB. Lymphangiography to treat postoperative lymphatic leakage: a technical review. *Korean J Radiol.* 2014;15(6):724-732.

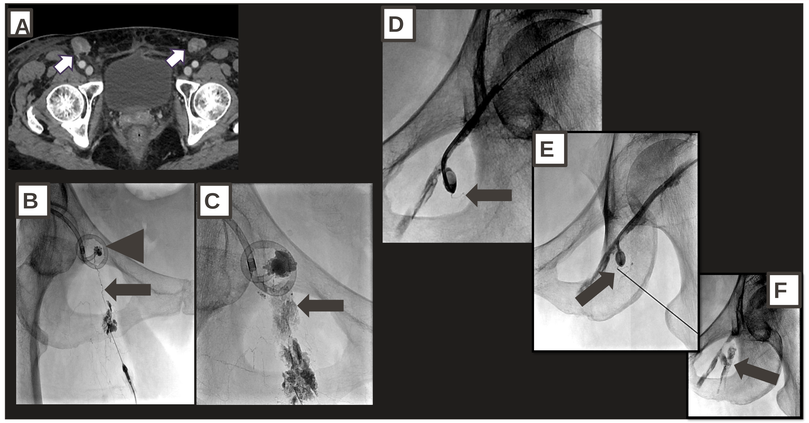

Case 1: Focal bilateral inguinal lymphatic leak embolization after resection of large painful inguinal lymphadenopathy (A, arrows). Injection of lipiodol through a benign right inguinal lymph node (A), with lymphangiogram delineating a channel passing directly and leaking into the surgical bed (A, arrow and arrowhead respectively). The leaking duct was cannulated with a 21g needle and embolized with histoacryl glue (C, arrow). The existing left drain access was cannulaed with a 5 Fr catheter, and forced injection of contrast demonstrated a lymphatic source (D, arrow), which was cannulated (E, arrow), and embolized with glue injection (F, arrow).

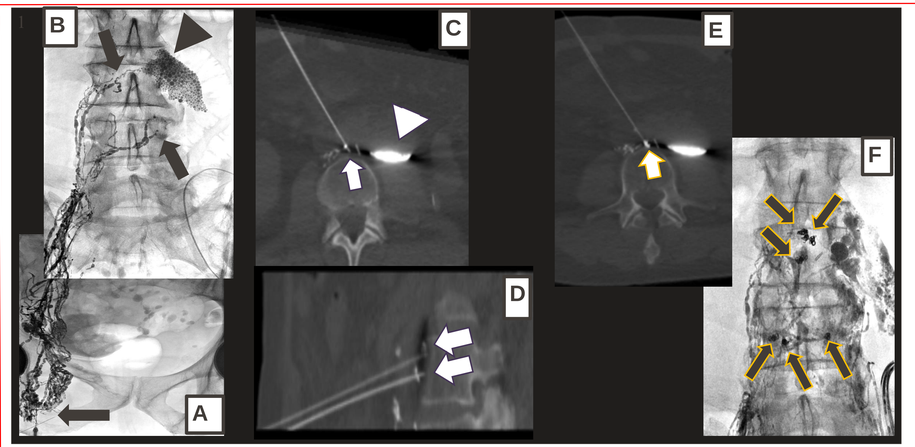

Case 2: Focal retroperitoneal lymphatic leak embolization. Injection of lipiodol through right inguinal lymph nodes (A, arrows), with lymphangiogram delineating a total of 6 focal leaking retroperitoneal lymphatic ducts at site of lymph node dissection with lipiodol pooling within the nephrectomy surgical bed (B, arrow and arrowhead respectively). The leaking ducts were cannulated one by one percutaneously with 21g needles (C and D, arrow demonstrating cannulation, arrowhead demonstrating pooling of lipiodol in surgical bed). Coils were passed through the needles into sources of leakage, followed by histoacryl glue to embolize (E and F, arrows show coils).

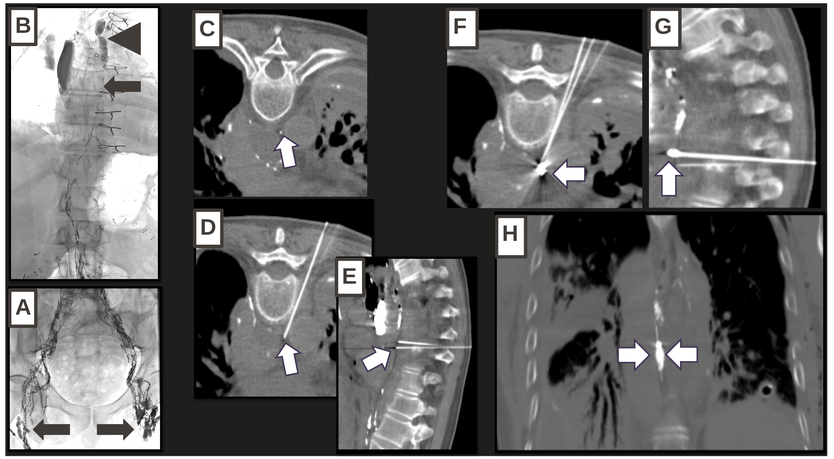

Case 3: Focal thoracic duct leak embolization. Injection of lipiodol through bilateral inguinal lymph nodes (A, arrows), with lymphangiogram delineating lower thoracic duct and focal leak at the mid thorax (B, arrow and arrowhead respectively). The duct was visualized on CT (C, arrow), and cannulated percutaneously with two 21g needles (D and E, arrows). Coils were passed through the needles into duct, followed by histoacryl glue to embolize (F, G, H arrows).

Radiation Segmentectomy as Primary Therapy for Solitary Hepatocellular Carcinoma

Authors: S. Ali Montazeri, MD, MPH; Zlatko Devcic, MD; Xi Li, MD, PhD; Ricardo Paz-Fumagalli, MD; Andrew R. Lewis, MD; Gregory T. Frey, MD, MPH; Charles A. Ritchie, MD; J. Mark McKinney, MD; Beau B. Toskich, MD
Division of Interventional Radiology, Department of Radiology, Mayo Clinic, Jacksonville, Florida

PURPOSE

To evaluate the outcomes of radiation segmentectomy (RS) as primary therapy for solitary hepatocellular carcinoma (HCC).

INTRODUCTION

High dose radioembolization to sublobar volumes of liver with RS is increasingly being utilized. There is increasing evidence to support the notion of ablative intent radioembolization, but the literature remains sparse for solitary HCC.

METHODS

A retrospective, single-center analysis of patients with imaging or biopsy-proven solitary HCC who received RS as primary therapy between January 2017 and December 2019 was performed. The institutional review board approved this study and waived the need for written consent due to the retrospective design.

All treatments utilized Y-90 glass microspheres (TheraSphere, Boston Scientific, Marlborough, MA) and MIRD dosimetry. Response was characterized at 3 and 6 months per mRECIST guidelines (1).

Adverse events were reported per CTCAE v5.0 (2). Patient demographics, tumor characteristics, RS technical parameters, time-to-progression (TTP), and overall survival (OS) censored for transplant were analyzed.

Inclusion criteria were: solitary HCC located in one or two liver segments, RS as the primary treatment without any additional treatment to the tumor, no vascular invasion, dose > 100 Gy.

Kaplan Meier method was used to depict survival and progression curves of primary HCC. Data are shown as median (IQR 25-75) or frequency (percentages) when appropriate.

RESULTS

BASELINE CHARACTERISTICS

Sixty-three patients (median age 68 years; range, 36-87 years) were treated with RS. 81% of patients were BCLC stage 0 or A. Median tumor diameter was 2.5 cm (range 1.1-7.8 cm). The most common causes of liver disease in this study were hepatitis C virus (HCV) and non-alcoholic fatty liver disease (NAFLD), accounting for 68% of all patients. Fifty-two percent of the tumors were located in segments 8, 7, or 4a.

DOSIMETRY

The median treatment dose, activity, and volume was 380 Gy (range 107-884), 1.31 GBq (range 0.23-5.71), and 160 ml (range 30-1000). 35% of patients received administrations to vascular watersheds. 61 patients (97%) received a single treatment. Y-90 administration was in a single segment in 41 (65%) patients. Lung shunt fraction was 1.4 % (IQR, 0.8%-2.9%).

SAFETY, RESPONSE, AND SURVIVAL

The median follow-up was 9.8 months (range 3.1-40.2). There were no grade 3 or higher adverse events at 3 or 6 months after RS.

Complete response was achieved in 78% and 88% of targeted tumors at 3 and 6 months, respectively (Table 1). A single patient developed an in-field (targeted lesion) progression. Out-of-field (non-targeted liver) progression occurred in 11 patients (17%).

26 patients were bridged to liver transplant. Four patients died during the study and median OS was not reached (Figures 2, 3).

TABLE 1: IMAGING RESPONSE

mRECIST	3rd month (n=62*)	6th month (n=51^)
Complete response	49 (78%)	45 (88%)
Partial response	12 (19%)	5 (10%)
Stable disease	1 (2%)	1 (2%)
In-field progression	0	0

FIGURE 1. IMAGING RESPONSE AFTER RADIATION SEGMENTECTOMY

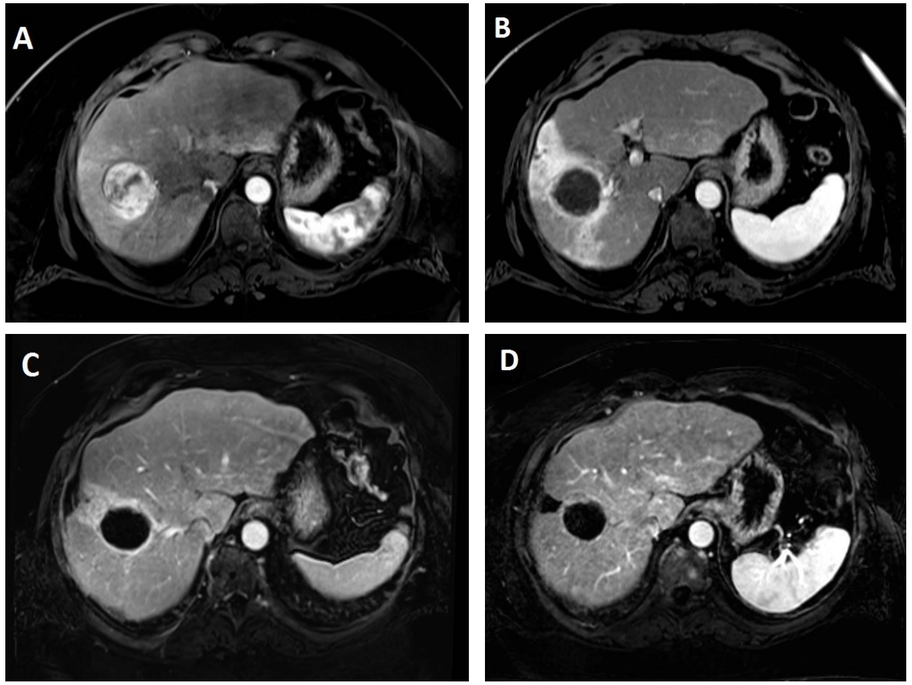

(A) Post contrast T1 weighted MRI of the liver demonstrating a 5.6 cm segment 8 HCC abutting the central portal triad.
Post contrast T1 weighted MRI of the liver at (B) 3 months, (C) 6 months, and (D) 38 months after radiation segmentectomy demonstrating eventual mRECIST complete response and ablation of the treated angiosome. Administered activity was 5.7 GBq, Dose 679 Gy MIRD, estimated 8 million particles 5 days after calibration.

CONCLUSION

Radiation segmentectomy is safe and effective for the primary treatment of solitary HCC.

FIGURE 2. OVERALL SURVIVAL

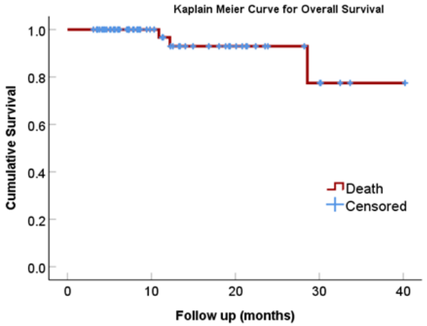

FIGURE 3. IN-FIELD PROGRESSION

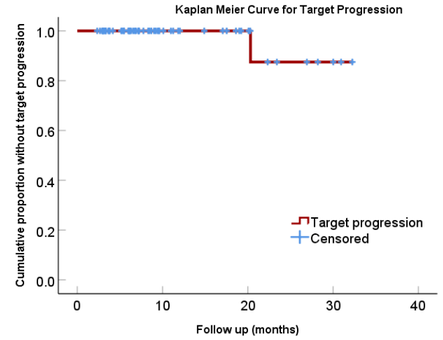

REFERENCES

1. Lencioni R, Llovet JM. Modified RECIST (mRECIST) assessment for hepatocellular carcinoma. InSeminars in liver disease 2010 Feb (Vol. 30, No. 01, pp. 052-060). © Thieme Medical Publishers.
2. US Department of Health and Human Services. Common terminology criteria for adverse events (CTCAE) Version 5.0. 2017.

*A single patient in the study did not have 3 month imaging available
^26 patients received liver trasnplant
Abbreviations:
mRECIST, modified response evaluation criteria in solid tumors
CTCAE, common terminology criteria for adverse events

Radiologic-Pathologic Analysis of Novel Ethanol Gel Formulation for Percutaneous Ablation in an Animal Model

Erika Chelales[1], Robert Morhard[1], Alan Alper Sag[2], Nimmi Ramanujam[1]

1. Department of Biomedical Engineering, Duke University, Durham, USA 2. Department of Radiology, Division of Vascular and Interventional Radiology, Duke University Medical Center, Durham, USA

Corresponding author: Erika Chelales
Email: erika.chelales@duke.edu

Duke BIOMEDICAL ENGINEERING

Global Women's Health Technologies

Abstract

Motivation

- Ethanol ablation, the direct injection of ethanol into a lesion, induces rapid necrosis by denaturing proteins and dehydrating cytoplasm[1].
- It is suitable for use in low- and middle-income countries because it is inexpensive, portable, and electricity-independent. However, its use is limited due to irregular and unpredictable ethanol distributions resulting in incomplete tumor coverage[2], and off-target damage[3].

Objective

- To improve ablation localization and efficacy using the ethanol-soluble, water-insoluble polymer, ethyl cellulose (EC). EC increases ethanol viscosity and induces a liquid-to-gel phase-change upon injection, sequestering cytotoxic ethanol at the target region.

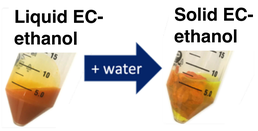

Fluorescent dye added for visualization

Approach

Develop a robust, non-invasive technique to quantify ethanol spatial distribution and concentration in tissue → Determine optimal formulation of EC-ethanol to maximize ethanol distribution volume → Compare efficacy optimal EC-ethanol concentration to pure ethanol ablation *in vivo* and assess relationship of pathology and imaging

Methods

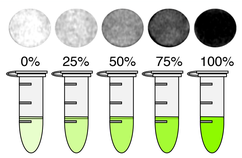

Measurement of ethanol radiodensity

- Ethanol-water solutions at 0%, 25%, 50%, 75%, and 100% ethanol (n= 20)
- Computed tomography (CT) imaging
- Radiodensity converted to estimated ethanol concentration

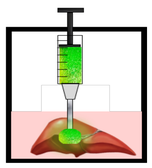

Optimization of ethyl cellulose concentration in rat liver *ex vivo*

- 100 μL of 0%, 6%, 8%, 10%, 12%, or 15% EC-ethanol (n=6)
- 10 mL/hour
- Tissue submerged in buffer to prevent air absorption
- Pre- and post-ablation CT imaging

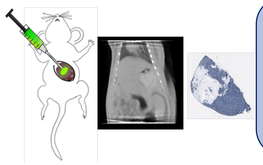

Radiologic-pathologic comparison to pure ethanol in rat liver *in vivo*

- 100 μL 12% EC-ethanol or pure ethanol (n=6)
- 10 mL/hour
- Pre- and post-ablation CT imaging
- Tissue stained for viability with NADH-diaphorase (24 hours post-ablation)

Image Analysis

Radiodensity was converted to estimated ethanol concentration with a two-point calibration equation (**Equation 1**). The total error in the concentration estimate was computed using the root-sum-square method from the random (variance) and the systematic (difference between predicted and true value) errors (**Equation 2**).

Ethanol distribution volume and aspect ratio were quantified. The aspect ratio (**Equation 3**) is defined as the ratio of the average distance of each point in the distribution to the centroid (radius of gyration) to the radius of a spherical distribution of equivalent volume (effective radius).

$$Ethanol\ concentration = \frac{Radiodensity_{sample} - Radiodensity_{0\%\ ethanol}}{Radiodensity_{100\%\ ethanol} - Radiodensity_{0\%\ ethanol}} \quad \textbf{(Equation 1)}$$

$$Total\ measurement\ error\ (\%) = \frac{\sqrt{Systematic\ error(HU)^2 + Random\ error\ (HU)^2}}{Radiodensity_{100\%\ ethanol} - Radiodensity_{0\%\ ethanol}} \quad \textbf{(Equation 2)}$$

$$Aspect\ ratio = \frac{Radius\ of\ gyration}{Effective\ radius} = \frac{\sum^{Distance\ from\ centroid}/_{number\ of\ pixels}}{\sqrt[3]{3*Volume/_{4\pi}}} \quad \textbf{(Equation 3)}$$

Quantifying ethanol concentration

The radiodensity difference between ethanol and water provides contrast on CT.

Mean radiodensity decreases with increasing ethanol concentration (-66.5 ± 20.3 HU for pure water vs -340.3 ± 29.1 HU for pure ethanol; n=20, p<0.0001).
Radiodensity was not impacted EC concentration, verifying that CT imaging assesses the impact of EC on the spread of injected ethanol and not the presence of EC itself.

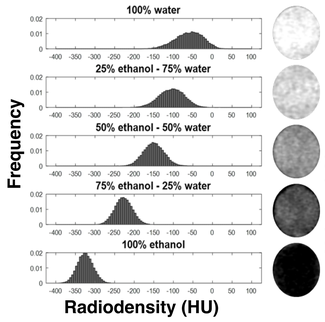

Average systematic error: 7.7% ± 6.8% (n=20)
Average random error: 20.8 ± 6.5 HU (n=20)
Total measurement error : 13.4% ± 3.7%.

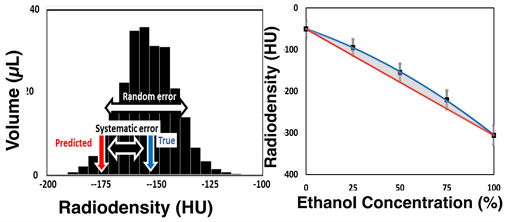

Optimal formulation

Representative transverse and frontal cross-sections of CT images acquired 5 minutes post-ablation of *ex vivo* rat liver

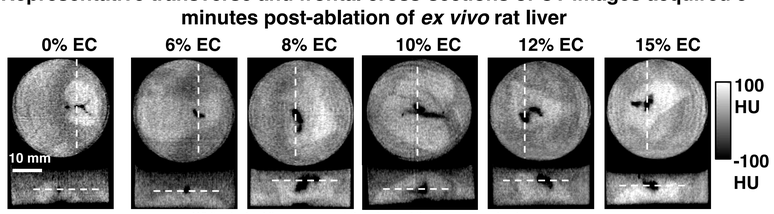

White dashed lines represent the plane of the accompanying image.

Representative transverse and frontal maximum concentration projections

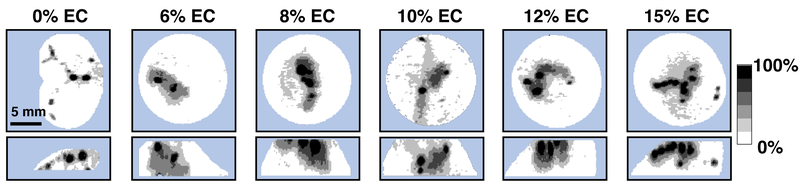

3D segmentations of ethanol distributions at different EC concentrations

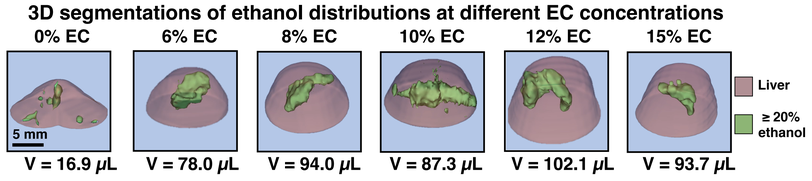

12% EC-ethanol results in the largest distribution of ≥ 20% ethanol in tissue and a more spherical distribution

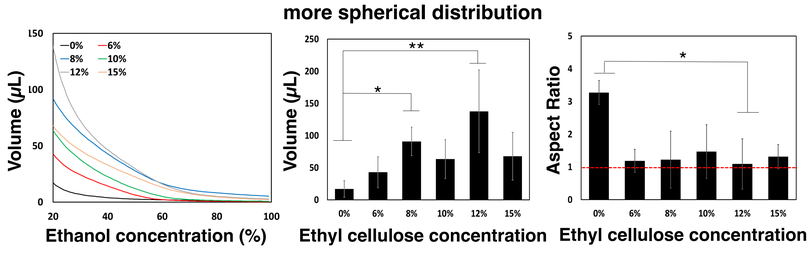

Pure ethanol and 12% EC-ethanol yielded the smallest and greatest distribution volumes, respectively (17.1 ± 12.9 μL vs. 137.7 ± 64.3 μL, p<0.01). 12% EC-ethanol also yielded significantly greater distribution volumes than 6% (42.9 ± 24.8 μL, p<0.01), 10% (63.5 ± 30.2 μL, p<0.05), and 15% EC-ethanol (67.9 ± 37.0 μL, p<0.05). 12% EC-ethanol yielded a significantly lower aspect ratio than pure ethanol (1.09 ± 0.12 vs. 3.27 ± 2.83, p<0.05), indicating a more spherical distribution. Red dotted line indicates aspect ratio of a sphere.

Radiologic-pathologic comparison *in vivo*

Frontal plane computed tomography images of *in vivo* rat liver
(arrow indicates ethanol)

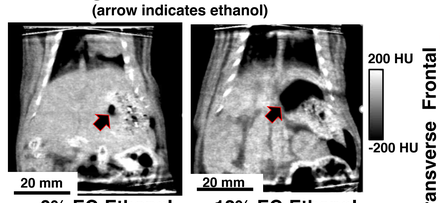

3D segmentations containing at least 20% ethanol by concentration *in vivo*

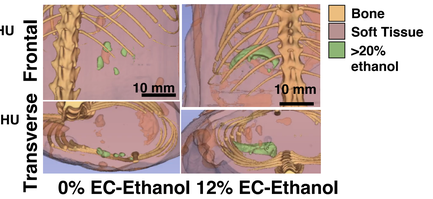

Maximum intensity projections

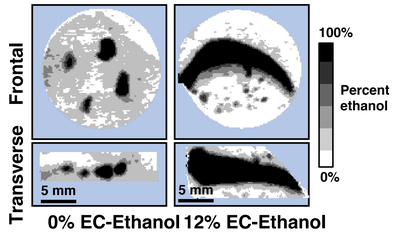

NADH-diaphorase viability staining

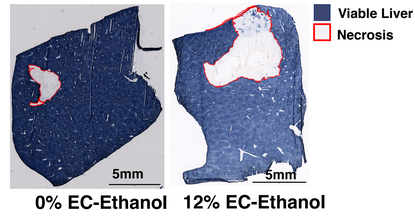

EC-ethanol improves efficacy compared to pure ethanol and CT distribution volume is an effective surrogate for histology

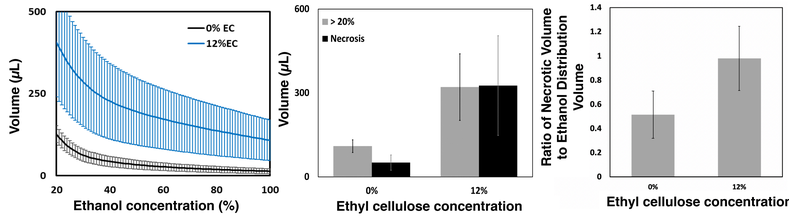

Both the volume of resultant necrosis and the ≥20% ethanol distribution volume are significantly greater for 12% EC-ethanol than for pure ethanol (p<0.05, n=6). The average ratio of the necrotic volume to ethanol distribution volume is closer to 1 for 12% EC than for pure ethanol (NS), indicating that CT imaging provides a more accurate prediction of necrosis for EC-ethanol than pure ethanol.

Conclusions

- We have demonstrated a robust and non-invasive technique to quantify ethanol spatial distribution and concentration in tissue from computed tomography images
- 12% EC-ethanol maximizes distribution volume and yields the most spherical distribution *ex vivo*
- Ethyl cellulose-ethanol ablation achieves superior distribution volume and necrosis compared to pure ethanol ablation *in vivo*
- Ethanol volume (> 20% ethanol concentration) visualized on CT could be an effective surrogate with histology

Future work

We plan to utilize this technique in a hepatocellular carcinoma model to elucidate the value of ethyl cellulose-ethanol as a local cancer therapy and investigate of the role of ethyl cellulose as a slow-release mechanism for intra-tumoral drug delivery.

Acknowledgements: This work is supported by the National Science Foundation Graduate Research Fellowship Program, NIH Grant R21CA241205-01, and the Core Facility Voucher Program through the Duke School of Medicine

For more information:
Contact Erika Chelales at **emc66@duke.edu** or **https://www.globalwomenshealthtechnologies.com**

References:
1. T. Chua, et al. *Gastrointest Endosc Clin N Am.* 2019.
2. M. Hamuro, et al. *Hepatogastroenterology.* 2002.
3. M. Koda, et al. *Gastrointest Radiol.* 1992.

Safety of Caudate Lobe Radiation Segmentectomy

Carlos A. Padula M.D., Zlatko Devcic M.D., Seyed Ali Montazeri M.D., Andrew R. Lewis M.D., J. Mark McKinney M.D., Ricardo Paz-Fumagalli M.D., Gregory T. Frey M.D. M.P.H., Charles A. Ritchie M.D., Beau B. Toskich M.D.

Division of Vascular and Interventional Radiology – Mayo Clinic, Jacksonville, FL

Purpose

Locoregional therapy of hepatic caudate lobe tumors can present a challenge due to variation in vascular supply and proximity to hilar plate. (1) There is discordance in the literature with regards to the safety of radioembolization of the caudate. (2,3) The purpose of the study was to evaluate the safety of caudate lobe radiation segmentectomy.

Methods

- IRB approved, single institutional, retrospective review
- Radiation segmentectomy of caudate lobe with glass microspheres
- Dose >190 Gy MIRD
- Solitary administration to caudate or part of overall liver treatment
- CT or MRI follow-up at 3-month intervals
- Adverse Events: CTCAE V.5
- Response: mRECIST

Response at 3 months (mRECIST)

HCC	12
Complete Response (CR)	7
Partial Response (PR)	3
Stable Disease (SD)	2
ICC	5
Complete Response (CR)	1
Partial Response (PR)	3
Stable Disease (SD)	1

Results

- 19 patients (14 HCC, 5 ICC)
- Median dose of 347.4 Gy (IQR; 269, 483)
- Median follow-up time of 11.8 mo (IQR; 8.7, 20.5)
- Mean TTP of 23.1 mo (CI, 15.9-30.9) (median not met)
- One Grade III encephalopathy 3 weeks post treatment
- No Grade III serologic adverse events or biliary injuries identified per imaging

Conclusion

Radiation segmentectomy of the caudate lobe does not appear to result in biliary injury.

Figure Legend

Fig A: MRI demonstrating 2.2 cm HCC in caudate lobe

Fig B: Cone beam CT of caudate artery arising from left hepatic artery showing complete coverage of tumor

Fig C: Post treatment Bremsstrahlung with intense focal activity in the caudate lobe

Fig D: 3-month follow up MRI demonstrating complete response (yellow arrow)

References

Kim HC, Miyayama S, Chung JW. Selective Chemoembolization of Caudate Lobe Hepatocellular Carcinoma: Anatomy and Procedural Techniques. RadioGraphics. 2019;39(1):289-302. Ibrahim SM, Kulik L, Baker T, et al. Treating and Downstaging Hepatocellular Carcinoma in the Caudate Lobe with Yttrium-90 Radioembolization. Cardiovasc Intervent Radiol. 2012;35(5):1094-1101. 3. Kim HC, Kim YJ, Lee JH, Suh KS, Chung JW. Feasibility of Boosted Radioembolization for Hepatocellular Carcinoma Larger than 5 cm. J Vasc Interv Radiol. 2019;30(1):1-8

Figures

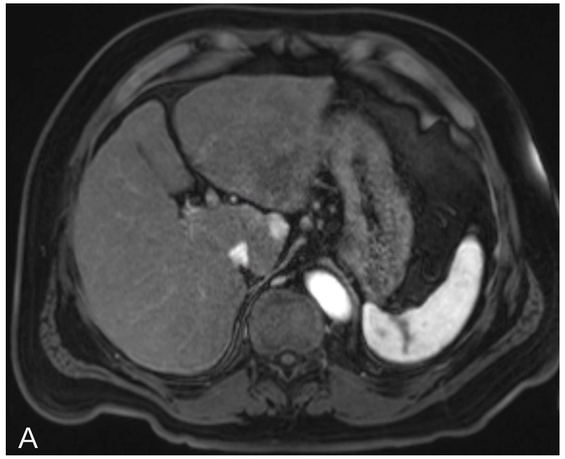

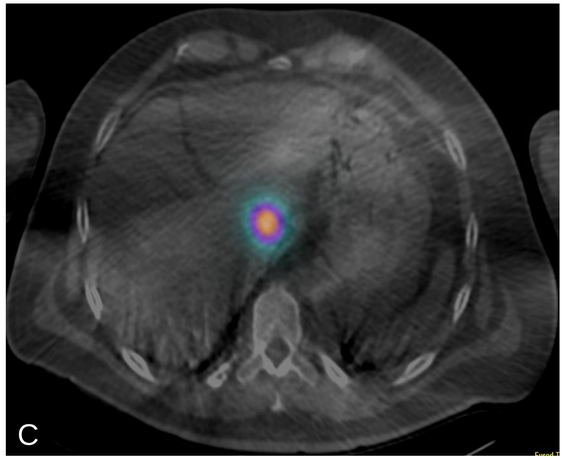

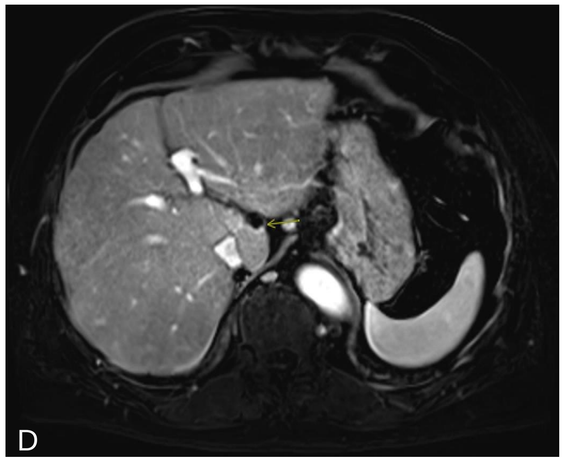

3D-PRINTED CUTTING GUIDES FOR INTERCALARY LONG BONE RESECTION AND ALLOGRAFT RECONSTRUCTION IN EXTREMITY BONE SARCOMA

M Gasparro, BS[1], C Gusho, BS[1], O Obioha, MD[1], M Batus MD[1], M Colman, MD[1], S Gitelis, MD[1], A Blank, MD, MS[1]

[1]RUSH UNIVERSITY MEDICAL CENTER

Disclosures: Please see AAOS/MSTS list of disclosures.

INTRODUCTION

Patient-specific 3D-printed cutting guides for the resection of long bone tumors and allograft reconstruction is a novel technique.

Prior to cutting guides, resection of long bone tumors was more difficult and resulted in less precise cuts with variable patient outcomes.[1,2]

This study aimed to validate the use of these 3D-printed cutting guides in the resection of long bone malignancies.

METHODS

A retrospective review of 6 patients was performed.

Patients were included if a 3D-printed cutting guide and intercalary allograft reconstruction were utilized during their long bone sarcoma surgery.

Margin status, union/nonunion, complications, and disease-related outcomes were recorded.

Case	Age/Sex	Diagnosis	Location
1	32 F	Osteosarcoma	Tibia
2	18 M	Ewing Sarcoma	Tibia
3	60 F	Ewing Sarcoma	Femur
4	21 M	Osteosarcoma	Tibia
5	35 F	Chondrosarcoma	Femur
6	19 M	Ewing Sarcoma	Femur

Table 1. Patient demographics and tumor characteristics.

METHODS (continued)

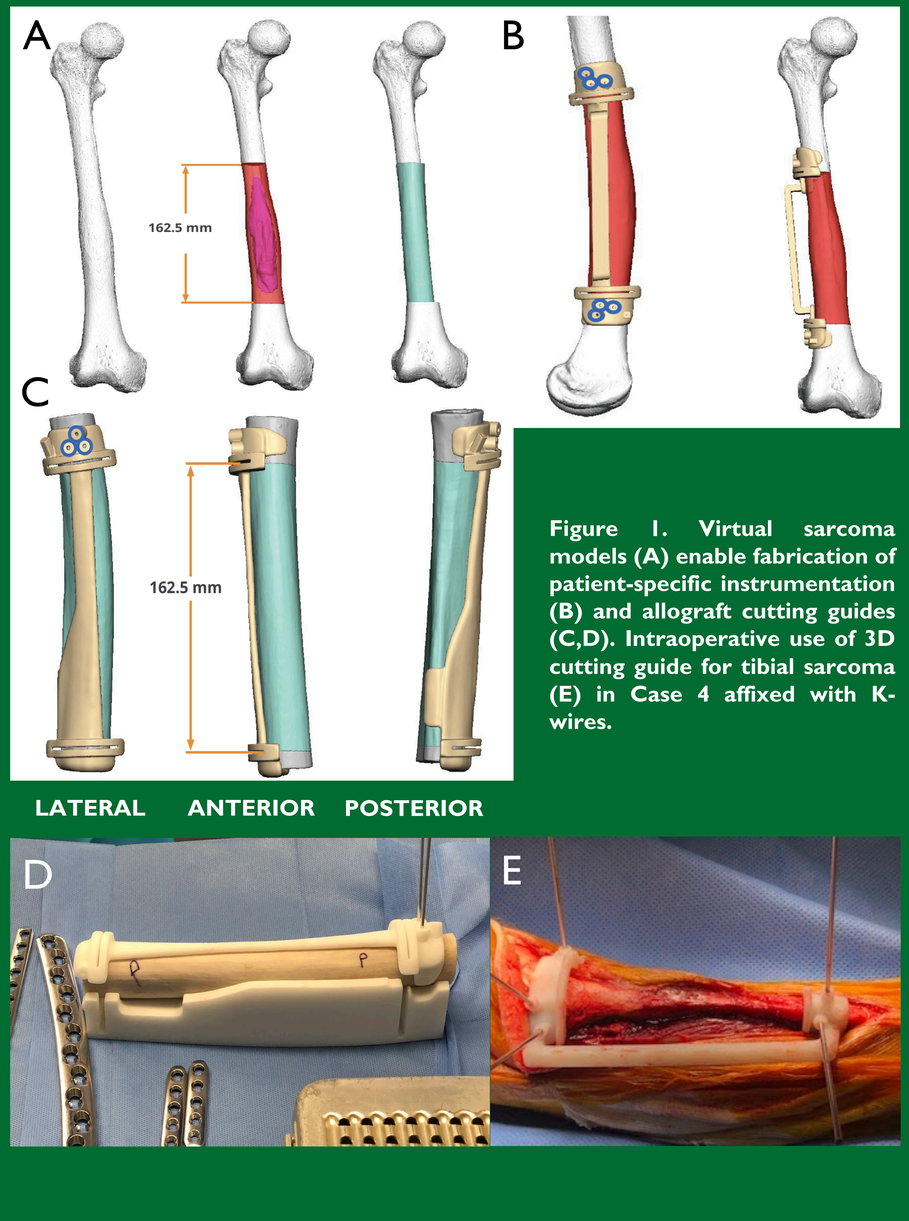

Figure 1. Virtual sarcoma models (A) enable fabrication of patient-specific instrumentation (B) and allograft cutting guides (C,D). Intraoperative use of 3D cutting guide for tibial sarcoma (E) in Case 4 affixed with K-wires.

RESULTS

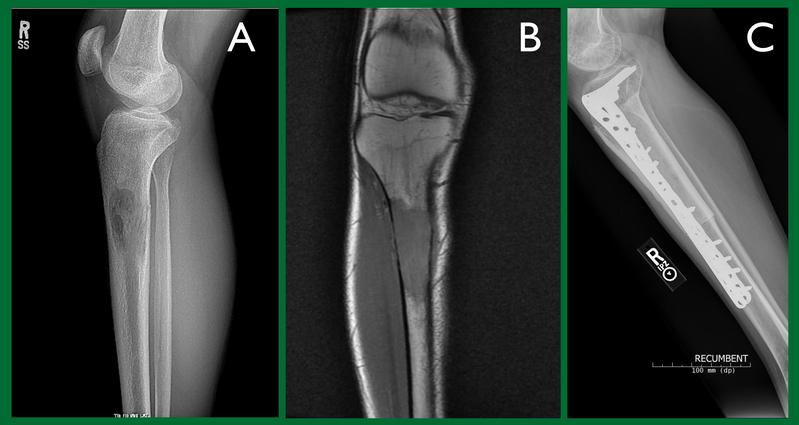

Figure 2. Case 4: Preoperative radiograph (A) and MRI (B) and postoperative lateral radiograph (C) showing bridging plate osteosynthesis going on to union.

- Nine of 12 (75%) cumulative osteotomy sites went on to union.
- 2 non-unions (66.7%) received adjuvant radiation therapy.
- 2 (33.3%) reconstructions failed (Henderson Type 3; implant failure).
- 0 local recurrences at maximum recorded follow-up of 4.05 years.
- 0 perioperative infections recorded.

SUMMARY

Our institution has successfully performed limb salvage surgery with patient-specific 3D-printed technology.

We demonstrate high rates of negative margin resection, low rates of infections, and acceptable rates of junctional union that align with historical and more recent series.[3,4]

REFERENCES

1. Frisoni T, Cevolani L, Giorgini A, Dozza B, Donati DM. Factors affecting outcome of massive intercalary bone allografts in the treatment of tumours of the femur. *J Bone Joint Surg Br*. 2012;94(6):836-841.
2. Liu Q, He H, Duan Z, et al. Intercalary Allograft to Reconstruct Large-Segment Diaphysis Defects After Resection of Lower Extremity Malignant Bone Tumor. *Cancer Manag Res*. 2020;12:4299-4308.
3. Park JW, Kang HG, Lim KM, Park DW, Kim JH, Kim HS. Bone tumor resection guide using three-dimensional printing for limb salvage surgery. *J Surg Oncol*. 2018;118(6):898-905.
4. Ma L, Zhou Y, Zhu Y, et al. 3D-printed guiding templates for improved osteosarcoma resection. *Sci Rep*. 2016;6(1):23335.

UTILIZATION OF THREE-DIMENSIONAL TECHNOLOGY IN THE RESECTION OF SPINOPELVIC SARCOMA OF BONE

M Gasparro, BS[1], C Gusho, BS[1], O Obioha, MD[1], S Gitelis, MD[1], A Blank, MD, MS[1], M Colman, MD[1]

[1]RUSH UNIVERSITY MEDICAL CENTER

Disclosures: Please see AAOS/MSTS list of disclosures.

INTRODUCTION

Wide-margin resection of pelvic tumors is a challenging procedure.

Advancements in 3D-printed patient-specific instrumentation may have benefits over traditional techniques.

Despite its promise, there is no consensus supporting its routine use in resection of spinal and pelvic tumors.

METHODS

A retrospective analysis of 13 cases over a ten-year consecutive period was performed at our tertiary academic center.

	Frequency	Percent
Chondrosarcoma	6	46.2
Metastatic bone disease	3	23.0
STS	2	15.4
Osteosarcoma	2	15.4
Total	13	100.0

Table 1. Preoperative diagnoses. STS, soft tissue sarcoma.

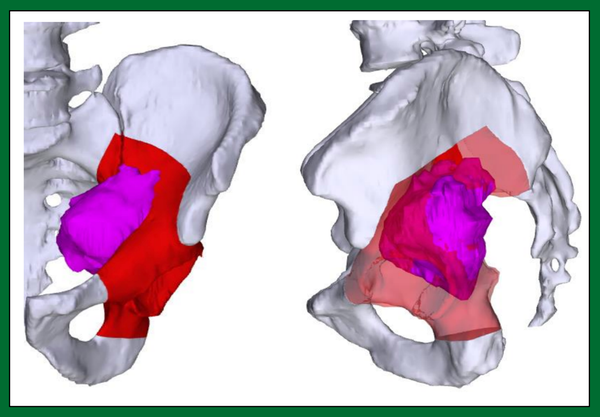

Figure 1. For each case engineers and surgeon meet to discuss tumor location and operative approach, during which a virtual model is constructed.

METHODS (continued)

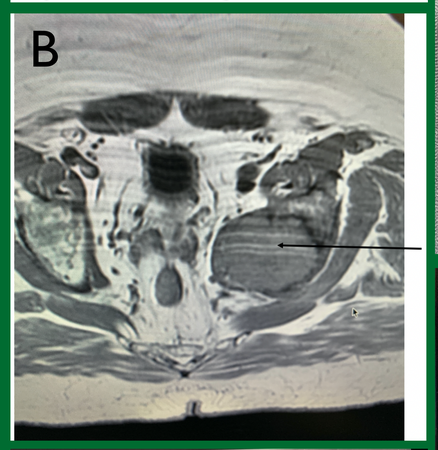

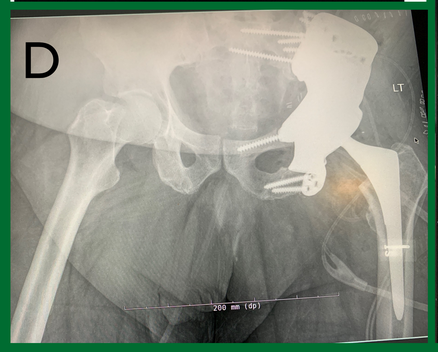

Figure 2. A tumor model (A) with adjacent structures (arrows) is made from patient imaging (B). The mass is then resected (C) and replaced with 3D-printed patient-specific instrumentation (D-E).

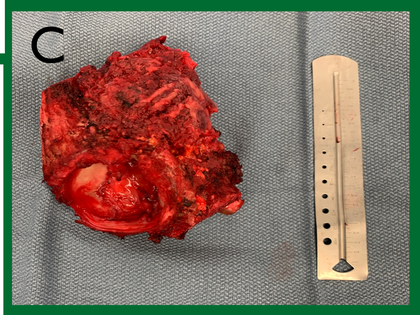

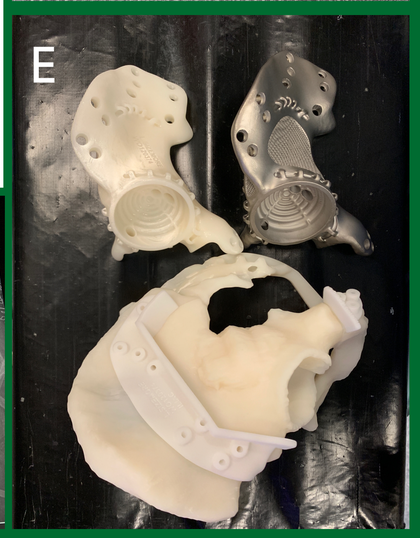

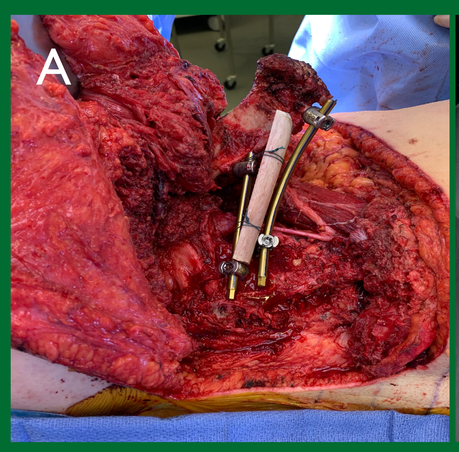

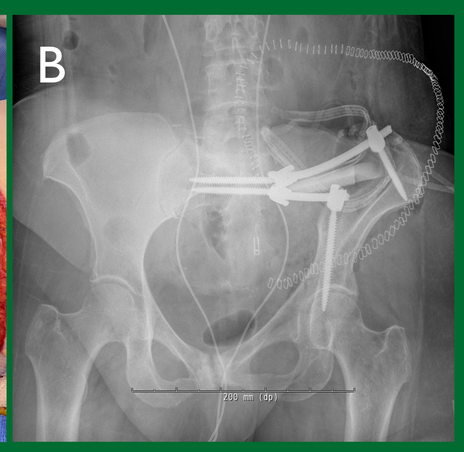

Figure 3. Pelvic reconstruction after resection using 3D-printed cutting guide and fibular strut allograft (A); post-operative anteroposterior radiograph (B).

RESULTS

- 3D-printed cutting guides were utilized in 7 (53.8%) cases, 3D-printed implants in 2 (15.4%), and for surgical simulation and demonstration in the remaining four.
- There were three deaths (all disease-related) in the immediate postoperative period at a mean 4.6 weeks (range, 1-10) weeks, and 1 disease-related death at 53 weeks following surgery.
- Three of 13 cases (23%) had microscopically contaminated margins.

CONCLUSIONS

This technology can be useful but has not emerged in our clinical practice as a clear determinant mostly due to rarity of use.

While we believe this technique offers advantages over freehand cutting and navigated surgical techniques, there is no substitute for anatomic understanding and operative experience for pelvic tumors.

REFERENCES

1. Ahlmann ER, Menendez LR, Kermani C, Gotha H. Survivorship and clinical outcome of modular endoprosthetic reconstruction for neoplastic disease of the lower limb. *J Bone Joint Surg Br*. 2006;88(6):790-795. doi:10.1302/0301-620X.88B6.17519
2. Bernthal NM, Greenberg M, Heberer K, Eckardt JJ, Fowler EG. What are the functional outcomes of endoprosthestic reconstructions after tumor resection? *Clin Orthop Relat Res*. 2015;473(3):812-819. doi:10.1007/s11999-014-3655-1
3. Cannon CP, Mirza AN, Lin PP, Lewis VO, Yasko AW. Proximal Femoral Endoprosthesis for the Treatment of Metastatic. *ORTHOPEDICS*. 2008;31(4):361-361. doi:10.3928/01477447-20080401-03
4. Chandrasekar CR, Grimer RJ, Carter SR, Tillman RM, Abudu AT. Modular endoprosthetic replacement for metastatic tumours of the proximal femur. *J Orthop Surg Res*. 2008;3:50. doi:10.1186/1749-799X-3-50

Liver Ablation and GB Fossa Tumors

Goel A, Jafroodifar A, Thibodeau R, Tewari SO, Jawed M

Department of Radiology, SUNY Upstate Medical University, Syracuse, NY

Introduction

Percutaneous liver ablation is classically done for both primary and secondary liver tumors. The most common indications include Hepatocellular carcinoma (HCC) and metastatic disease from the colon. Additional indications include the management of benign hepatic lesions such as hemangiomas and hepatic adenoma. Several imaging modalities (US, CT, MRI) can be used to complete the procedure. The choice of ablative technique will also vary (radiofrequency, microwave, etc.) depending on the structure and location of the hepatic pathology. It is important for a resident to know the basic steps and equipment involved.

Patient Selection

Indications

- HCC
  - Per the Barcelona Clinic Liver Cancer (BCLC) group recommendations [1], percutaneous ablation is recommended as an alternative to surgery for either:
    - Stage 0: single liver lesion measuring <2 cm (very early stage)
    - Stage A: solitary lesions >2 cm or early multifocal disease characterized by up to 3 lesions measuring less than 3 cm (early stage)
- Liver Metastases
  - Per expert consensus [2], percutaneous ablation is recommended when a patient is not a candidate for surgical resection or has failed other therapies. Additionally recommendations suggest that:
    - Lesion size < 3 cm, but with allowance to < 5cm when lesions are well located
    - Lesion number < 5, but with allowance to < 9 in select cases
- Benign Liver Lesions
  - Select applications of percutaneous ablation are recommended for benign liver lesions for either:
    - Prevention of rupture and/or hemorrhage
    - Potential malignant degeneration (most commonly in adenomas)

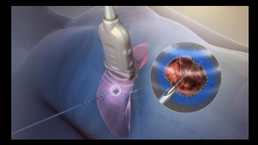

Figure 1: RF Ablation of Tumor [3]

Contraindications

- General: Uncontrollable bleeding, (abnormal coagulation studies), infection, poor ECOG performance status <3, Child-Pugh Score C

Figure 6: Choice of Image Guidance

1st Line
Ultrasound (US) and Computed Tomography (CT)

→

2nd Line (poor US-visibility or CT occult)
Magnetic Resonance Imaging (MRI), Contrast-Enhanced Ultrasound (CEUS) and PET/CT

Real-time registration between modalities has been shown to improve technical success of the procedure [9]

Figure 7: Procedural Technique

1. Sedation and local infiltration of anesthesia at puncture site
2. Place probe into the center of the lesion, confirm location using image-guidance
3. Activate probe to generate desired ablative properties
4. Ensure replacement of lesion with ablation zone, > 5 mm around circumference
5. Confirm appropriate ablation using post-procedure imaging technique based on planning imaging protocol
6. Note: Tumors near the GB fossa may be ablated after the administration of CCK to help decompress the GB and reduce the risk for thermal injury to GB wall.

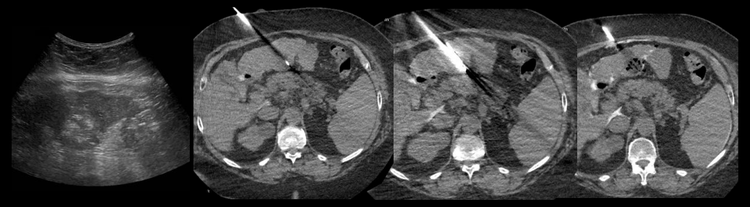

Procedure Details

Table 1: Most employed treatment modalities for percutaneous liver ablation

	Radiofrequency Ablation (Thermal)	Microwave Ablation (Thermal)	Cryoablation (Thermal)	Irreversible Electroporation (Non-thermal)
Mechanism	Needle electrode and grounding pad generate high frequency alternating electric current	Antenna delivers electromagnetic energy at microwave frequencies (915 – 2.45 Ghz)	Rapid reduction of tissue temperature promotes destruction of cellular architecture though formation of intracellular and extracellular ice crystals	Needle electrodes deliver high voltage electrical pulses that create nano-sized pores in the cell membrane -> leads to loss of homeostasis and cell death
Additional Details	- First technique to come to prominence but has variable outcomes due to tissue charring (alters tissue anatomy and conductivity) -Susceptible to "heat-sink effect" [3]	- Less susceptible to heat sink effect, faster ablation and ability to treat larger tumors than RFA	- Evidence suggests that RFA is superior - Risk of cryoshock (multiorgan failure, DIC, high mortality) and excessive bleeding	- No heat-sink effects - Preservation of the extracellular matrix and collagenous structures in ablation zone
Treatment time	5-10 minutes/probe	5-10 minutes/probe	15- 30 minutes/probe	50-100 microseconds/pulse 50-100 pulses typically used

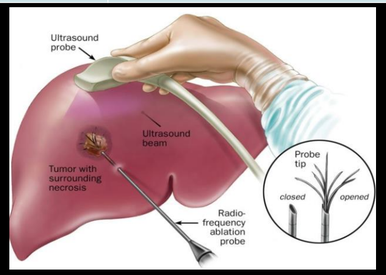

Figure 2: Schematic of Radiofrequency Ablation [5]

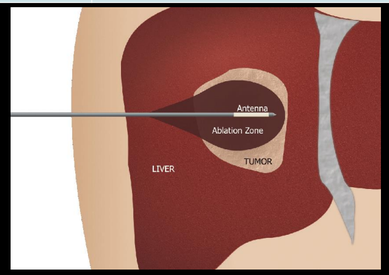

Figure 3: Schematic of Microwave Ablation [6]

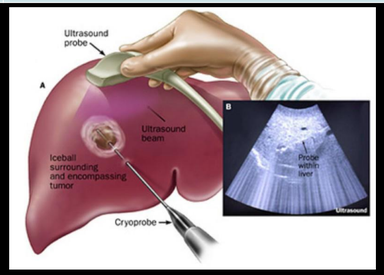

Figure 4: Schematic of Cryoblation [7]

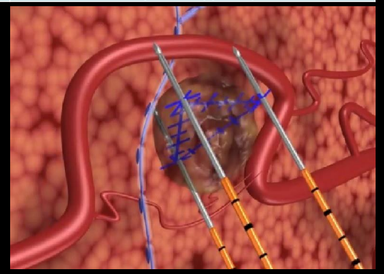

Figure 5: Schematic of Irreversible Electroporation for pancreatic tumor [8]

Complications

Infectious
- Hepatic Abscess (0.3-2%)
  - Prevention: Potentially prophylactic antibiotics
  - Management: Antibiotics if smaller, Drainage if larger or refractory to antibiotics alone

Vascular
- Hemorrhage (<2%, depending on hepatic parenchymal status & location of tumor)
  - Prevention: Correct coagulopathy, minimize passages through hepatic capsule and avoiding major vessels
  - Management: Conservatively if venous, Transfusion/embolization or surgery if arterial
- Portal venous thrombosis (1.7%), Hepatic venous thrombosis (1.4%)
  - Prevention: Avoid vascular structures, choose ablative options that minimize "heat-sink"
  - Management: Potentially systemic anticoagulation or local thrombolysis

Biliary
- Bile leakage, Biloma formation, Cholangitis, Abscess
  - Prevention: Choose ablative options that minimize "heat-sink," active biliary cooling via drainage tube
  - Management: Potentially percutaneous or endoscopic drainage for severe cases

References

1. Llovet JM, Bru C, Bruix J. Prognosis of Hepatocellular Carcinoma: The BCLC Staging Classification. Semin Liver Dis. 1999; 19(3): 329-38
2. Grundmann RT, Hermanek P, Merkel S, Germer CT, Grundmann RT, Hauss J, et al. Diagnosis and treatment of colorectal liver metastases - workflow. *Zentralbl Chir*. 2008 Jun. 133 (3):267-84.
3. https://www.scientificanimations.com/
4. Pillai, K., Akhter, J., Chua, T.C., Shehata, M., Alzahrani, N., Al-Alem, I., & Morris, D. L. (2015). Heat sink effect on tumor ablation characteristics as observed in monopolar radiofrequency, bipolar radiofrequency, and microwave, using ex vivo calf liver model. *Medicine*, *94*(9), e580.
5. https://southfloridasurgicaloncology.com/wp-content/uploads/2016/03/RADIOFREQUENCY-MICROWAVE-ABLATION.png
6. Brace, Christopher. (2010). Microwave Tissue Ablation: Biophysics, Technology, and Applications. Critical reviews in biomedical engineering. 38. 65-78. 10.1615/CritRevBiomedEng.v38.i1.60. (5)
7. Strykerinterventionalspecialists.ts.com/blog/archives
8. Interventionalnews.com
9. Abi-Jaoudeh N, Kruecker J, Kadoury S, et al. Multimodality image Fusion Guided procedures: Technique, accuracy, and applications. Cardiovasc Intervent Radiol 2012;35(5):986-98
10. Kim, K. R., & Thomas, S. (2014). Complications of image-guided thermal ablation of liver and kidney neoplasms. *Seminars in interventional radiology*, *31*(2), 138-148. https://doi.org/10.1055/s-0034-1373789

A Review of Thoracic Duct Embolization and Its Use in the Treatment of Malignant Chylothorax

Goel A, Labella D, Jafroodifar A, Thibodeau R, Tewari S, Jawed M
Department of Radiology, SUNY Upstate Medical University, Syracuse NY

Introduction:

Thoracic duct embolization is performed for the evaluation and treatment of traumatic, atraumatic, and iatrogenic chylothorax. Minimally invasive thoracic duct embolization was developed as an alternative to surgical options. The treatment consists of diagnostic pedal lymphangiography, followed by transabdominal catheterization of the thoracic duct and embolization of the thoracic duct proximal to the chyle leak.[1] Potential advantages include the minimally invasive nature of the procedure, which results in reduction of mortality and morbidity, as well as the ability to identify chyle leaks and variations in thoracic duct anatomy.[1,2]

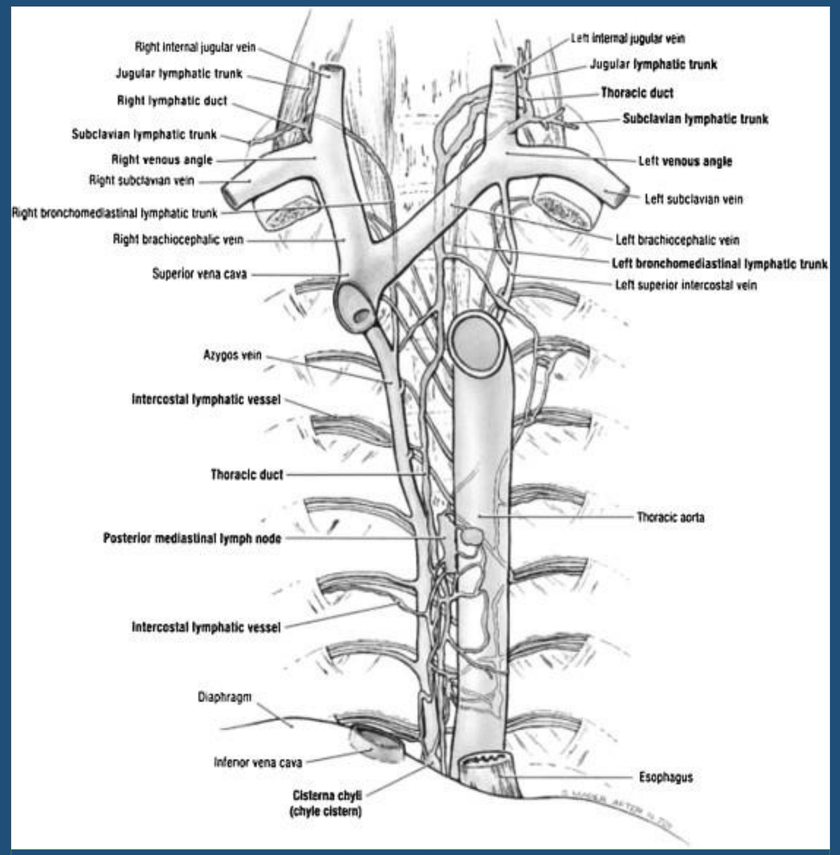

Figure 1: Anatomic rendering of the thoracic duct.[4]

Indications:

Patients with clinically significant chylothorax, chylopericardium, or post-surgical chyle leaks who fail conservative management. Clinically significant chylothorax can also arise from underlying disease including tuberculosis, sarcoidosis, or lymphoma.[2,3]

Contraindications:

Thoracic duct catheterization and embolization in patients with nonvisualization of the cisterna chyli or thoracic duct (18%) or inability to catheterize the thoracic duct (12%).[1] Additionally, significant major lower vessel venous occlusion should be ruled out prior to thoracic duct embolization.[3,6]

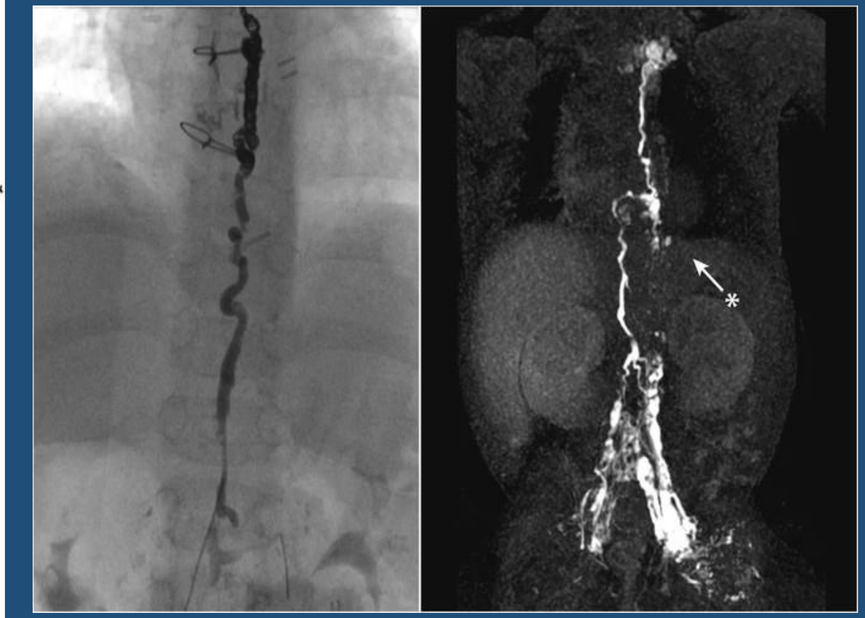

Figure 2: Fluoroscopic image of the thoracic duct after embolization, with microcoils and Truefill glue.[5]

Figure 3: Pre-procedure MR lymphangiography identifying abnormal lymphatic connections to the left pleural space.[5]

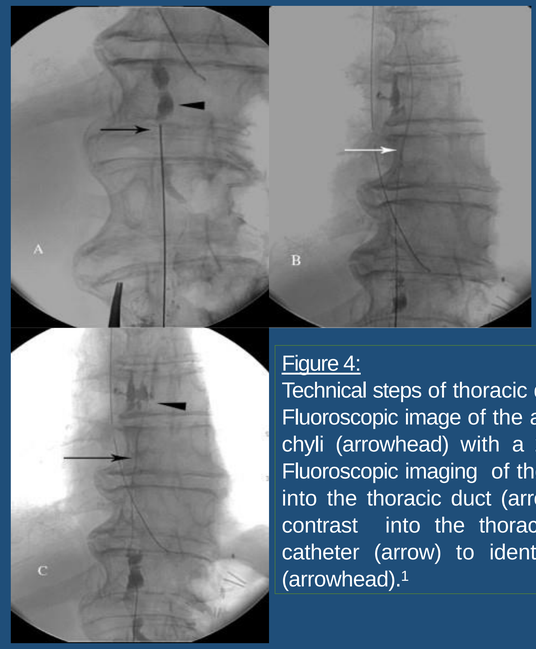

Figure 4: Technical steps of thoracic duct embolization. (A) Fluoroscopic image of the access of the cisterna chyli (arrowhead) with a 21-gauge needle. (B) Fluoroscopic imaging of the V-18 wire advanced into the thoracic duct (arrow). (C) Injection the contrast into the thoracic duct through the catheter (arrow) to identify the chylous leak (arrowhead).[1]

Procedure:

1. After identification of the cause of chyle leakage (extravasation or obstruction), embolization of the TD is performed proximally.
2. Coils are placed to provide a matrix for glue polymerization.
3. D5W is used to flush the catheter to prevent intracatheter glue polymerization.
4. n-Butyl cyanoacrylate (n-BCA) diluted 1:1 in Ethiodol is used for embolization.
5. The TD is filled with the glue mixture just proximal to the leak or occlusion.
6. Immediately after glue injection, the microcatheter is removed.
7. The foot incisions are closed with at least three vertical mattress sutures each, and the percutaneous access site is dressed with a bandage[5,6]

References:
1) Itkin M, Chen EH. Thoracic duct embolization. Semin Intervent Radiol. 2011;28(2):261-266. doi:10.1055/s-0031-1280676
2) Higgins, M.C.S.S., Park, A.W., Angle, J.F. Chylothorax: Percutaneous Embolization of the Thoracic Duct. (2015) Operative Techniques in Thoracic and Cardiovascular Surgery, 20 (4), pp. 402-412. doi: 10.1053/j.optechstcvs.2016.04.002
3) Luangrath, M.A., Pinchot, J. & Lamers, L.J. Case report description of a collaborative approach to thoracic duct embolization in patients with congenital heart disease. J Congenit Heart Dis 2, 2 (2018). https://doi.org/10.1186/s40949-018-0016-z
4) Adapted from Agur AMR, Dalley AF, Grant JCB. Grant's Atlas of Anatomy. 11th ed. Philadelphia: Lippincott Williams & Wilkins; 2005
5) Chen E, Itkin M. Thoracic duct embolization for chylous leaks. Semin Intervent Radiol. 2011;28(1):63-74. doi:10.1055/s-0031-1273941
6) Cope C: Diagnosis and treatment of postoperative chyle leakage via percutaneous transabdominal catheterization of the cisterna chyli: A preliminary study. J Vasc Interv Radiol 9:727–734, 19985.

An Unusual Presentation of an Uncommon Tumor: Transarterial Embolization of a Large Lower Extremity Hemangiopericytoma

Derrick Tran, M.D., Akram Sadeghi, M.D., Keri Conner, D.O.
University of Oklahoma Health Sciences Center, Department of Vascular and Interventional Radiology

Purpose

The purpose of this exhibit is to discuss the endovascular management for a patient presenting with a large lower extremity biopsy-proven hemangiopericytoma. More commonly found in the central nervous system, hemangiopericytomas are highly vascular tumors and embolization can be of benefit for prior to resection.

Material and Methods

Pre-procedural imaging was reviewed to assess the vasculature supplying the lesion. Access to the lesion was gained using standard catheter and exchange techniques. A 6 Fr vascular sheath, and several catheters and microcatheters were used for super-selective angiography. Embolization was carried out using 300-500 um particles and detachable Ruby coils. The patient went to the operative for resection, and was subsequently seen in clinic for follow up. All diagnostic imaging was reviewed on PACS workstation. Patient information was handled in accordance with HIPAA standards.

Case

A 45-year-old male with a history of testicular cancer was referred after imaging showed a highly vascular and hypermetabolic mass in the posterior left knee. The lesion was discovered to be a malignant hemangiopericytoma, and resection was the only curative option. Prior to resection however, pre-operative embolization was requested given the highly vascular nature of the mass and proximity to major blood vessels, elevating the risk of mortality and morbidity.

Results

Figure 1 and 2: Axial and sagittal fat-saturated post-contrast MR shows large enhancing posterior knee mass. Note prominent vasculature.

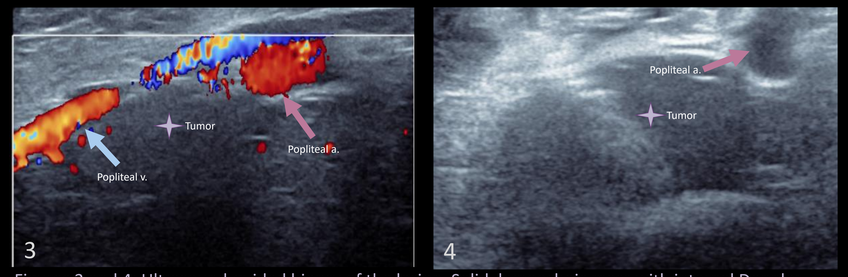

Figures 3 and 4: Ultrasound-guided biopsy of the lesion. Solid, hypoechoic mass with internal Doppler flow. Note popliteal vasculature abutted by the lesion.

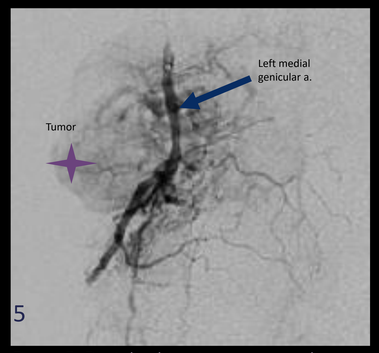

Figure 5: Digital-subtraction angiography (DSA) of the left medial genicular artery with prominent tumor opacification.

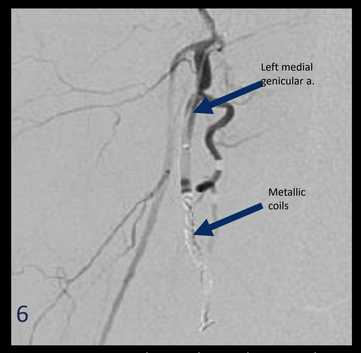

Figure 6: Post-coil DSA showed minimal opacification. 300-500 um particles were administered in the distal branches, and coils were deployed proximally.

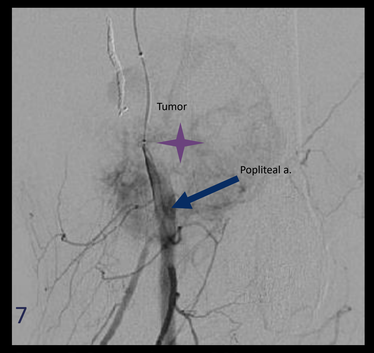

Figure 7: Popliteal artery DSA shows prominent residual tumor opacification.

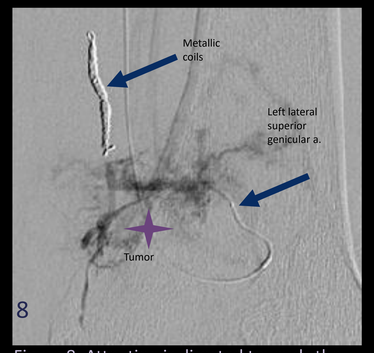

Figure 8: Attention is directed towards the lateral superior genicular artery.

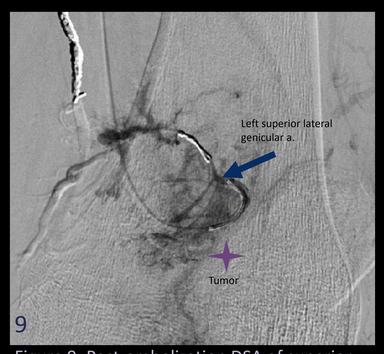

Figure 9: Post-embolization DSA of superior lateral genicular artery after particles and coils. Note residual tumor opacification.

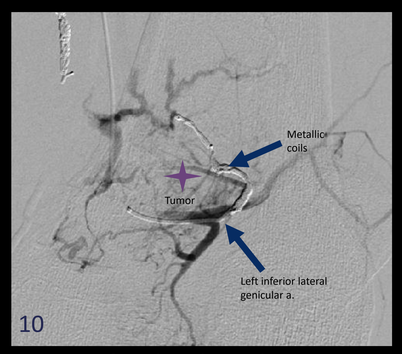

Figure 10: Inferior lateral genicular artery DSA shows subtle tumor opacification.

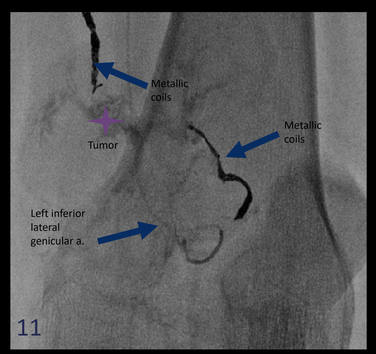

Figure 11: Post-embolization angiography, left inferior lateral genicular artery.

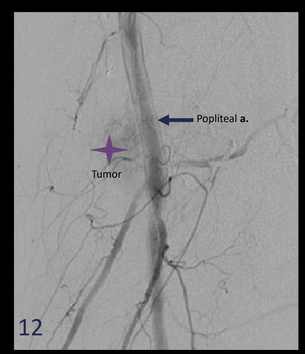

Figure 12: Final DSA shows contrast-retention from embolized tumor.

Radiologic-Pathologic Correlation

After trans-arterial embolization, the patient immediately went to the operating room for resection. Pathology demonstrated a well-circumscribed mass with spindle cells and "staghorn-like" vasculature. The lesion stained positive for CD99, CD34, and BCL-2, while staining negative for S100 and SMA. S100 identifies nerve-sheath cells and melanocytes, while SMA identifies desmoid tumors. The final diagnosis was hemangiopericytoma, part of the family of solid fibrous tumors.

Relevant Lower Extremity Vascular Anatomy

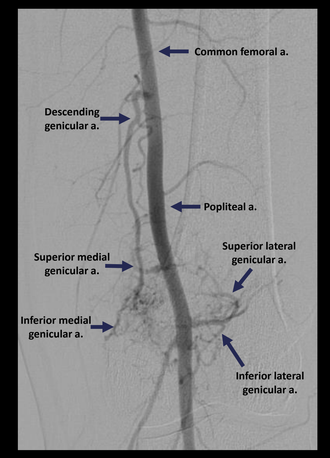

Discussion

Hemangiopericytomas fall under the family of solid fibrous tumors. These neoplasms can be benign or malignant, but are often locally aggressive. Hemangiopericytomas are most often seen within the CNS, however since they are of mesenchymal origin, can arise in any part of the body. Presentation within an extremity, as in our case, is rare.

Review of the imaging shows a highly vascular mass. This is the hallmark of hemangiopericytoma. On MRI, there is extensive vascularity accompanied by avid enhancement. This provides superb visualization on catheter angiography in fact, these tumors were once referred to as "angioblastic meningiomas," given their similar appearance compared to meningiomas when identified in the CNS.

The location of the lesion in our case made pre-operative embolization essential. The hypervascular lesion was adherent to the popliteal artery and common tibial nerve. Embolization allowed for minimal complications during resection, and although the encased neurovasculature was unable to be saved, the lesion was resected in its entirety and the patient recovered well without evidence of recurrence to this date.

References:

1. Llovet JM, Real MI, Montaña X, et al. Arterial embolisation or chemoembolisation versus symptomatic treatment in patients with unresectable hepatocellular carcinoma: a randomised controlled trial. Lancet 2002; 359:1734.
2. Brown KT, Do RK, Gonen M, et al. Randomized Trial of Hepatic Artery Embolization for Hepatocellular Carcinoma Using Doxorubicin-Eluting Microspheres Compared With Embolization With Microspheres Alone. J Clin Oncol 2016; 34:2046.
3. Moustafa AS, Aal AKA, Ertel N, Saad N, Dubay D, Saddekni S. Chemoembolization of Hepatocellular Carcinoma with Extrahepatic Collateral Blood Supply: Anatomic and Technical Considerations. RadioGraphics. 2017;37(3):963-977. doi:10.1148/rg.2017160122.
4. Moustafa AS, Aal AKA, Ertel N, Saad N, Dubay D, Saddekni S. Chemoembolization of Hepatocellular Carcinoma with Extrahepatic Collateral Blood Supply: Anatomic and Technical Considerations. RadioGraphics. 2017;37(3):963-977. doi:10.1148/rg.2017160122.
5. Choi J-Y, Lee J-M, Sirlin CB. CT and MR Imaging Diagnosis and Staging of Hepatocellular Carcinoma: Part I. Development, Growth, and Spread: Key Pathologic and Imaging Aspects. Radiology. 2014;272(3):635-654. doi:10.1148/radiol.14132361.
6. Wible BC. Diagnostic Imaging: Interventional Procedures. Philadelphia: Elsevier; 2018.

Antenna Fracture During Microwave Ablation of RCC: What is the Frequency?

Jacob Miller MD, Tushar Garg MD, Nicholas Pigg DO, and Brian Baigorri MD | HCA

Aventura Hospital and Medical Center

Purpose

We describe a case of retained antenna probe fragment after an otherwise uneventful percutaneous RCC ablation. In this scenario, the interventionist must choose between leaving a retained foreign body and risking further intervention for retrieval. Additionally, we provide a review of the literature available on this topic to illustrate the need for development of evidence-based prevention or mitigation strategies as well as management recommendations.

Methods and Materials

A 58-year-old gentleman presented for minimally invasive treatment of stage T1a renal cell carcinoma. CT and MRI imaging demonstrate a 3.1 cm renal mass (figures 1-2). Patient underwent CT-guided biopsy and subsequent microwave ablation of the left renal mass using two 17-gauge PR 15 (Neuwave) microwave probes at 65 watts for 10 and 5 minutes. One of the two probes unexpectedly stopped working before completion, though adequate coverage of tumoral margins was demonstrated. Upon removal, it was noted that the faulty probe tip was fractured and two 7x20 mm metallic fragments in the perirenal fat were noted on post-procedure CT (figures 3 and 4).

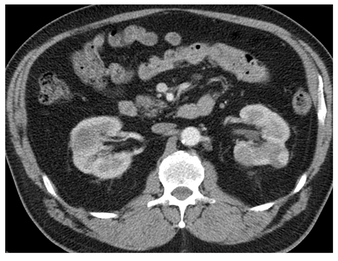

Figure 1: Axial contrast-enhanced preprocedural CT demonstrates a 3.1 cm enhancing mass at the mid pole of the left kidney.

Figure 2: Intraprocedural contrast-enhanced axial CT demonstrates proper positioning of the 17G PR 15 microwave probe.

Figure 3: Post-procedural axial unenhanced CT demonstrates metallic fragments adjacent to the ablation site.

Results/Discussion

The patient experienced no adverse events after the intervention and was discharged in excellent clinical condition. Follow-up imaging demonstrated expected post-ablation changes with an unchanged appearance of the retained fragments. No additional interventions are planned for this patient.

Analysis of the broken probe by the manufacturer and review of the ablation data was inconclusive for cause of failure. Six events of tip breakage of PR 15 cm probes were reported in the FDA's Manufacturer and User Facility Device Experience (MAUDE) database, three of which were described during removal of char. One case occurred during percutaneous bone ablation. One case of tip dislodgement in the liver was noted during percutaneous hepatic ablation.

Only two cases of antenna breakage are described during percutaneous ablation in the literature, with one attributed to shearing force of costal cartilage during lung ablation (Acculis), and the other described in hepatic ablation.[1,2] The antenna used during the hepatic ablation was not specified, though only Covidien, Amica, and Microsulis devices were used in the study.[2] Notably, no major study examining complications associated with percutaneous microwave ablation describes antenna breakage.

Conclusion

While this complication has not been described in the literature for this procedure or this device, antenna breakage has been reported in percutaneous ablation, and incident reports submitted to MAUDE's database confirm this complication is not novel.

Whether lack of data in the literature about this complication during percutaneous procedures is due to its rarity or a failure in its reporting is not entirely clear. Knowledge of this complication may allow for elucidation of risk factors, and in the development of prevention strategies and guidelines for management.

Figure 4: Photograph of fractured antenna probe at time of the procedure.

References

1. Danaher L and Steinke K. Hot tips on hot tips: technical problems with percutaneous insertion of a microwave antenna through rigid tissue. *Journal of Medical Imaging and Radiation Oncology.* 2013. 15(1): 57-60.
2. Mbaliske EC et al. Image-guided microwave thermoablation of hepatic tumors using novel robotic guidance: an early experience. *Eur Radiol.* 2015. 25:454-462.

This research was supported (in whole or in part) by HCA and/or an HCA affiliated entity. The views expressed in this publication represent those of the author(s) and do not necessarily represent the official views of HCA or any of its affiliated entities.

HCA Healthcare℠

Chemosaturation with Percutaneous Hepatic Perfusion for Unresectable Hepatic Metastasis: A Review of the Literature

Tushar Garg[1], Jacob Miller, MD[2], Thomas J Vogl, MD, PHD[3]

1:Seth GS Medical College & KEM Hospital; 2:Aventura Hospital and Medical Center, 3: University Hospital, Frankfurt

INTRODUCTION

- Chemosaturation with percutaneous hepatic perfusion (CS-PHP) (PHP; Hepatic CHEMOSTAT® Delivery System; Delcath Systems Inc, USA) is a minimally invasive, regional therapy developed for liver-dominant metastatic disease in patients unresponsive to systemic therapy and tumor burden not amenable to resection, embolization, or ablation.
- Since the first experimental study for this technique was performed in 2000, few trials have been performed to elucidate its role in the oncology treatment paradigm.
- As evidence continues to grow for the safety and efficacy of this procedure, the interventionalist may benefit from knowledge of both its technical components in addition to evidence that may support its use

METHODS AND MATERIALS

- A literature search was conducted in PubMed and Google scholar engine, and a total of 10 clinical trials were identified and reviewed systematically to determine the number of patients treated, the number of procedures performed, the type of tumor, and selected outcomes.

RESULTS

- A total of 237 patients underwent treatment with CS-PHP with a total of 541 procedures between them.
- The types of primary tumor for the hepatic metastasis are: Ocular melanoma (n=167, 70.46%) followed by cholangiocarcinoma (n=30, 12.6%), colorectal carcinoma (n=11, 4.6%), cutaneous melanoma (n=8, 3.3%), hepatocellular carcinoma (n=6, 2.5%), breast carcinoma (n=2, 1.2%), pancreatic adenocarcinoma (n=2, 1.2%), neuroendocrine tumor (n=2, 1.2%), periampullary cancer (n=2, 1.2%), endometrial carcinoma (n=1, 0.4%), sarcoma (n=1, 0.4%), and unknown primary melanoma (n=1, 0.4%).

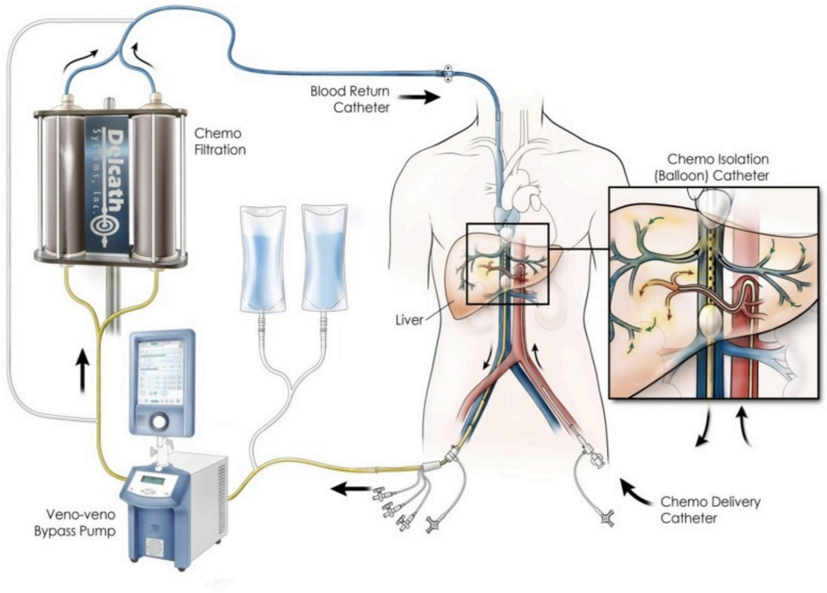

Overview of CS-PHP system

- A total of 9 patients (3.7%) showed complete response, and 89 patients (37.55%) showed partial response. The disease stabilized in 108 patients (45.56%) but 34 patients (14.34%) showed progressive disease and 4 patients (1.6%) died either during or after the procedure.

CONCLUSION

- Analysis of results from the randomized controlled trials and several retrospective studies show CS-PHP good tumor response rates in patients with unresectable hepatic metastases from various primary tumors.

Study	No. of Study Patients	Type of Primary Tumor (n)	No. of treatments received	Median No. of Treatments	Selected Outcomes	Comment
Schonfeld et al	60	Ocular Melanoma (30) Cholangiocarcinoma (14) HCC (6) Colorectal cancer (2) Pancreatic cancer (2) Periampullary cancer (2) Neuroendocrine Tumor (2) Breast cancer (1) Endometrial cancer (1)	141	2	CR=1 PR=14 SD=38 PD=15	
Artzner et al	16	Ocular Melanoma (16)	28	Not reported	CR=0 PR=9 SD=5 PD=1	1 patient died due to intra-procedure cardiac arrest
Marquart et al	15	Cholangiocarcinoma (15)	26	Not reported	CR=1 PR=2 SD=8 PD=3	1 patient died after procedure due to sepsis and liver failure
Karydis et al	51	Ocular Melanoma (51)	134	2	CR=3 PR=22 SD=17 PD=7	
Hughes et al	44	Ocular Melanoma (39) Cutaneous Melanoma (5)	120	3	CR=0 PR=16 SD=23 PD=5	Death associated with treatment =1
Van Etten et al	10	Colorectal cancer (9) Ocular melanoma (1)	10	Not reported	CR=0 PR=2 SD=6 PD=2	
Abbott et al	10	Ocular Melanoma (4) Sarcoma (1) Unknown primary melanoma (1)	30	3	CR=1 PR=5 SD=4 PD=0	
Hickson et al	18	Ocular Melanoma (18)	34	2	CR=2 PR=13 SD=2 PD=1	
Vogl et al	13	Ocular Melanoma (8) Cutaneous Melanoma (3) Breast cancer (1) Cholangiocarcinoma(1)	18	1	CR=1 PR=6 SD=5 PD=0	Death associated with treatment =1

References

1. Vogel A, Gupta S, Zeile M, von Haken R, Brüning R, Lotz G, Vahrmeijer A, Vogl T, Wacker F. Chemosaturation percutaneous hepatic perfusion: a systematic review. Advances in therapy. 2016 Dec 1;33(12):2122-38.
2. Artzner C, Mossakowski O, Hefferman G, Grosse U, Hoffmann R, Forschner A, Eigentler T, Syha R, Grözinger G. Chemosaturation with percutaneous hepatic perfusion of melphalan for liver-dominant metastatic uveal melanoma: a single center experience. Cancer Imaging. 2019 Dec 1;19(1):31.

Combined Radiofrequency Ablation and Augmentation for the Palliation of Vertebral Metastasis: Case Examples and Review.

Christian Sleeper, BA[a/b], Matthew Moccia, DO[b], Joseph Gerding, MD[b] and Ethan Dobrow, MD[c]

a - Tufts University School of Medicine, Boston, MA; b - Maine Medical Center, Portland, Maine; c - Veterans Affairs Maine Healthcare System, Augusta, Maine

Purpose:

This exhibit will review radiofrequency ablation (RFA) and percutaneous vertebral augmentation (PVA) in the palliative treatment of painful spinal metastases through a series of case examples. We will also review the current literature supporting the use of these combined therapeutic modalities, in particular the choice of RFA as the ablative modality for spinal lesions.

Introduction:

Bone represents the third most frequent site of solid tumor metastasis, with breast, prostate, lung, thyroid, and kidney primaries being implicated in 80 percent of cases[1]. The vertebral bodies are the most susceptible to metastatic spread, with an estimated 30 to 70 percent of oncology patients developing vertebral metastasis during their disease course[2]. The presence of vertebral metastatic disease is associated with significant morbidity including pain, fracture, hypercalcemia, and spinal cord damage. It has been reported that up to 80 percent of patients will experience severe pain before palliative treatment is initiated[3]. Traditional management has often utilized a multidisciplinary approach, with external beam radiation being the gold standard for palliative management[4]. NSAIDs, opioids, bisphosphonates, and radiopharmaceuticals are also used for supplemental therapy and pain control. Despite these measures, patients often experience refractory pain and significantly reduced quality of life[5]. In these patients, both vertebral augmentation and local ablation therapies have been discussed in the literature as potential therapeutic options[6-13]. Although a variety of ablative methods have been discussed within the literature, bipolar RFA is our preferred modality due to the reported insulating effects of cortical bone and decreased heat transmission through cancellous bone[14]. In patients whose vertebral cortex is intact, ablation zones are therefore less likely to extend beyond the cortex and damage surround neural structures. More recently, emerging data has shown that concomitant use of radiofrequency ablation (RFA) and percutaneous vertebral augmentation (PVA) may play an important role in management of refractory vertebral metastasis by providing both pain palliation and local tumor control[15-19]. In this presentation, we describe a procedural technique for combined RFA and PVA as well as review four patient cases who successfully underwent treatment for management of refractory metastatic disease.

Methods:

A total of four patients with symptomatic vertebral metastatic lesions underwent kyphoplasty with concomitant radiofrequency ablation at a single tertiary care center. Under fluoroscopic guidance, trocars were advanced into the vertebral body via a transpedicular approach in the lumbar spine or an extrapedicular approach in the thoracic spine. Once appropriately positioned, radiofrequency ablation probes were inserted into the trocars and activated. Ablation times varied between 6 and 15 minutes depending on size of the probe used. Upon ablation completion, kyphoplasty balloons were inserted into the same trocars and inflated within the vertebral body. Finally, polymethylmethacrylate cement was prepared and inserted into the trocars to fill the vertebral body and complete the procedure.

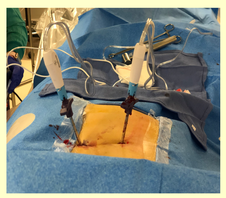

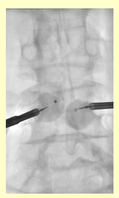

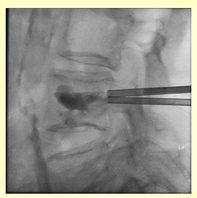

Case #1 – Metastatic Renal Cell Carcinoma

A 61 y/o male with metastatic renal cell carcinoma presents with upper back pain. CT revealed near complete replacement of T5 with a lytic metastasis. He underwent combined RFA and PVA. Follow up CT revealed adequate cement fill in the T5 vertebral body without cement extravasation.

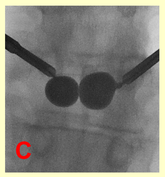

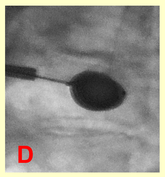

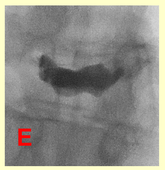

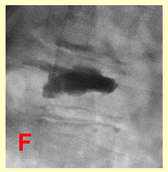

AP and lateral intraprocedural spot fluoroscopic images (ablation not imaged). **C-D:** Bilateral 15mm balloons are slowly inflated via bipedicular access. **E-F:** Final spot fluoroscopic images reveal cement filling the T5 vertebral body.

Preprocedural Imaging. **A:** Coronal CT reveals a lytic lesion involving T5 with destruction of the lateral cortex. **B:** Sagittal CT demonstrates near complete lytic replacement of T5.

Postprocedural Imaging. **G-H:** Coronal and sagittal CT images reveal adequate cement fill within the the T5 body without cement extrusion.

Case #2 –Metastatic Breast Cancer

A 66 y/o female with newly diagnosed primary breast cancer presents with worsening low back pain. A CT revealed multiple lytic lesions throughout the lumbar spine. A contrast enhanced MRI demonstrated pathologic compression fractures of L1 and L5. Using bi-pedicular technique, combination RFA and PVA was performed. Following the procedure, the patient reported reduction in her lower back pain. Subsequent imaging revealed excellent cement fill in the L1 and L5 vertebral bodies.

Preprocedural imaging. **A:** Sagittal CT demonstrates diffuse lytic lesions throughout the lumbar spine; **B-C:** Sagittal T2WI and T1WI C+ more clearly demonstrate pathologic compression deformities of L1 and L5 (red arrows).

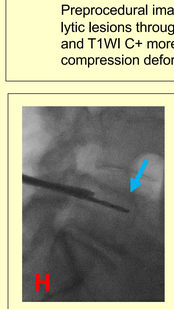

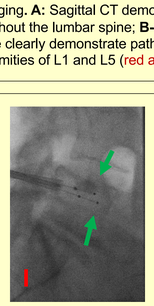

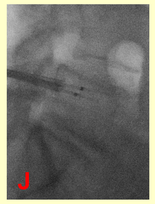

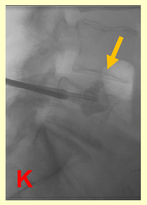

Intraprocedural spot fluoroscopic images. **H:** L5 accessed using bipedicular technique, a bone drill is advanced on the left to the anterior one third of the vertebral body (blue arrow). **I:** The thermal ablation probes are positioned within the vertebral body (green arrows). **J:** A 15 mm kyphoplasty balloon is slowly inflated on the right (left side not included). **K:** Cement is slowly administered into the vertebral body with some extrusion superiorly (orange arrow). **L:** A final spot fluoroscopic image reveals adequate cement fill in the L1 and L5 vertebral bodies.

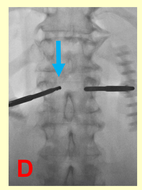

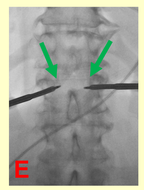

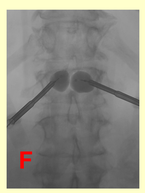

Intraprocedural spot fluoroscopic images of the L1 vertebral body. **D:** L1 accessed using bipedicular technique, a bone drill is advanced on the left (blue arrow). **E**: The thermal ablation probes are advanced into the vertebral body (green arrows). **F:** 15 mm kyphoplasty balloons are inflated bilaterally. **G:** Cement is slowly administered into the vertebral body.

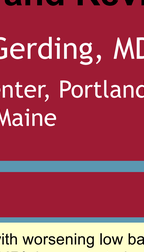

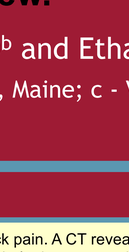

Postprocedural images. **M-N:** Sagittal CT and T1WI demonstrate cement fill within L1 and L5 without clinically significant extrusion of cement (red arrows).

Case #3 – Metastatic Gastric Cancer

A 43 y/o male with a history of gastric adenocarcinoma presents with pain secondary to multiple PET avid spinal metastases involving the T3-T5 vertebral bodies. Combined RFA and PVA was performed utilizing a bilateral extrapedicular technique at all levels. Follow up PET-CT revealed excellent cement fill and absent FDG uptake at the treated levels.

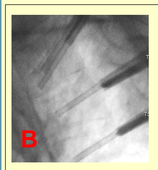

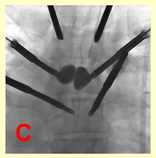

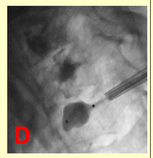

AP and lateral intraprocedural spot fluoroscopic images (ablation not imaged). **B-C:** Bilateral 15 mm balloons are slowly inflated via bipedicular access. **D-E**: Final spot fluoroscopic images reveal cement filling the T3-T5 vertebral bodies.

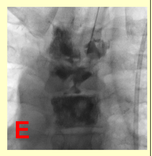

Preprocedural images. **A**: PET-CT reveals intense uptake within the T3-T5 vertebral bodies.

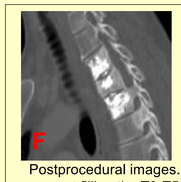

Postprocedural images. **F-G:** Sagittal CT with cement filling the T3-T5 vertebral bodies. PET-CT reveals resolution of the previously intense uptake within T3-T5.

Case #4 – Metastatic Renal Cell Carcinoma

A 50 y/o male with primary renal cell carcinoma presents with an isolated, asymmetric L5 spinal metastasis with associated pathologic fracture. He subsequently underwent unipedicular RFA and PVA. Follow up CT revealed cement filling the entirety of the asymmetric lytic lesion with minimal cement extrusion through the disrupted lateral cortex.

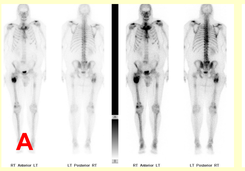

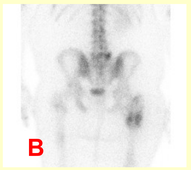

Preprocedural imaging. **A-B:** Whole body bone scan reveals focal uptake within the L5 vertebral body concerning for metastatic disease. **C:** Axial CT reveals an asymmetric lytic lesion involving the right side of L5. **D-E:** Sagittal and coronal CT images demonstrate destruction of the inferior endplate (red arrows).

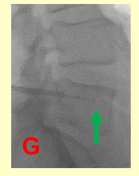

AP and lateral intraprocedural spot fluoroscopic images: **F:** The right pedicle of L5 is accessed utilizing unipedicular technique. **G:** A thermal ablation probe is advanced to the anterior one third of the vertebral body (green arrow). **H:** A 15mm balloon is inflated within L5. **I:** Cement is slowly instilled into the right side of the L5 vertebral body. **J-K:** Final AP and lateral spot images demonstrate cement fill within L5 with minimal cement extrusion along the right margin of the inferior endplate (blue arrow).

Postprocedural images. **L-N:** Axial, sagittal and coronal CT images with cement filling the entirety of the previous L5 lytic lesion. The coronal image demonstrates minimal extrusion of cement from the right margin of the inferior endplate which was not clinically significant (blue arrow).

Conclusions

All four patients underwent technically successful vertebral augmentation with radiofrequency ablation. This method appears to be a safe and technically feasible approach for the management of painful osseous vertebral metastasis.

Citations

1: Aaron, A. D. "Treatment of Metastatic Adenocarcinoma of the Pelvis and the Extremities." *Journal of Bone and Joint Surgery. American Volume* 79.6 (1997): 917. Web.
2: Coleman, Robert E. "Clinical Features of Metastatic Bone Disease and Risk of Skeletal Morbidity." *Clinical Cancer Research* 12.20 (2006): 6243s-249s. Web.
3: Janjan, Nora. "Bone Metastases: Approaches to Management." *Seminars in Oncology* 28.4 Suppl 11 (2001): 28-34. Web.
4: Lutz S, Berk L, Chang E, et al. Palliative radiotherapy for bone metastases: an AS- TRO evidence-based guideline. Int J Ra- diat Oncol Biol Phys 2011;79(4):965–976.
5: Rosenthal, Daniel, and Callstrom, Matthew R. "Critical Review and State of the Art in Interventional Oncology: Benign and Metastatic Disease Involving Bone." *Radiology* 262.3 (2012): 765-80. Web.
6: Health Quality Ontario. Vertebral augmentation involving vertebroplasty or kyphoplasty for cancer related vertebral compression fractures: a systematic review. Ont Health Technol Assess Ser [Internet]. 2016 May;16(11):1–202. Available from: http://www.hqontario.ca/Evidence-to-ImproveCare/Journal-Ontario-Health-Technology-Assessment-Series.
7: Gennaro, Nicolò, Sconfienza, Luca Maria, Ambrogi, Federico, Boveri, Sara, and Lanza, Ezio. "Thermal Ablation to Relieve Pain from Metastatic Bone Disease: A Systematic Review." *Skeletal Radiology* 48.8 (2019): 1161-169. Web.
8: Berenson, James, Pflugmacher, Robert, Jarzem, Peter, Zonder, Jeffrey, Schechtman, Kenneth, Tillman, John B, Bastian, Leonard, Ashraf, Talat, and Vrionis, Frank. "Balloon Kyphoplasty versus Non-surgical Fracture Management for Treatment of Painful Vertebral Body Compression Fractures in Patients with Cancer: A Multicenter, Randomized Controlled Trial." *The Lancet Oncology* 12.3 (2011): 225-35. Web.
9: Hillen, Travis J, Anchala, Praveen, Friedman, Michael V, and Jennings, Jack W. "Treatment of Metastatic Posterior Vertebral Body Osseous Tumors by Using a Targeted Bipolar Radiofrequency Ablation Device: Technical Note." *Radiology* 273.1 (2014): 261-67. Web.
10: Thanos, L, Mylona, S, Galani, P, Tzavoulis, D, Kalioras, V, Tanteles, S, and Pomoni, M. "Radiofrequency Ablation of Osseous Metastases for the Palliation of Pain." *Skeletal Radiology* 37.3 (2008): 189-94. Web.
11: Buy, Xavier, Catena, Vittorio, Roubaud, Guilhem, Crombe, Amandine, Kind, Michèle, and Palussiere, Jean. "Image-Guided Bone Consolidation in Oncology." *Seminars in Interventional Radiology* 35.4 (2018): 221-28. Web.
12: Yevich, Steven, Tselikas, Lambros, Gravel, Guillaume, De Baère, Thierry, and Deschamps, Frederic. "Percutaneous Cement Injection for the Palliative Treatment of Osseous Metastases: A Technical Review." *Seminars in Interventional Radiology* 35.4 (2018): 268-80. Web.
13: Moynagh, Michael R, Kurup, A. Nicholas, and Callstrom, Matthew R. "Thermal Ablation of Bone Metastases." *Seminars in Interventional Radiology* 35.4 (2018): 299-308. Web.
14: Dupuy, D E, Hong, R, Oliver, B, and Goldberg, S N. "Radiofrequency Ablation of Spinal Tumors: Temperature Distribution in the Spinal Canal." *American Journal of Roentgenology (1976)* 175.5 (2000): 1263-266. Web.
15: Bagla, Sandeep, Sayed, Dawood, Smirniotopoulos, John, Brower, Jayson, Neal Rutledge, J, Dick, Bradley, Carlisle, James, Lekht, Ilya, and Georgy, Bassem. "Multicenter Prospective Clinical Series Evaluating Radiofrequency Ablation in the Treatment of Painful Spine Metastases." *CardioVascular and Interventional Radiology* 39.9 (2016): 1289-297. Web.
16: Tomasian, Anderanik, Madaelil, Thomas P, Wallace, Adam N, Wiesner, Elizabeth, and Jennings, Jack W. "Percutaneous Thermal Ablation Alone or in Combination with Cementoplasty for Renal Cell Carcinoma Osseous Metastases: Pain Palliation and Local Tumour Control." *Journal of Medical Imaging and Radiation Oncology* 64.1 (2020): 96-103. Web.
17: Sayed D, Jacobs D, Sowder T, Haines D, Orr W. Spinal Radiofrequency Ablation Combined with Cement Augmentation for Painful Spinal Vertebral Metastasis: A Single-Center Prospective Study. *Pain Physician*. 2019;22(5):E441-E449.
18: Tomasian, A. Hillen, T.J. Chang, R.O. and Jennings, J.W. "Simultaneous Bipedicular Radiofrequency Ablation Combined with Vertebral Augmentation for Local Tumor Control of Spinal Metastases." *American Journal of Neuroradiology: AJNR* 39.9 (2018): 1768-773. Web.
19: Kelekis, Alexis, Cornelis, Francois H, Tutton, Sean, and Filippiadis, Dimitrios. "Metastatic Osseous Pain Control: Bone Ablation and Cementoplasty." *Seminars in Interventional Radiology* 34.4 (2017): 328-36. Web.

Contrast-Enhanced Ultrasound as a Useful Targeting Aid During Microwave Ablation of Hepatic Malignancies

Derrick Tran, M.D., Akram Sadeghi, M.D., Keri Conner, D.O.

The University of Oklahoma Health Sciences Center

The UNIVERSITY of OKLAHOMA Health Sciences Center

Purpose

The purpose of this exhibit is to review the basic principles behind contrast-enhanced ultrasound and to discuss the benefits provided during the microwave ablation of liver metastases, particularly when the lesion is small or difficult to visualize.

Materials and Methods

Images were reviewed on a PACS workstation, with relevant history obtained from the hospital electronic medical record. Microwave ablation was performed under contrast-enhanced ultrasound guidance, with a pre-procedural non-contrast CT scan to provide a global picture of the surrounding structures. All information was handled in accordance with HIPAA standards.

Basic Principle of Contrast-Enhanced Ultrasound

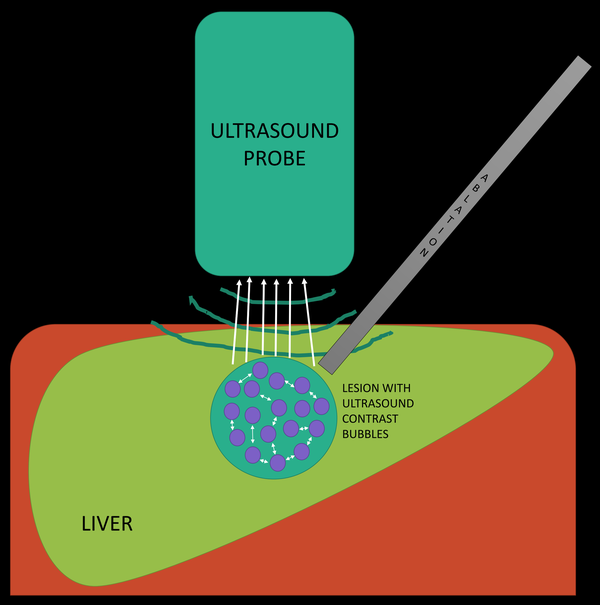

Figure 1: Simplified schematic of contrast-enhanced ultrasound. The underlying principle is the significant echogenicity difference between gas (highly echogenic) and body fluid (low echogenicity). Tissue is less echogenic given its relatively high fluid content. Ultrasound contrast agents are gas bubbles suspended in a solution, which is injected intravenously. Ultrasound waves strike the gas bubbles, causing essentially a reverberation, visualized as an echo. Since these bubbles are carried in the bloodstream, a dynamic evaluation of different organs is possible, and the contrast-enhancement characteristics mirror that of CT or MRI techniques.

Case 1

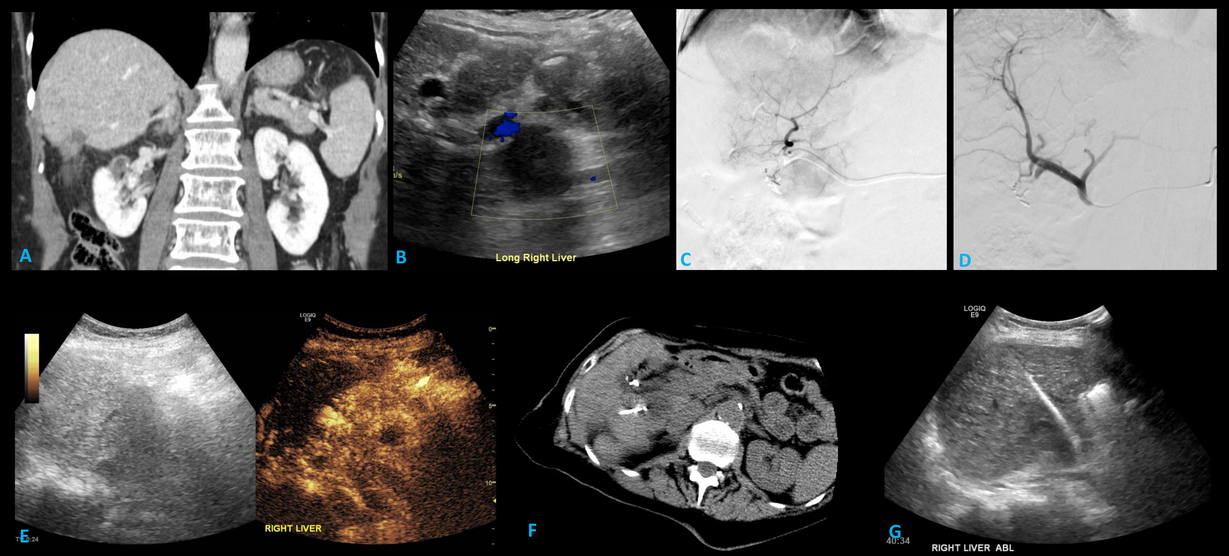

Figure 2: (A) Coronal CT shows hypoattenuating lesion with desmoplastic reaction in inferior right hepatic lobe. (B) Corresponding ultrasound appearance (C) Right hepatic artery DSA prior to particle chemoembolization, showing subtle tumor vascularity and opacification. (D) Post-chemoembolization DSA performed after microcatheter is withdrawn proximally. (E) Greyscale and contrast-enhanced ultrasound of the treated lesion. Note the difficulty in discerning the lesion, which becomes much more conspicuous after contrast. Echogenic areas indicate residual viable tumor, while hypoechoic center represents necrosis. (F) planning CT to identify surrounding structures. Note close proximity to bowel and IVC. (G) Successful microwave ablation of the lesion.

Case 2

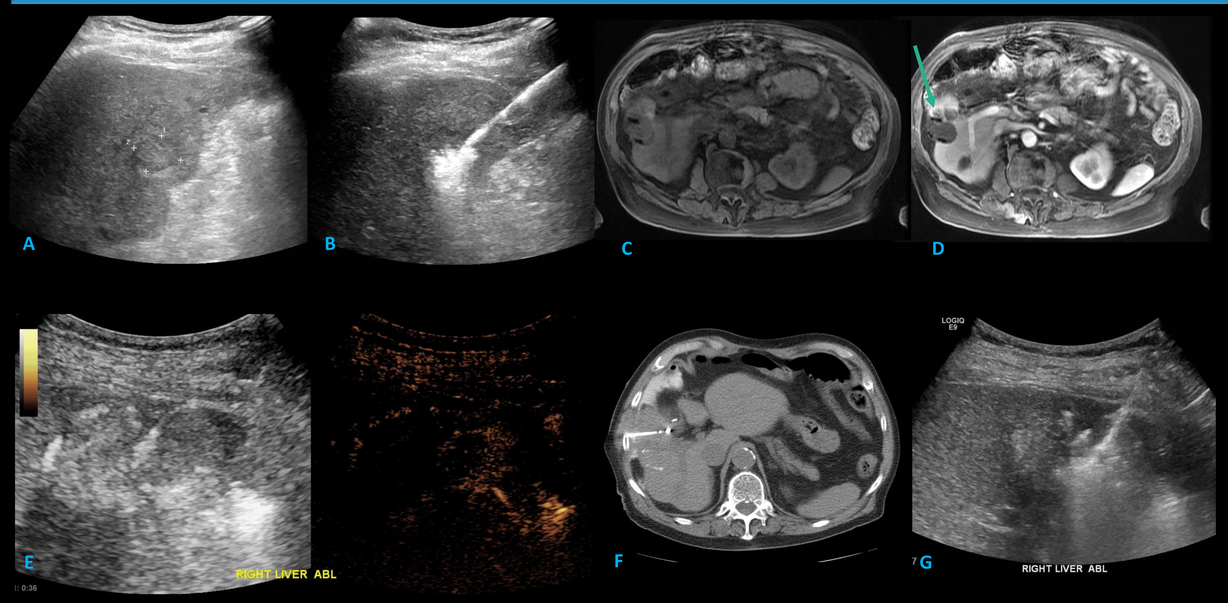

Figure 3: (A) Mostly isoechoic lesion in the right hemiliver. (B) Microwave ablation of the lesion. (C) Noncontrast and (D) postcontrast MR 3 months post-ablation shows small region of residual enhancement concerning for viable tumor (green arrow). (E) Contrast-enhanced ultrasound shows a peripheral rim of enhancement, greater on the left, compatible with residual tumor. Note adjacent bowel gas. (F) planning CT confirms ablation probe placement. Contrast was injected into the peritoneal cavity to "push" bowel away from the ablation zone. (G) Successful microwave ablation of the lesion.

Discussion and Conclusion

Microwave ablation with contrast-enhanced ultrasound was technically successful in these cases and highlighted the advantages of real-time imaging while performing the procedure. As can be seen, the contrast enhancement of viable tumor allows the operator to precisely target the zone of therapy while avoiding collateral damage to the surrounding structures.

Oftentimes, lesions that have been treated whether by ablation or embolization, become more difficult to visualize due to the presence of scar and necrosis which can closely match the attenuation of viable tumor. Intravenous iodinated contrast cannot be used during CT-guided ablation because contrast timing cannot be practically coordinated with the procedure. Contrast-enhanced ultrasound fills this role, allowing better visualization of viable tumor, while also allowing the radiologist to manipulate structures to optimize the treatment. Furthermore, ultrasound contrast can be replenished while scanning. The inherent lack of ionizing radiation also reduces the dose to the patient, radiologist, and their staff.

Contrast-enhanced ultrasound is an emerging modality to augment diagnostic imaging. It too, can augment the vascular and interventional radiologist's toolset when dealing with difficult lesions.

References

1. Eng O, Tsang A, Moore D et al. Outcomes of microwave ablation for colorectal cancer liver metastases: A single center experience. J Surg Oncol. 2014;111(4):410-413. doi:10.1002/jso.23849
2. Chiou Y. US-Guide Microwave and Radiofrequency Ablation for Liver Tumors. Ultrasound Med Biol. 2017;43:S152. doi:10.1016/j.ultrasmedbio.2017.08.1496
3. Cosgrove D. Contrast-Enhanced Ultrasound of Liver Lesions. Ultrasound Med Biol. 2010;36(12):2146. doi:10.1016/j.ultrasmedbio.2010.06.011
4. Lorentzen T. The Use of Contrast Enhanced US in Interventional Application of Liver. Ultrasound Med Biol. 2017;43:S151. doi:10.1016/j.ultrasmedbio.2017.08.1492
5. Wible B. Diagnostic Imaging. 2nd ed. Philadelphia: Elsevier; 2018.
6. Gores G. Chemoembolization as a bridge to transplantation for hepatocellular carcinoma. Liver Transplantation. 2001;7(11):998. doi:10.1053/jlts.2001.21341
7. Minocha J, Salem R, Lewandowski R. Transarterial Chemoembolization and Yittrium-90 for Liver Cancer and Other Lesions. Clin Liver Dis. 2014;18(4):877-890. doi:10.1016/j.cld.2014.07.007

Contrast-Enhanced Ultrasound: A Comprehensive Review and a Look at Its Role in the Arsenal of the Modern Interventionalist

Goel A, Thibodeau R, Jafroodifar A, Labella D, Jawed M, Tewari SO

Department of Radiology, SUNY Upstate Medical University, Syracuse NY

CIOctober Symposium on Clinical Interventional Oncology 2020 ONLINE

UPSTATE MEDICAL UNIVERSITY

Introduction:

- Patients with cirrhosis are at high-risk for developing hepatocellular carcinoma (HCC) → guidelines recommend ultrasonography guidance every 6 months +/- alpha-fetoprotein serum assay

Ultrasonography (US)

- Gray-scale US is non-specific for focal liver lesions and while US with Doppler may provide more information, it is still relatively non-specific and prone to motion artifact
- Contrast-enhanced US (CEUS) is growing in popularity for focal liver lesions with reported sensitivity and specificity values approaching CT/MRI[1] and can reveal vascular architecture (microcirculation and microcirculation) and contrast enhancement
  - CEUS Is a real-time dynamic US that uses microbubble-based contrast (1-10 μm) to reveal focal liver lesions without ionizing radiation (vs CT) and has a much higher temporal resolution (vs MRI and CT) [2,3]
- Microbubble-based contrast agents are not nephrotoxic and can be used in patients with renal failure/obstruction or COPD

Table 1: CEUSAdverse Event Rates[4]

Risk for Adverse Event	0.0086%
Death Rate	0.0%
Life-threatening Anaphylactoid Rate	0.002%

Table 2: Pooled Statistics for CEUS[5]

Sensitivity	92%
Specificity	87%
Diagnostic Odds Ratio	104.20
Positive Likelihood Ratio	7.38
Negative Likelihood Ratio	0.09
Area Under the Curve	0.9665

Contrast agent	Year	Components	Approval
Echovist®	1991	Galactose with air	Shunt imaging in cardiology and in hysterosalpingo-contrast sonography[33,34]
Albunex®	1995	Perflutren shell with air	Cardiology
Levovist®	1995	Mix of galactose and palmitic acid with air	Cardiology, liver imaging, and intracavitary application for imaging of vesicoureteral reflux
Optison®	1997	Albumin shell with perflutren	LV opacification and endocardial border definition
SonoVue®	2001	Phospholipid shell with sulfur hexafluoride	LV opacification and endocardial border definition, breast, liver, portal vein, extracranial carotid and peripheral arteries, USA: Only approved for LV opacification and endocardial border definition, Canada: Only approved for LV opacification, endocardial border definition and diagnostic assessment of vessels
Definity®	2001	Phospholipid shell with octafluoropropane	LV opacification and endocardial border definition, Australia, Brazil, Mexico, India, Israel, and New Zealand: Imaging of liver and kidney, Canada: Liver, kidney, spleen, pancreas, bladder, bowel, ovary, uterus, testicles
Sonazoid®	2007	Lipid shell with perfluorobutane	Imaging of focal liver lesions, Japan: Focal breast lesions

Figure 2 (left): Contrast-enhancing agents[6]

A Contrast-enhanced ultrasonography (CEUS) diagnostic criteria for characterising focal liver lesions

Lesion type	Postcontrast appearance
Cyst	Nonenhancing in all dynamic phases
Haemangioma	Globular peripheral or rim-like enhancement during the arterial phase, with progressive centripetal fill-in in the extended portal phase
Focal nodular hyperplasia	Spoke-wheel appearance in the early arterial phase, homogeneously hypervascular in the late arterial phase, iso/hypervascular in the portal-venous and delayed phase; central hypovascular scar in the delayed phase
Hepatocellular adenoma	Subcapsular arteries with centripetal or mixed fill-in; isoenhancing to the liver parenchyma in the extended portal phase, often inhomogeneous
Focal fatty sparing	Isovascular to the surrounding liver parenchyma during all vascular phases
Focal fatty change	Isovascular to the surrounding liver parenchyma during all vascular phases
Regenerative nodule	Hypo/ isovascular in the arterial phase, indistinguishable from the surrounding liver parenchyma in the extended portal phase
Hepatocellular carcinoma	Diffuse, homogeneous or heterogeneous enhancement during the arterial phase with hypovascular appearance during the extended portal phase
Metastasis	Variable enhancement in the arterial phase, with hypovascular appearance in the extended portal phase
Cholangiocarcinoma	Heterogeneous, prevalently peripheral enhancement in the arterial phase; hypovascular in the extended portal phase

B Computed tomography (CT) and magnetic resonance (MRI) diagnostic criteria for characterising focal liver lesions

Lesions	Precontrast appearance	Postcontrast appearance
Cysts	Fluid density (±10 HU), T1 hypointensity and marked T2 hyperintensity	Avascular throughout the dynamic study
Haemangioma	Homogeneous T2 hyperintensity	Globular peripheral or rim-like enhancement during the arterial phase, with progressive centripetal fill-in in the portal-venous and/or equilibrium phase; isodensity/isointensity to vessels
Focal nodular hyperplasia	Isointensity to liver in T1/T2 Hyperintense "central scar" in T2	Homogeneously and markedly hypervascular in the arterial phase, isohypervascular in the portal-venous and/or equilibrium phase, delayed enhancement of the central scar; isohypervascular during the liver-specific phase of MRI
Hepatocellular adenoma	Fatty (reduced signal intensity on out-of-phase T1 images) or haemorrhagic (heterogeneous hyperdensity or T1 hyperintensity)	Homogeneous and diffuse or heterogeneous enhancement during the arterial phase, isoenhancing to the liver parenchyma during the portal-venous and equilibrium phase, homogeneous or heterogeneous; hypovascular during the liver-specific phase of MRI
Focal fatty sparing	Hyperdensity in the context of a low-attenuation parenchyma Hyperintensity on out-of-phase T1 images	Isovascular to the surrounding parenchyma during all vascular phases
Focal fatty change	Hypodensity in the context of a normally attenuating parenchyma Reduced signal intensity on out-of-phase T1 images	Isovascular to the surrounding parenchyma during all vascular phases
Regenerative nodule	Hyperdensity or T1 hyperintensity/T2 hypointensity	Hypo/isovascular in the arterial phase, indistinguishable from the surrounding parenchyma in the portal-venous and equilibrium phase
Hepatocellular carcinoma	Moderate and heterogeneous T2 hyperintensity Satellite nodules, presence of fatty component	Homogeneous or heterogeneous diffuse enhancement during the arterial phase with washout in the portal-venous and/or equilibrium phase
Metastasis	–	Peripheral uptake, variable vascularity during the arterial phase, hypovascular during the portal-venous and/or equilibrium phase
Cholangiocarcinoma	–	Heterogeneous, predominantly peripheral, enhancement, uptake during the equilibrium phase

Figure 1 (right): Findings of focal liver lesions in CEUS (A) vs CT/MRI with contrast (B)[2]

Liver phases: arterial, portal venous, and late (sinusoidal)

- With some US contrast agents, there may be a fourth phase: post-vascular phase (Kupffer cell phase)
- CEUS may alter differential based on vascularity and contrast enhancement pattern during arterial, portal, and late phase
  - Highest diagnostic accuracy in the differential diagnosis of small (≤20 mm) focal liver lesions
  - In part, due to visualized high vascularity and wash-out phenomenon of malignant lesions (compared to benign lesions)

Characterization of CEUS findings:

- *Enhancement* = contrast behavior of lesion or region of interest in terms of the degree (hypo-, iso-, hyperenhancement relative to adjacent parenchyma) and timing (phase)
  - Must know if liver tissue is healthy or disease (cirrhosis, fibrosis, steatosis) in advance due to affect on enhancement
- *Wash-in vs wash-out*
  - Wash-in = progressive enhancement within region of interest from arrival of microbubbles, to peak enhancement
  - Wash-out = reduction in enhancement which follows peak enhancement

Tips and Tricks

- Curvilinear array is usually transducer of choice for liver CEUS
- May need to lower transducer frequency for better penetration for assessing >12-15 cm or if liver disease is present (cirrhosis)
- Focus should be positioned just deep to lesion for most US scanners
- Gain is usually set very slightly above noise floor so pre-contrast imaging is dark with very mild noise
- When assessing liver lesions, frame rates ≥10 hertz are recommended
- Avoid significant increases in mechanical index (↑MI = ↑microbubble destruction)

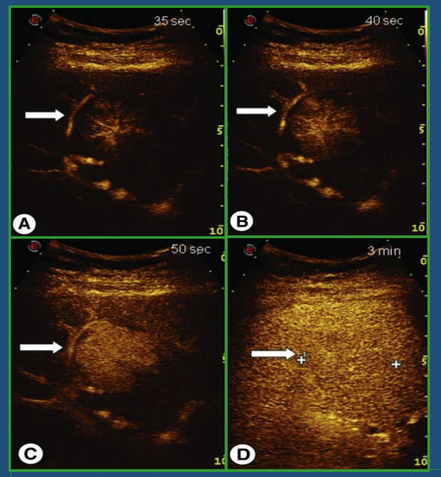

Figure 4 (above): Focal nodular hyperplasia (benign lesion)[7]
CEUS showing central arterial hyper-enhancement (A), rapid filling from center outward (B, C), and iso-enhancement phases (D)

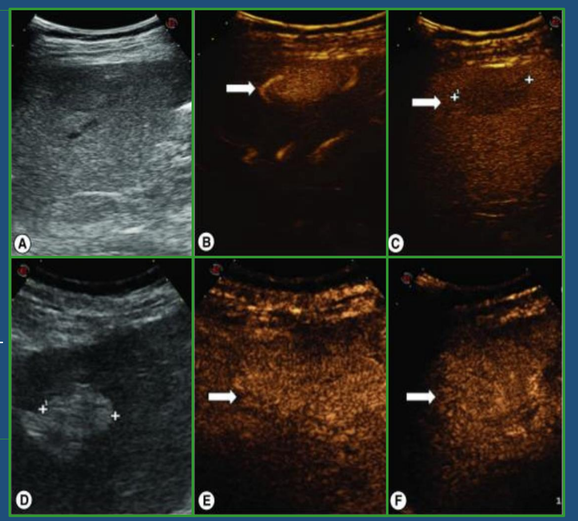

Figure 3 (right): HCC[7]
Gray-scale US showing HCC (A)
CEUS revealing hyper-enhancement in arterial phase (B) and wash-out at hypo-enhancement in late phase at ~2 minutes (C). Atypical vascularity of HCC (D) can be characterized by CEUS as iso-enhancement in the arterial phase (E) and iso-enhancement without washout in the late phase (F)

References

1) Bartolotta TV, Taibbi A, Midiri M, La Grutta L, De Maria M, Lagalla R. Characterisation of focal liver lesions undetermined at grey-scale US: contrast-enhanced US versus 64-row MDCT and MRI with liver-specific contrast agent. *Radiol Med*. 2010;115(5):714-731. doi:10.1007/s11547-010-0506-3
2) Bartolotta TV, Vernuccio F, Taibbi A, Lagalla R. Contrast-Enhanced Ultrasound in Focal Liver Lesions: Where Do We Stand?. *Semin Ultrasound CT MR*. 2016;37(6):573-586. doi:10.1053/j.sult.2016.10.003
3) Dietrich CF, Averkiou M, Nielsen MB, et al. How to perform Contrast-Enhanced Ultrasound (CEUS). *Ultrasound Int Open*. 2018;4(1):E2-E15. doi:10.1055/s-0043-123931
4) Piscaglia F, Bolondi L; Italian Society for Ultrasound in Medicine and Biology (SIUMB) Study Group on Ultrasound Contrast Agents. The safety of Sonovue in abdominal applications: retrospective analysis of 23188 investigations. *Ultrasound Med Biol*. 2006;32(9):1369-1375. doi:10.1016/j.ultrasmedbio.2006.05.031
5) Wu M, Li L, Wang J, et al. Contrast-enhanced US for characterization of focal liver lesions: a comprehensive meta-analysis. *Eur Radiol*. 2018;28(5):2077-2088. doi:10.1007/s00330-017-5152-x
6) Ignee A, Atkinson NS, Schuessler G, Dietrich CF. Ultrasound contrast agents. *Endosc Ultrasound*. 2016;5(6):355-362. doi:10.4103/2303-9027.193594
7) Leoni S, Serio I, Pecorelli A, Marinelli S, Bolondi L. Contrast-enhanced ultrasound in liver cancer. *Hepat Oncol*. 2015;2(1):51-62. doi:10.2217/hep.14.25

DISTAL FEMORAL REPLACEMENT FOR THE TREATMENT OF LOWER EXTREMITY TUMORS: THE EXPERIENCE OF A SINGLE INSTITUTION

C Gusho BS[1], B Clayton MD[1], J Greenspoon MD[1], J Bauer BS[1], M Colman MD[1], S Gitelis MD[1], A Blank, MD, MS[1]

[1]RUSH UNIVERSITY MEDICAL CENTER

Disclosures: Please see AAOS/MSTS list of disclosures.

INTRODUCTION

Modular endoprostheses for limb salvage are commonly performed.

Distal femoral modular endoprostheses are fraught with high rates of complications.[1-2] Some series describe 10 and 20-year survival estimates of 50%.[3-4]

This study sought to determine overall complication rates, revisions, and survival of cases performed within a 15-year period by a single institution to evaluate trends over time.

METHODS

A retrospective review of a prospectively maintained surgical database was performed.

One-hundred one patients who underwent reconstruction of the distal femur using custom expandable or modular endoprostheses were included.

For records with available data, the prosthetic system and manufacturer were noted.

	FREQUENCY	%
Chondrosarcoma	3	3.0
GCTB	7	6.9
MBD	13	12.9
Osteosarcoma	59	58.4
Other/Revision Surgery	18	17.8
Total	**101**	**100.0**

Table 1. Pre-procedure diagnoses. MBD, metastatic bone disease. GCTB, giant cell tumor of bone.

METHODS (continued)

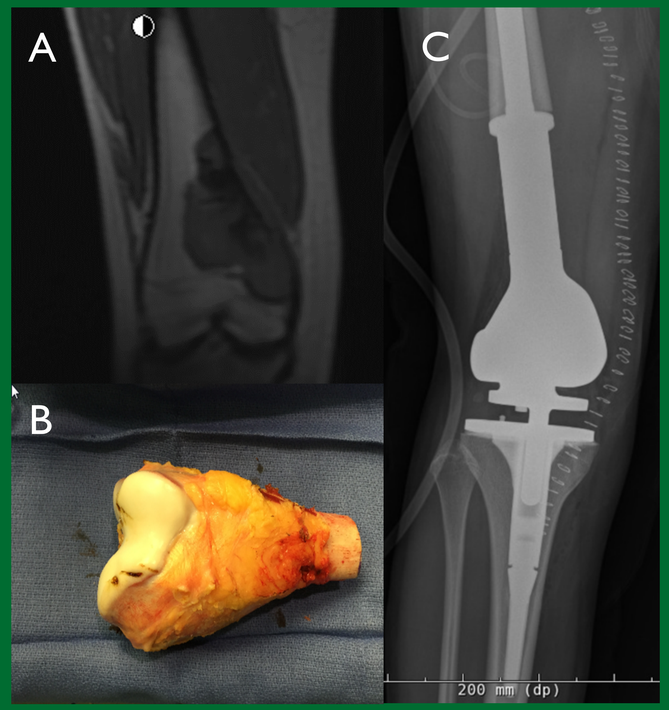

Figure 1. MRI (A) of distal femoral osteosarcoma (B) in a 13-year-old who was reconstructed with a modular endoprosthesis (C).

RESULTS

	FREQUENCY	%
Cemented stem system	79	78.2
Press-Fit stem system	18	17.8
Other/Not recorded	4	4.0
Structural failure*	9 (n=34)	26.5
Aseptic loosening*	8 (n=34)	23.5
Infection*	8 (n=34)	23.5
Patellar revision	5 (n=34)	14.7

Table II. Fixation and revision. Remaining revisions: osteolysis (n=2), metallosis (n=1), and periprosthetic fracture (n=1). *: Henderson Classification.[5]

RESULTS (continued)

- All-cause revision rate was 34% (n=34); Cemented (21 all-cause revisions), Press-Fit (10 all-cause revisions).

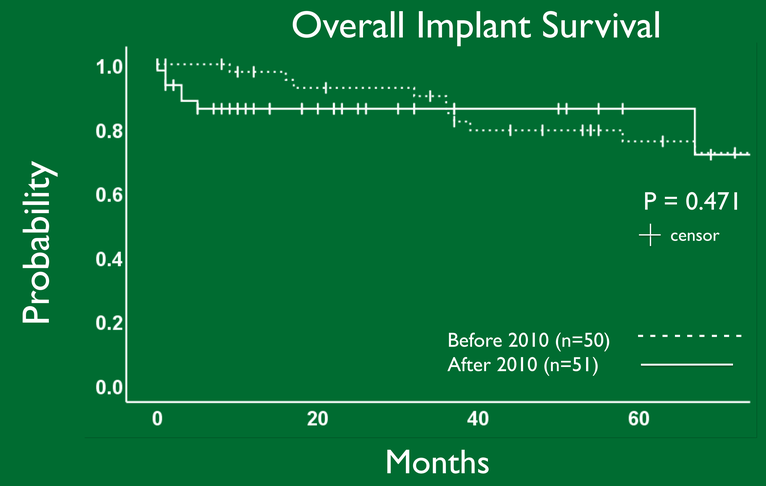

Figure 2. Distal femoral implant survivorship.

SUMMARY

Cases before 2010 had a 5-year survival probability of 75.9% while cases after 2010 had 5-year probability of 86.1%. Cumulative median overall implant survival was 120.9 months.

Despite a reliable and safe procedure and slight implant innovation, rates of revision are high, especially after 5 years duration.

The significant rate of revision surgery is an important factor to discuss during preoperative counseling.

REFERENCES

1. Portney DA, Bi AS, Christian RA, Butler BA, Peabody TD. Outcomes of Expandable Prostheses for Primary Bone Malignancies in Skeletally Immature Patients: A Systematic Review and Pooled Data Analysis. *Journal of Pediatric Orthopaedics*. 2020;40(6):e487. doi:10.1097/BPO.0000000000001459
2. Myers GJC, Abudu AT, Carter SR, Tillman RM, Grimer RJ. Endoprosthetic replacement of the distal femur for bone tumours: long-term results. *The Journal of bone and joint surgery British volume*. 2007;89(4):521–526.
3. Bhangu AA, Kramer MJ, Grimer RJ, O'Donnell RJ. Early distal femoral endoprosthetic survival: cemented stems versus the Compress® implant. *International Orthopaedics (SICOT)*. 2006;30(6):465-472. doi:10.1007/s00264-006-0186-8
4. Jeys LM, Grimer RJ, Carter SR, Tillman RM. Periprosthetic infection in patients treated for an orthopaedic oncological condition. *J Bone Joint Surg Am*. 2005;87(4):842-849. doi:10.2106/JBJS.C.01222
5. Henderson ER, Groundland JS, Pala E, et al. Failure mode classification for tumor endoprostheses: retrospective review of five institutions and a literature review. *J Bone Joint Surg Am*. 2011;93(5):418-429. doi:10.2106/JBJS.J.00834

Durvalumab ± Bevacizumab as Adjuvant Therapy in Patients With HCC at Risk of Recurrence After Curative Therapy: EMERALD-2

Riccardo Lencioni,[1] Jennifer Knox,[2] Ann-Lii Cheng,[3] Sean Cleary,[4] Peter Galle,[5] Norihiro Kokudo,[6] Joong-Won Park,[7] Jian Zhou,[8] Philip He,[9] Shethah Morgan,[10] Gordon Cohen,[9] Jia Fan[8]

[1]University of Pisa School of Medicine, Pisa, Italy; [2]Princess Margaret Cancer Centre, University of Toronto, Toronto, ON, Canada; [3]National Taiwan University, Taipei City, Taiwan; [4]Mayo Clinic, Rochester, MN, USA; [5]University Medical Center Mainz, Mainz, Germany; [6]National Center for Global Health and Medicine, Tokyo, Japan; [7]National Cancer Center, Goyang, South Korea; [8]Zhongshan Hospital, Fudan University, Shanghai, China; [9]AstraZeneca, Gaithersburg, MD, USA; [10]AstraZeneca, Cambridge, United Kingdom

Summary

- The EMERALD-2 study will expand the understanding of the efficacy and safety of durvalumab with or without bevacizumab as adjuvant HCC therapy for patients who are at high risk for recurrence after curative hepatic resection or ablation.

Introduction

- Many patients with early-stage HCC undergo hepatic resection or ablation as standard of care, but while potentially curative, **the risk of cancer recurrence following resection is as high as 44%–79% at 5 years.**[1–3]
- Effective adjuvant therapy has not been identified to date, and the **prevention and/or delay of recurrence of HCC after curative treatment presents a high unmet medical need.**
- Adjuvant therapy given after resection or ablation has the potential to reduce the risk of relapse and is an effective therapeutic approach in the treatment of many solid tumors.
- Encouraging clinical evidence shows that **adjuvant therapy involving agents that engage the immune response can prolong RFS in patients with early-stage HCC.**[4–7]
- In addition, data suggest that **inhibiting the VEGF pathway may enhance activity of programmed death ligand-1 blockade** in patients with more advanced HCC.[8–10]

Methods

- **EMERALD-2 (NCT03847428)** is a Phase 3 randomized, double-blind, placebo-controlled study evaluating the efficacy and safety of durvalumab monotherapy and durvalumab combined with bevacizumab as adjuvant therapy in patients with HCC within 12 weeks of completion of curative hepatic resection or final curative ablation procedure (which may include embolization) who are at high risk of recurrence.
- Following hepatic resection and ablation, approximately 888 patients will be randomized 1:1:1 to Arm A, B, or C (**Figure 1**).

Figure 1. EMERALD-2 study design

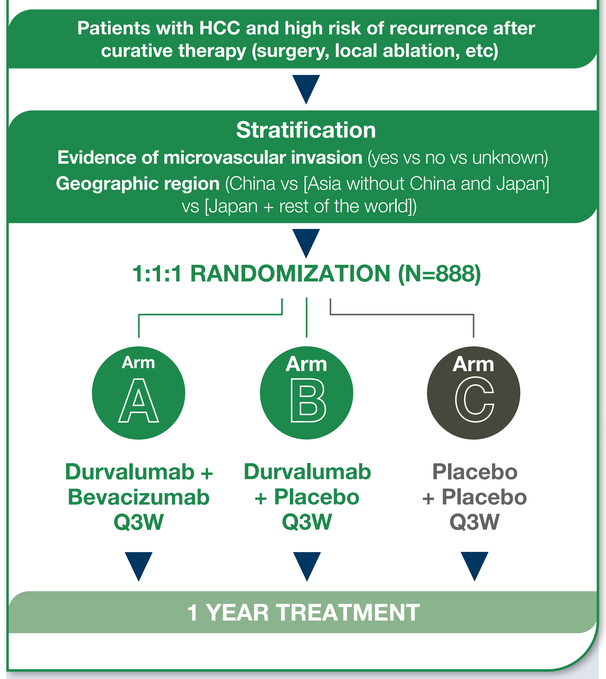

- A tumor tissue sample is mandatory for biomarker analysis.
- Patients with HBV or HCV alone may be enrolled, but patients who are HBV+ must have adequately controlled viral suppression prior to enrollment, and HBV/HCV replication will be monitored during the study and treated if appropriate.
- Patients are required to have an upper endoscopy (or contrast-enhanced cross-sectional imaging) performed within 6 months of randomization; patients with varices at risk of bleeding should be excluded.
- There are currently 18 countries and regions participating in the EMERALD-2 study (**Figure 2**).

Figure 2. EMERALD-2 participating regions

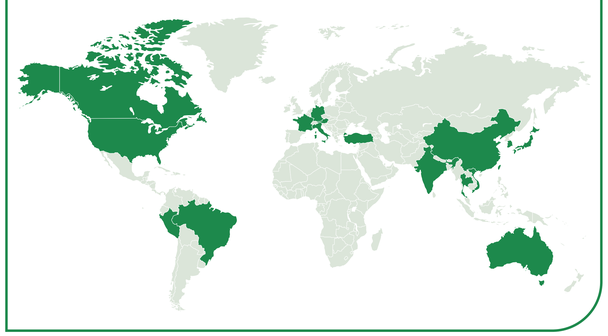

Study Endpoints

1. **Assess RFS of Arm B vs Arm C (by BICR using RECIST v 1.1)**
2. Assess RFS of Arm A vs Arm C (by BICR using RECIST v 1.1)
   - Evaluate 24-month RFS for all arms (by BICR using RECIST v 1.1)
   - Measure time to relapse for all arms (by BICR using RECIST v 1.1)
   - Evaluate overall survival for all arms
   - Investigate the relationship between a patient's baseline PD-L1 expression and efficacy outcomes
   - Assess disease-related symptoms, impacts, and HRQoL for all arms
   - Evaluate safety and tolerability profile of all arms

Key exploratory objectives

- Investigate the association of candidate biomarkers with efficacy measures using blood and tissue samples
- Explore the impact of treatment and disease state on health care utility and resources (EQ-5D-5L, HOSPAD)

Key Inclusion Criteria

- Aged ≥18 years
- Successful completion of curative therapy (resection or ablation) with imaging to confirm disease-free status ≤28 days prior to randomization
- Histologically or cytologically confirmed HCC
- No prior systemic therapy for HCC
- Child-Pugh score of 5 or 6
- ECOG PS of 0 or 1 at enrollment

Key Exclusion Criteria

- Known fibrolamellar HCC, sarcomatoid HCC, or mixed cholangiocarcinoma and HCC
- Any evidence of metastatic, macrovascular invasion, or co-existing malignant disease on baseline imaging
- Evidence of portal vein thrombosis
- Prior systemic anticancer therapy for HCC
- Patients with varices at risk of bleeding
- Patients who are candidates for liver transplantation

References

1. Bruix J, Sherman M. *Hepatology*. 2005;42:1208-1236.
2. Imamura H, et al. *J Hepatol*. 2003;38:200-207.
3. Kianmanesh R, et al. *Surg Oncol Clin N Am*. 2003;12:51-63.
4. Yin J, et al. *J Clin Oncol*. 2013;31:3647-3655.
5. Huang G, et al. *Ann Surg*. 2015;261:56-66.
6. Xu J, et al. *Adv Clin Exp Med*. 2015;24:331-340.
7. Lee JH, et al. *Gastroenterology*. 2015;148:1383-1391.
8. Pishvaian MJ, et al. *Ann Oncol*. 2018;29 (Suppl 8;abstr LBA26).
9. Ikeda M, et al. *J Clin Oncol*. 2018;36 (Suppl;abstr 4076).
10. Finn RS, et al. *N Engl J Med*. 2020;382:1894-1905.

Abbreviations

BICR, blinded independent central review; ECOG PS, Eastern Cooperative Oncology Group performance status; EQ-5D-5L, EuroQol 5-dimension, 5-level, health state utility index; HBV, hepatitis B virus; HCC, hepatocellular carcinoma; HCV, hepatitis C virus; HOSPAD, hospital admission form; HRQoL, health-related quality of life; PD-L1, programmed death ligand-1; Q3W, every 3 weeks; RECIST, Response Evaluation Criteria In Solid Tumors; RFS, recurrence-free survival; VEGF, vascular endothelial growth factor.

Acknowledgments

This study was funded by AstraZeneca. The authors would like to thank the patients, their families and caregivers, and all investigators involved in this study. Medical writing support, which was in accordance with Good Publication Practice (GPP3) guidelines, was provided by Anne-Marie Manwaring of Parexel (Littlehampton, UK) and was funded by AstraZeneca.

Contact Information

gordon.cohen@astrazeneca.com

Presented at the Symposium on Clinical Interventional Oncology I Virtual Meeting I October 2020

Embolization and Sclerotherapy of Recurrent Aneurysmal Bone Cyst that Failed Numerous Operative Interventions

Derrick Tran, M.D., Akram Sadeghi, M.D., Sean Duguay, M.D.

University of Oklahoma Health Sciences Center

The UNIVERSITY of OKLAHOMA Health Sciences Center

Purpose

The purpose of this exhibit is to report and discuss an unusual case of a massive pelvic aneurysmal bone cyst, and to review the treatment approaches to such a lesion.

Materials and Methods

All imaging was reviewed on a PACS workstation and access to the lesion was gained using standard catheter and microcatheter techniques, utilizing a variety of catheters. Embolization was performed using 100-300 um particles. Percutaneous sclerotherapy was performed with sodium tetrodecyl sulfate foam. All information was handled in accordance with HIPAA standards.

Case

This is a 30 year old female who presented with recurrent right hip pain and immobility. Initial imaging showed a massive lytic lesion in the right acetabulum with features compatible with aneurysmal bone cyst. Over the next year she underwent 6 cycles of curettage, chemical ablation, and argon beam coagulation. Unfortunately, followup imaging demonstrated the lesion to actually be growing rather than regressing. At that point, vascular and interventional radiology was consulted for embolization. Transarterial embolization was carried out in two phases separated by approximately 4.5 months apart. Particle embolization was performed initially, which was followed by n-butyl cyanoacrylate (NBCA) glue embolization and sodium tetrodecyl sulfate (STS) foam sclerotherapy. Primary blood supply was from a replaced right obturator artery arising from the inferior epigastric artery. Follow-up imaging demonstrated persistent, but reduced, cyst size.

Results

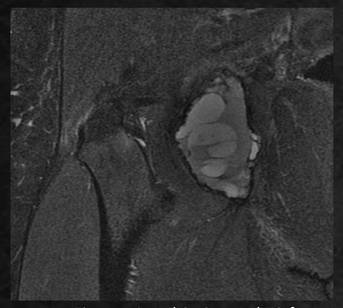

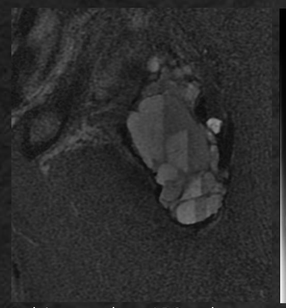

Figures 1 and 2: Coronal T2 fat-saturated images show ABC and characteristic expansive morphology with fluid-fluid levels

Figure 3: Frontal view shows the expansile and lytic right hip lesion

Figure 4: Axial CT shows expansile ABC

Figure 5: Spot angiogram in right obturator artery shows ABC with contrast opacification

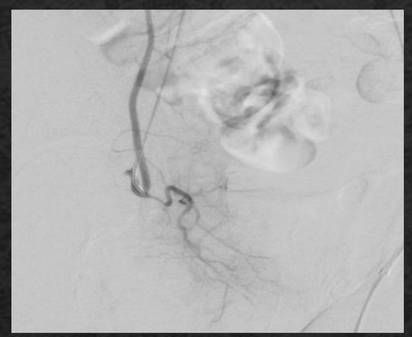

Figure 6: Right obturator artery DSA showing supply to ABC

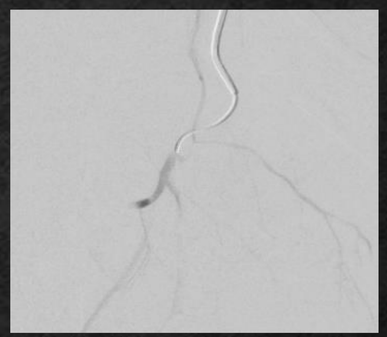

Figure 7: 1st phase embolization; DSA after particle embolization

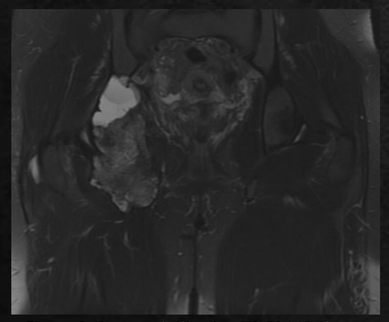

Figure 8: Post-embolization T2 FS MR shows less cystic component

Figure 9: Right obturator artery DSA shows minimal tumor opacification

Figure 10: Spot angiogram shows tumor contrast retention

Figure 11: Post-NBCA embolization spot angiogram

Figure 12: Confirming site of sclerotherapy. Note the cystic area of concern on pre-procedural imaging

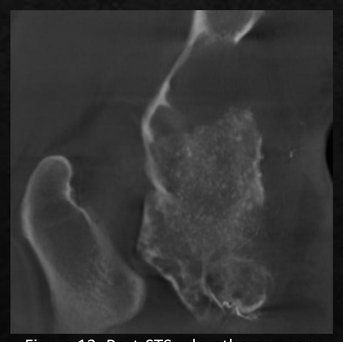

Figure 13: Post-STS sclerotherapy cone beam CT

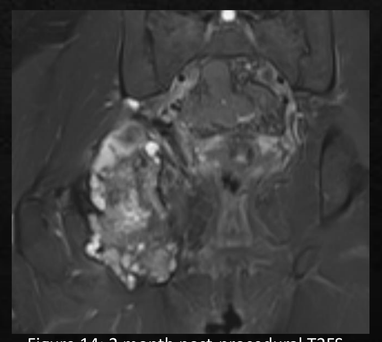

Figure 14: 2 month post-procedural T2FS image shows minimal, but favorable response.

Discussion

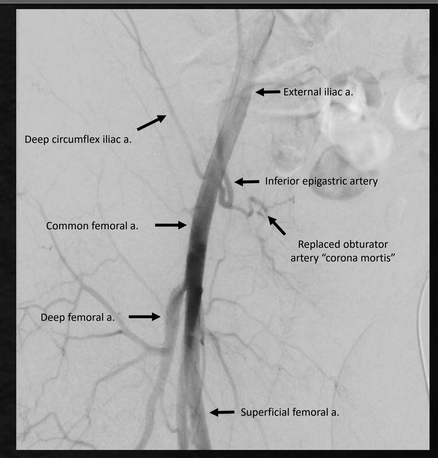

The case highlights the tenacity and difficulty in managing these aggressive, but benign, lesions. Aneurysmal bone cysts are highly vascular and composed of blood and fluid-filled trabeculae lined primarily by giant cells. Their etiology is unknown, but since a portion of these lesions occur secondary to a primary lesions, such as giant cell tumor, non-ossifying fibroma, and osteosarcoma, it is surmised that the destructive nature of ABC's may be related to an uncontrolled osteoclast response.

Similarly, there is debate as to what is the best approach to management for these lesions. Currently, operative management has been the standard of care, yet ABC's may recur in up to 50% of cases. Embolization, ablation, and sclerotherapy can be important adjuncts that may serve to decrease blood flow and osteoclast response. Although the patient had minimal improvement after 2 embolizations and sclerotherapy, the lesion did not grow in size, possibly paving the way for further advances in minimally-invasive treatment options.

An interesting aspect of the case illustrates the replaced right obturator artery, arising from the inferior epigastric artery. This is a common variant, but has important implications in the trauma setting. Pelvic fractures or surgery may injury this artery leading to life-threatening hemorrhage, and is known as the "corona mortis." In conclusion, our patient benefited from the procedure and as our technology evolves, so do our options for these young patients.

References:

1. Wible B. *Diagnostic Imaging*. 2nd ed. Philadelphia: Elsevier; 2018.
2. Mavrogenis A, Rossi G, Rimondi E, Ruggieri P. Aneurysmal bone cyst of the acromion treated by selective arterial embolization. *Journal of Pediatric Orthopaedics B*. 2011;20(5):354-358. doi:10.1097/bpb.0b013e3283453506
3. Batisse F, Schmitt A, Vendeuvre T, Herbreteau D, Bonnard C. Aneurysmal bone cyst: A 19-case series managed by percutaneous sclerotherapy. *Orthopaedics & Traumatology: Surgery & Research*. 2016;102(2):213-216. doi:10.1016/j.otsr.2015.11.016
4. Aneurysmal Bone Cyst of the Pelvis: A Challenge in Treatment: Review of the Literature. *The Internet Journal of Orthopedic Surgery*. 2008;8(1). doi:10.5580/c52
5. Gaillard F. Aneurysmal bone cyst | Radiology Reference Article | Radiopaedia.org. Radiopaedia.org. https://radiopaedia.org/articles/aneurysmal-bone-cyst?lang=us. Published 2020. Accessed September 18, 2020.

Endovascular Management of Atypical Renal Cell Carcinoma Metastases: A Case Series

Derrick Tran, M.D., Akram Sadeghi, M.D. Lindsey Schroeder, B.S., Maha Jarmakani, D.O., Sean Duguay, M.D., Shadi Saleem, M.D., Keri Conner, D.O., William Vanlandingham M.D.

The UNIVERSITY of OKLAHOMA Health Sciences Center

Purpose

The purpose of this exhibit is to discuss several unique cases of renal cell carcinoma metastases involving the musculoskeletal system, and review the endovascular approach to management. Renal cell carcinoma is a highly vascular tumor, and pre-operative intervention may be necessary to decrease morbidity and mortality associated with resection. We also sought to evaluate the suitability of pre-operative embolization to improve patient outcomes.

Materials and Methods

Cases were classified as singular metastasis or multifocal metastases, defined as two or more lesions. Tumor size was recorded for each. Embolization was performed with standard catheter techniques, utilizing various particles and coils. Technical success was defined as minimal tumor opacification post-embolization. Cases were reviewed on a PACS workstation with relevant history and course reviewed using the standard hospital electronic medical record. All information was handled in accordance with HIPAA standards.

Results: Case 1

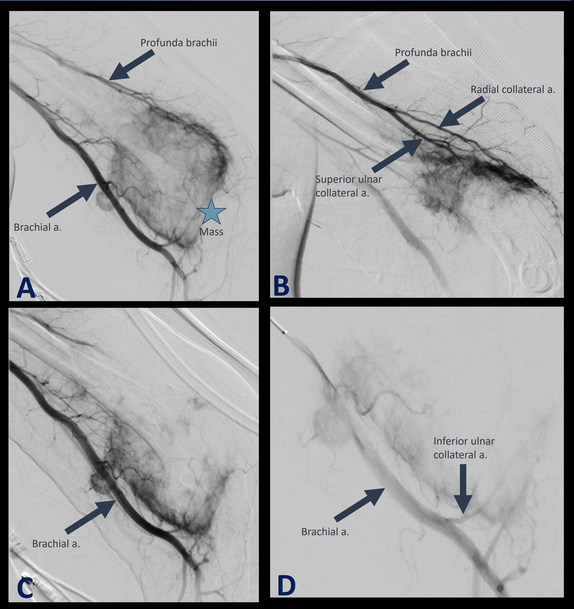

Figure 1: (A) right proximal brachial artery DSA reveals large hypervascular lesion. (B) selective deep brachial DSA. (C) distal right brachial artery DSA with tumor hypervascularity. (D) post-particle embolization DSA shows significantly reduced tumor vascularity. Patient underwent resection and radial nerve reconstruction without major complications, suffering approximately 200 mL blood loss.

Results: Case 2

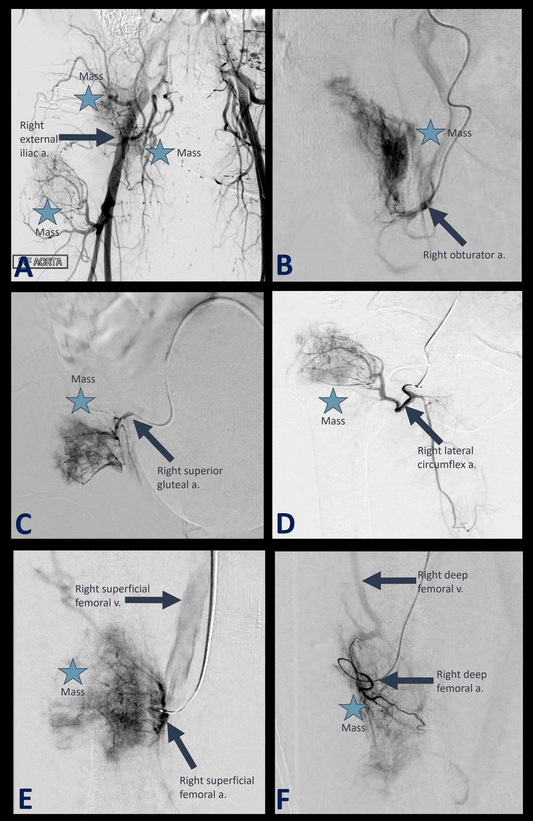

Figure 2: (A) Aortic bifurcation DSA shows multiple hypervascular lesions. (B) Right obturator artery DSA. (C) Right superior gluteal artery DSA. (D) Right lateral circumflex femoral artery DSA. (E) Right distal superficial femoral artery DSA. Note the large AVF created by the lesion. (F) Right deep femoral artery DSA. Again, abnormal AV connection. All of these lesions were embolized, and the patient went to the operating room the following day for intramedullary nailing. The patient suffered no significant complications or blood loss.

Results: Case 3

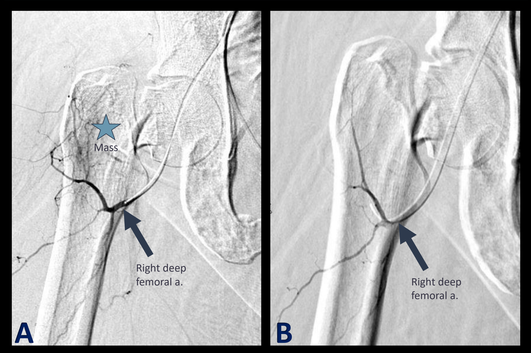

Figure 3: (A) Right deep femoral artery DSA shows lesion in the proximal right femur. Note the pathological femoral neck fracture. (B) Post-embolization DSA shows no significant tumor opacification. Patient went to the operating room for total right hip arthroplasty and suffered only 100 mL blood loss without any significant complications.

Results: Case 4

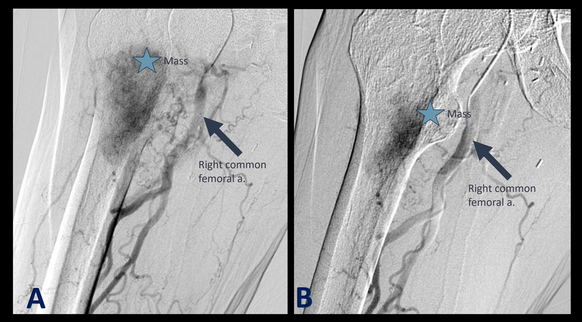

Figure 4: Right common femoral DSA images show hypervascular lesion in the proximal right femur. Patient did not tolerate the therapeutic portion, and proceeded directly to the operating room. Patient experienced 1000 mL of blood loss, and requiring 2units of packed red-blood cells and 3 L of saline fluid resuscitation.

Results: Case 5

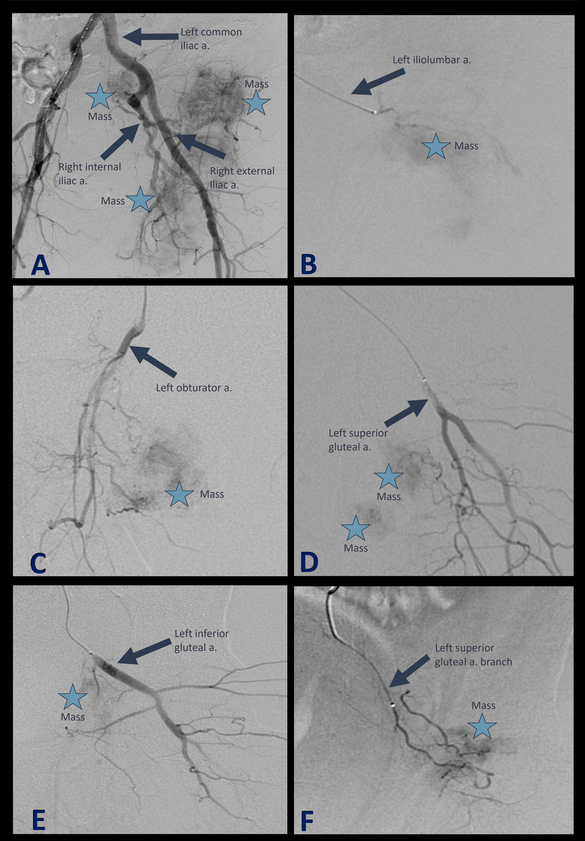

Figure 5: (A) Aortic bifurcation DSA shows massive hypervascular lesion in the left hemipelvis. (B) Left iliolumbar artery DSA. (C) left obturator artery DSA. (D) left superior gluteal artery DSA. (E) left inferior gluteal artery DSA. (F) super selective DSA of a left superior gluteal artery branch. All of these lesions were embolized. Patient went to the operating room for complex left hip arthroplasty with curettage and cementing of the lesion, experiencing approximately 1250 mL of blood loss. The patient did not suffer any significant complications.

Results: Case 6

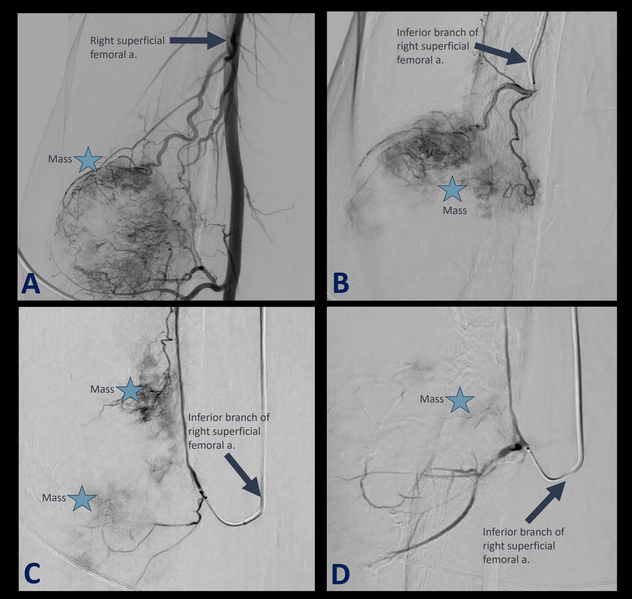

Figure 6: (A) right superficial femoral artery DSA with extensive neovascularity to a large destructive lesion. (B) selective DSA of a superior branch. (C) selective DSA of inferior branch. (D) post-embolization DSA shows minimal tumor opacification. Patient went to operating room for resection and nailing, experiencing approximately 600 mL of blood loss and suffered no significant complications.

Discussion and Conclusion

Renal cell carcinoma is a highly vascular malignancy that often metastasizes to the musculoskeletal system leading to pathologic fractures and increased morbidity. The rich vascular supply generated by these lesions, and their propensity to form arteriovenous connections, elevates the risk of operative mortality. These cases demonstrate the benefits pre-operative embolization plays to reduce blood less. Furthermore, our surgeons reported greater confidence during their surgeries cementing the benefit that vascular and interventional radiologists provide for these patients.

References

1. Chatziioannou AN, Johnson ME, Pneumaticos SG, Lawrence DD, Carrasco CH. Preoperative embolization of bone metastases from renal cell carcinoma. Eur Radiol. 2000;10(4):593-596. doi:10.1007/s003300050969.
2. Gatto L, Facchini G, Saponara M, et al. Successful selective arterial embolizations for bone metastases in renal cell carcinoma integrated with systemic therapies: A case report. Radiol Case Rep. 2017;12(4):775-779. Published 2017 Aug 16. doi:10.1016/j.radcr.2017.07.008.
3. Rossi G, Mavrogenis AF, Casadei R, et al. Embolisation of bone metastases from renal cancer. Radiol Med. 2013;118(2):291-302. doi:10.1007/s11547-012-0802-4.
4. Leenknegt, B., Pesapane, F., & Huang, D. (2019). Pre-Operative Trans-Arterial Embolization of a Hypervascular Bone Metastasis. Journal of the Belgian Society of Radiology, 103(1), 9. DOI: http://doi.org/10.5334/jbsr.1694.
5.Grünwald, V., Eberhardt, B., Bex, A. et al. An interdisciplinary consensus on the management of bone metastases from renal cell carcinoma. Nat Rev Urol 15, 511–521 (2018). https://doi.org/10.1038/s41585-018-0034-9.
6.Ma J, Tullius T, Van Ha TG. Update on Preoperative Embolization of Bone Metastases. Semin Intervent Radiol. 2019;36(3):241-248. doi:10.1055/s-0039-1693120.
7. Errani C, Bazzocchi A, Spinnato P, et al. What's new in management of bone metastases?. Eur J Orthop Surg Traumatol. 2019;29(7):1367-1375. doi:10.1007/s00590-019-02446-y.
8. Ralph K, Christian W, Hanno H, Harald MB, Karin L, Martin B, and Jürgen T. Interventional Management of Hypervascular Osseous Metastasis: Role of Embolotherapy Before Orthopedic Tumor Resection and Bone Stabilization. American Journal of Roentgenology 2008 191:6, W240-W247.

Feasibility and Safety of a Novel Bland Embolization Using Biodegradable Ekobi® Embolization Microspheres in an Office Based Lab

Grigoriy Malyutin, MD[1], Edgar D. St. Amour, MD[2]

1 Department of Diagnostic and Interventional Radiology, University of Arkansas for Medical Sciences, Little Rock, AR, USA
2 Department of Diagnostic and Interventional Radiology, CARTI Cancer Center, Little Rock, AR, USA

INTRODUCTION

Bland intra-arterial embolization has been shown to be of equal overall survival when compared with doxorubicin eluting beads for chemoembolization or Y90 trans-arterial radioembolization. Recent advancements in organic synthesis have shown poly-lactic-co-glycolic acid (PLGA) to be biodegradable within 4-6 months and biocompatible. A novel bland embolization particle, the Ekobi embolization microspheres, uses the FDA-approved PLGA polymer as an embolic agent. Therefore, the purpose of this study was to evaluate the feasibility and safety of using biodegradable Ekobi embolization microspheres in an office based interventional oncology practice.

METHODS

Retrospective chart review of bland embolization utilizing Ekobi microspheres between January and June 2020 in 3 patients who were previously treated with Yttrium 90 and were poor candidates for further radioembolization. Feasibility was defined as a patient tolerating the treatment in an office based lab without requiring hospitalization. Safety was defined as no major adverse events at the time of, and subsequent to, the treatment.

Figure 1.
Spot fluoroscopic image demonstrating catheter directed bland embolization using Ekobi microbeads of the segment 7 hepatic artery.

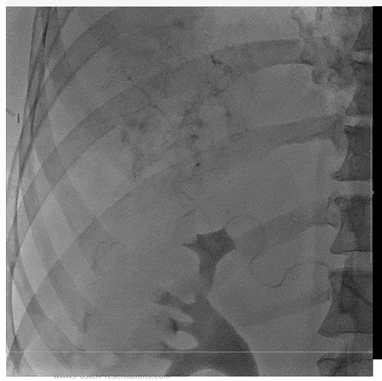

Figure 2.
Post embolization CT image demonstrating contrast uptake within metastatic foci within hepatic segment 7.

RESULTS

All patients were able to undergo bland embolization utilizing Ekobi microspheres in an office based lab without need for hospitalization. Only one patient had post-procedure symptoms, and that was fatigue which lasted approximately 1 week. No patient had any significant post-embolization pain and none developed post-embolization syndrome. No patient had any significant change in their liver function tests, and those with imaging all had stable disease up to 3 months. Two patients had a total of 400 mg of Ekobi microspheres injected, while the third had 800 mg injected. Rudimentary institutional cost data shows Ekobi microspheres cost to be $500, Embozene $205, and Oncozene $1700 per vial.

Figure 3.
Spot fluoroscopic image of microcatheter directed bland embolization using Ekobi microbeads of the replaced right hepatic artery supplying the hyper vascular segment 6 metastatic lesion.

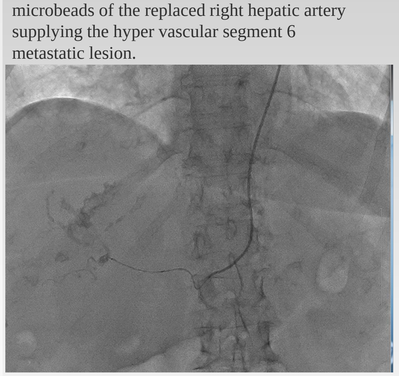

Figure 4.
Post embolization CT image demonstrating successful contrast uptake in segment 6 metastatic lesion.

Figure 5.
Spot fluoroscopic image of micro catheter directed embolization using Ekobi microbeads of the segment 1/7 branch of the right hepatic artery supplying the hyper vascular tumor.

Figure 5.
Post embolization CT image demonstrating contrast uptake in the region of the hepatic segment 1/7 tumor.

Age	Gender	Primary Cancer type	ECOG	Child Pugh Score	Prior Radiation	Prior Chemotherapy	Ekobi Dose
51	F	Breast	0	A	Yes	Yes	400 mg
88	F	Colon Adenocarcinoma	1	A	Yes	Yes	400 mg
80	M	Hepatocellular Carcinoma	2	B8	Yes	No	800 mg

CONCLUSION

Bland embolization using Ekobi embolization microspheres is both safe and feasible when used in an office based lab. There were no major adverse events or need for hospitalization. Ekobi microspheres may be an excellent alternative to other embolization products, and further research is warranted to evaluate response to treatment with comparison to established embolization techniques. When compared to DEB-TACE or radioembolization, bland embolization demonstrates promising cost-savings.

REFERENCES

Makadia HK, Siegel SJ. Poly Lactic-co-Glycolic Acid (PLGA) as Biodegradable Controlled Drug Delivery Carrier. *Polymers (Basel)*. 2011;3(3):1377-1397. doi:10.3390/polym3031377

Brown KT, Do RK, Gonen M, et al. Randomized Trial of Hepatic Artery Embolization for Hepatocellular Carcinoma Using Doxorubicin-Eluting Microspheres Compared With Embolization With Microspheres Alone. *J Clin Oncol*. 2016;34(17):2046-2053. doi:10.1200/JCO.2015.64.0821

Implementing Quality Measure Adjustments of the 2020 Merit-Based Incentive Payment System in the Interventional Radiology Practice.

Muhammad Noor, MD[1]; Eugene Bivins, MD[1]; Ronak Patel, BS[2]; Barbara Manchec, MD[1]; Thomas J Ward, MD[1]

1. Diagnostic and Interventional Radiology - AdventHealth, Orlando, FL
2. UCF College of Medicine

Introduction

The Merit-Based Incentive Payment System (MIPS) is a quality-based payment system proposed by CMS in 2015. MIPS has four essential performance categories, each weighted differently in the payment model: Quality, Cost, Promoting Interoperability, and Practice Improvement. Each year, CMS makes several changes to MIPS. In general, the Quality Measure (QM) category has the highest weight (85%) for most radiology practice. A practice can submit using MIPS Clinical Quality Measures (CQMs) or Qualified Clinical Data Registries (QCDRs). There are several *cross-cutting* measures, those which broadly apply to clinical services, which may be implemented in an IR clinic, as well.

Purpose

1. To provide a brief explanation of Quality Measure scoring
2. To provide IR physicians with high value quality measures
3. To demonstrate the relative importance of IR in meeting radiology performance goals in MIPS.

Quality Measures Explained

- In general – practice submit **6 measures**. Goal is **60 points**
- A measure must have a **benchmark** and have a **non-capped** status to be worth 10 points (6 x 10 = 60)
- **Benchmark –** a specific goal established for a given measure which is broken into 10 deciles. Each decile category gets a certain amount of points (up to 10 points for non-capped measures)
- **Topped-out** – measures with an exceptionally high national median performance rate (≥95%).
- Topped-out measures may be **capped at 7 points** after 2 years of being topped-out. CMS reserves the right to delete topped-out measures after four consecutive years.

No financial disclosures to report

IR Related Measures Worth 10-Points

Measure #	Title	Description
374	Closing the Referral Loop: Receipt of Specialist Report	% patients referred to the IR for which the referring provider receives a note back documenting treatment/diagnosis
404	Anesthesiology Smoking Abstinence	% of smokers who abstain from cigarettes prior to anesthesia on the day of elective surgery or procedure – they must be told day before and can simply be asked y/n the day of
418	Osteoporosis Management in Women Who Had a Fracture	% women (50-85) who suffered a fracture and who either had a DEXA or received treatment for osteoporosis in the six months after the fracture
437	Rate of Surgical Conversion from Lower Extremity Endovascular Revascularization Procedure	Inpatients assigned to endovascular treatment for obstructive arterial disease, % patients who undergo unplanned major amputation or surgical bypass within 48 hours of the index procedure (inverse measure average in 2019 = 1.86%)

Examples of Cross-Cutting Measures Worth 10-Points

Measure #	Title	Description
47	Advance Care Plan	% patients (≥ 65 years) who have an advance care plan or surrogate decision maker documented in the medical record, or the patient did not wish or was not able to name a surrogate decision maker or provide an advance care plan
110	Influenza Immunization	% patients seen between October 1 and March 31 who received an influenza immunization OR who reported previous receipt.
111	Pneumococcal Vaccination for Older Adults	% patients (≥ 65 years) who have ever received pneumococcal vaccine.
112	Breast Cancer Screening	% women (50-74) who had a mammogram to screen for breast cancer in the 27 months prior to the end of the measurement period.
128	Body Mass Index (BMI) Screening and Follow-Up Plan	% patients (≥ 18 years) with abnormal BMI documented during the current encounter or previous 12 months, a follow-up plan is documented during the encounter or during the previous 12 months.
226	Tobacco Use: Screening and Cessation Intervention	% patients (≥ 18 years) who were screened for tobacco use one or more times within 24 months AND who received tobacco cessation intervention if identified as a tobacco user.
317	Screening for High Blood Pressure and Follow-Up Documented	% patients (≥ 18 years) who were screened for high blood pressure AND a recommended follow-up plan is documented based on the current blood pressure (BP) reading as indicated.
236	Controlling High Blood Pressure	% patients (18-85) with diagnosis of hypertension during measurement period and whose most recent blood pressure was adequately controlled (<140/90mmHg) during the measurement period.

DR Related Measures Worth 10-Points

Measure #	Title	Description
225	Radiology: Reminder System for Mammograms	% patients undergoing a screening mammogram whose information is entered into a reminder system with a target due date for the next mammogram
364	Follow-up CT for Incidentally Detected Pulmonary Nodules According to Rec. Guidelines	% of final reports for CT Chest for patients ≥ 18 years with documented f/up recommendations for incidentally detected pulmonary nodules based at a minimum on nodule size AND patient risk factors

QCDR Measures Worth 10-Points (DR)

Measure Code	Title
ACRAD15	Report Turnaround Time: Radiography
ACRAD16	Report Turnaround Time: Ultrasound (Excluding Breast US)
ACRAD17	Report Turnaround Time: MRI
ACRAD18	Report Turnaround Time: CT
ACRAD19	Report Turnaround Time: PET
ACRAD25	Report Turnaround Time: Mammography

Conclusion

In MIPS CQM submissions, only **2** DR measures worth 10-points are available versus **>12** IR related measures. If a practices chooses to submit via a QCDR, there are **6** additional DR related measures worth 10-points.

References/Contact

Muhammad Noor, MD

Cell Phone: (321) 946-6143

Email: Muhammad.Noor.MD@adventhealth.com

Golding LP, Nicola GN, Duszak R, Rosenkrantz AB. The Quality Measure Crunch: How CMS Topped Out Scoring and Removal Policies Disproportionately Disadvantage Radiologists. J Am Coll Radiol. 2020;17(1 Pt B):110-117.

Centers for Medicare & Medicaid Services. 2020 Quality benchmarks. Available at: https://qpp.cms.gov/mips/explore-measures?tab=qualityMeasures&py=2020. Accessed September 8, 2020.

Modified Bland Transarterial Embolization of Hepatocellular carcinoma

Elie Barakat, Bela Kis, Nainesh Parikh, Junsung Choi, Jennifer Sweeney, Ghassan El-Haddad

Department of Diagnostic Imaging and Interventional Radiology, Moffitt Cancer Center, Tampa, Florida, USA

No Disclosures

Purpose

Lipiodol® has been historically used as an emulsifying and microembolic vehicle for delivering chemotherapeutic agents in liver tumors chemoembolization. Recent studies Showed no significant difference between drug-eluting chemoembolization and bland embolization of hepatocellular carcinoma, negating the added benefit of chemotherapy agent. We hypothesized that the benefit of chemoembolization stems from the Lipiodol-based emulsion and not chemotherapy and aimed to evaluate radiographic response and survival of patients with HCC who received a modified bland embolization using Lipiodol-Isovue emulsion and bland particles.

Materials and Methods

From March 2016 to September 2019, 25 patients (22 male, 3 female) with median age of 72.4 years (range:57-90) were treated for HCC (12 BCLC-A, 13 BCLC-B) with transarterial embolization using Lipiodol/Isovue emulsion and bland microspheres. Retrospective review of medical records and imaging was performed to evaluate response to treatment, local hepatic progression free survival (HPFS), and overall survival (OS). Median follow-up was 7.7 months (range:3-26). Survival data was analyzed by Kaplan-Meier method. CTCAE was used to grade adverse events. Radiographic response was evaluated using mRECIST.

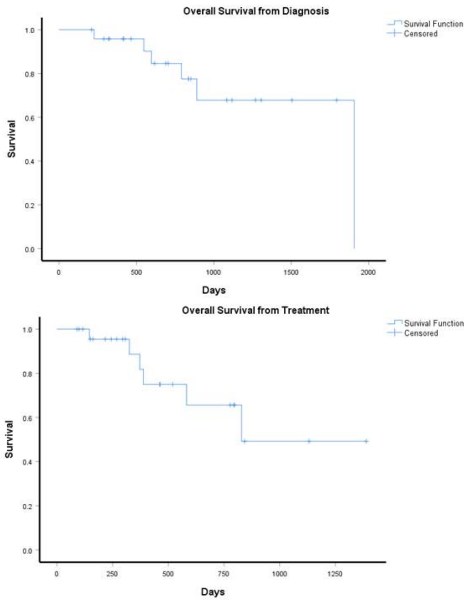

Results

9 patients had unilobar, 15 segmental, and 1 bilobar embolization. 2 patients had prior systemic chemotherapy and17 patients had liver directed therapy before embolization (thermal ablation, radioembolization, and chemoembolization). At 6 months post-treatment 7 of 25 patients had complete response, 4 patients had progressive disease, and 7 partial response. The remaining patients were either lost to follow-up (n=1), died (n=2), or had less than 6-month follow-up (n=4). Median HPFS from embolization was 13 months (95% CI, 1.6-24.3). Median OS from diagnosis and from embolization was 63.5 months and 27.6 months, respectively. All adverse events after embolization were graded 1 or 2.

Work-up angiogram in a 77-year-old male with a biopsy proven well to moderately differentiated Hepatocellular carcinoma.

The tumor was supplied by both anterior and posterior division branches

Since selective radioembolization could not be performed without exposing the rest of the right hepatic lobe to radiomicrospheres, the decision to perform a bland embolization was made

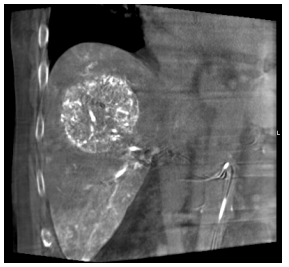

Pre embolization cone-beam CT with injection of contrast in the right hepatic artery

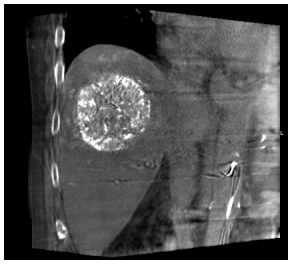

Post embolization cone-beam CT

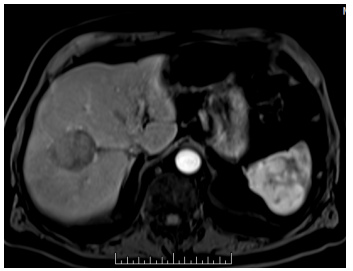

Arterial phase MRI 31 months post embolizations hows a 4cm non enhancing residual mass

Conclusion

Transarterial bland embolization using lipiodol emulsion with microspheres without chemotherapy shows promising preliminary results for the treatment of HCC even in a heavily pretreated population with an efficacy comparable to other intra-arterial therapies.

Overcoming Limitations in the Treatment of Locally Advanced Pancreatic Cancer with Transarterial Microperfusion Utilizing a Novel Dual Balloon Catheter

Barbara Manchec[1], M.D., Ripal Gandhi[2,3], M.D.

[1] Advent Health
[2] Miami Cardiac and Vascular Institute
[3] Miami Cancer Institute

Miami Cancer Institute
BAPTIST HEALTH SOUTH FLORIDA

Miami Cardiac & Vascular Institute
BAPTIST HEALTH SOUTH FLORIDA

AdventHealth

Learning Objectives

Review the current challenges of treating locally advanced pancreatic cancer (LAPC), introduce transarterial microperfusion utilizing a novel dual balloon catheter (RenovoCath), and present early results of patients with LAPC who were treated with intra-arterial (IA) Gemcitabine.

Background

Pancreatic cancer is the 3rd leading cause of cancer mortality in the US, with a median overall survival of only 9-12 weeks [1]. The US alone has over 50,000 new cases per year. There has been little improvement in mortality despite advancements in detection and treatment. LAPC accounts for approximately 30% of pancreatic cancers and includes patients with unresectable tumors (due to vascular involvement) who have not developed distant metastasis. Traditionally, these patients have been treated with intravenous (IV) gemcitabine, however effectiveness is limited by tumor hypovascularity, a dense tumor matrix and systemic side effects/toxicity.

Catheter Mechanics

The RenovoCath (RC-120) is a dual balloon catheter designed to overcome the limitations of drug penetration secondary to tumor hypovascularity. After advancing the catheter into the hepatic, superior mesenteric or splenic artery, the balloons are inflated at the proximal and distal edge of the tumor border. Gemcitabine is then infused by power injection between the balloons causing an IA pressure high enough to diffuse the drug into the adjacent tumor (Figure 1).

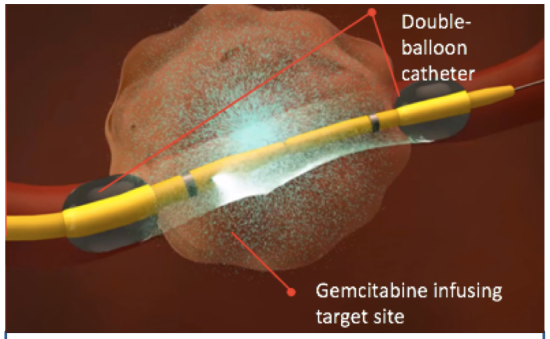

Figure 1. RenovoCath is positioned within the artery with balloons inflated at the proximal and distal aspect of the pancreatic mass. Gemcitabine is then infused under pressure resulting in drug diffusion into the adjacent tumor.

Contact Information

Barbara Manchec
Barbara.Manchec.MD@adventhealth.com
Twitter: @Manchec_MD
Phone: 954-851-2543

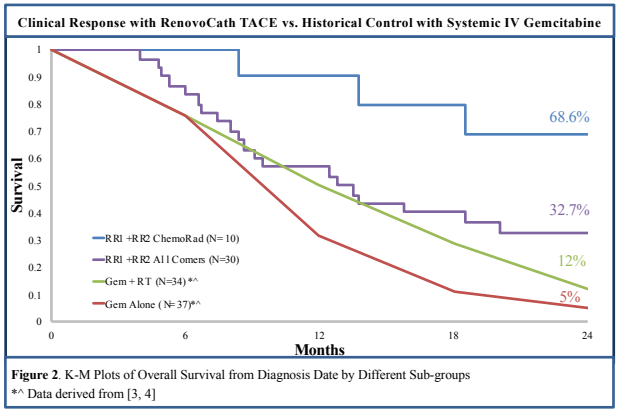

Figure 2. K-M Plots of Overall Survival from Diagnosis Date by Different Sub-groups
*^ Data derived from [3, 4]

Phase I and II Outcomes

In total, 43 patients have been treated with IA gemcitabine using the RC-120 catheter. The initial RRI (safety) study included 20 patients that received dose escalated gemcitabine [2, QR Code], and the following RR2 (registry) study included 25 patients previously treated with radiation that received full dose (1000 mg/m^2) twice monthly treatments (2 patients rolled over). The average number of treatments was 4 (range 1-14). 30% of patients completed the intended 4 cycles of IA therapy.

The median survival of the cohort was 12.4 months. Patients who received prior chemoradiation and had ≥3 IA gemcitabine treatments (n=10) had a 2-year survival of 68.6% and a median survival of 27.8 months (Figure 2). The improved results in this subgroup is believed to be secondary to radiation-induced reduction in microvascular washout.

Teaching Points

IA gemcitabine using the RC-120 catheter to increase drug diffusion demonstrates encouraging early results in treating LAPC, especially in patients who received prior chemoradiation.

RR1 Study

Figure 3. A. Celiac trunk angiogram. B. Splenic artery angiogram with the RenovoCath markers (arrows) distal to the base catheter. C. RenovoCath with proximal and distal inflated balloons (arrows) in the splenic artery. D. Injection through the RenovoCath demonstrates contained contrast between the two balloons.

Future Directions: Phase III

Trans (Intra)-arterial Gemcitabine vs. Continuation of IV Gemcitabine and Nab-Paclitaxel following Radiotherapy for LAPC (TIGeR-PaC) is a prospective, multicenter, phase III randomized controlled trial currently enrolling patients. Primary endpoint is overall survival.

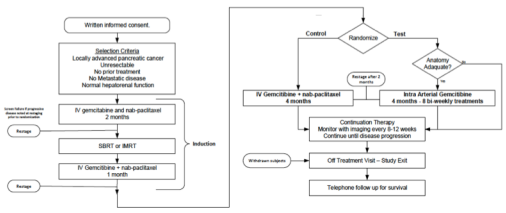

References

1. Ilic, M. and I. Ilic, *Epidemiology of pancreatic cancer.* World J Gastroenterol, 2016. **22**(44): p. 9694-9705.
2. Rosemurgy, A.S., et al., *Safety Study of Targeted and Localized Intra-Arterial Delivery of Gemcitabine in Patients with Locally Advanced Pancreatic Adenocarcinoma.* J Pancreat Cancer, 2017. **3**(1): p. 58-65.
3. Chauffert, B. et al. Phase III trial comparing intensive induction chemoradiotherapy (60 Gy, infusional 5-FU and intermittent cisplatin) followed by maintenance gemcitabine with gemcitabine alone for locally advanced unresectable pancreatic cancer. Definitive results of the 2000-01 FFCD/SFRO study. Annals of Oncology 19, 1592–1599 (2008).
4. Loehrer, P. J. et al. Alone Versus Gemcitabine Plus Radiotherapy in Patients With Locally Advanced Pancreatic Cancer: An Eastern Cooperative Oncology Group Trial. Journal of Clinical Oncology 29, 4105–4112 (2011).

Percutaneous Irreversible Electroporation for Locally Advanced Pancreatic Carcinoma: A Review of Literature

Tushar Garg[1], Jacob Miller, MD[2], Roberto Fourzali, MD[2]

1:Seth GS Medical College & KEM Hospital; 2:Aventura Hospital and Medical Center

INTRODUCTION

- Irreversible electroporation (IRE) is a non-thermal ablative technique that uses high-voltage, low-energy direct current pulses to induce cell death.
- IRE is uniquely suited for this patient population as it is not bound by the same risks as traditional thermal ablative techniques. This poster reviews the available evidence for the use of percutaneous IRE in locally advanced pancreatic carcinoma (LAPC).
- An illustrative review of the technical and clinical aspects of the procedure is provided.

METHODS AND MATERIALS

- A literature search was conducted in PubMed and Google Scholar, and a total of 7 studies were identified and reviewed systematically to determine the number and mean age of patients treated, tumor size before treatment, number of patients treated with radiotherapy and chemotherapy before the procedure, median survival after diagnosis, as well as procedure-related complications, and mortality.

RESULTS

- A total of 264 patients underwent percutaneous IRE for LAPC in these 7 studies.
- The median age of treated patients ranged from 61-68.5 years, and the median tumor size ranged from 3.2- 4.5 cm, 25.28% (n=44) patients underwent radiotherapy before the procedure, and 91.95% (n=174) patients underwent chemotherapy before the procedure.
- The mean overall survival (MOS) of patients from the time of diagnosis ranged from 14- 27.9 months compared to reported MOS of 11 months for patients treated with chemotherapy alone.

Study	Number of Patients (n)	Mean Age of Patients	Median Tumor Size	Prior Radiotherapy (Number of Patient)	Prior Chemotherapy	Complication Rate	Median Survival (in months from diagnosis)	Mortality
Belfiore et al	29	68.5	4.5	Not reported	NA	0	14	0
Mansson et al	24	65	3.5	10	22	45.8	17.9	4
Narayanan et al	50	62.5	3.2	30	50	20	27	6
Leen et al	75	63.4	0	4	75	25	27 from treatment	0
Zhang et al	21	0	3.5	Not reported	Not reported	0	0	Not reported
Scheffer et al	25	61	4	0	13	40	17	0
Ruarus et al	50	61	4	Not reported	Not reported	58	17	4

- The complication rate ranged from 20- 58%, and these include abdominal pain, pancreatitis, hematoma, spontaneous pneumothorax, portal vein thrombosis, and sepsis. The mortality rate in these studies ranged from 0-6%.

PROCEDURE

(A) ceCT of the LAPC in the head of the pancreas (white arrows) and biliary stent (black arrow) prior to IRE treatment.
(B) Axial view of 3 of the 7 needle electrodes in situ.
(C) Coronal view of all 7 needle electrodes in situ. The needles were successfully placed, bypassing all major blood vessels.
(D) Sagittal view of 3 of the 7 needle electrodes in situ.
(E) ceCT directly post IRE treatment. The white arrows depict the outline of the ablated lesion, in which intra-lesional gas pockets are visible (just to the left of the asterisk).
(F) ceCT 24 hours post IRE treatment. The ablated region with hyperattenuating peripheral rim is outlined by the white arrows.

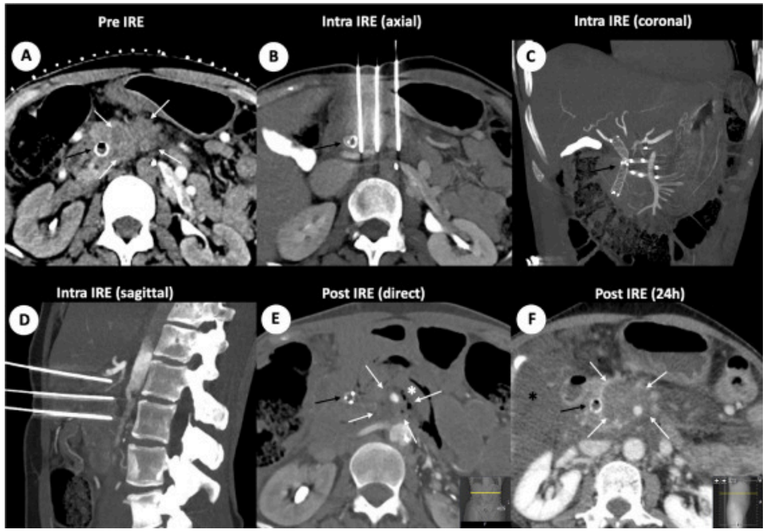

Irreversible electroporation (IRE) for locally advanced pancreatic cancer (LAPC) treatment timeline.

CONCLUSION

- LAPC carries an extremely poor prognosis, with few viable treatment options. IRE is a promising minimally invasive procedure for patients with LAPC, though it carries a high complication rate and should be considered a high-risk procedure.

References

1. Martin RC, McFarland K, Ellis S, Velanovich V. Irreversible electroporation in locally advanced pancreatic cancer: potential improved overall survival. Annals of surgical oncology. 2013 Dec 1;20(3):443-9.
2. Narayanan, G., Hosein, P.J., Beulaygue, I.C., Froud, T., Scheffer, H.J., Venkat, S.R., Echenique, A.M., Hevert, E.C., Livingstone, A.S., Rocha-Lima, C.M. and Merchan, J.R., 2017. Percutaneous image-guided irreversible electroporation for the treatment of unresectable, locally advanced pancreatic adenocarcinoma. *Journal of Vascular and Interventional Radiology*, *28*(3), pp.342-348.
3. Narayanan G. Irreversible electroporation. InSeminars in interventional radiology 2015 Dec (Vol. 32, No. 4, p. 349). Thieme Medical Publishers.

CT guided Microwave Ablation of Primary Peripheral Lung Tumors: A Single-Institution Retrospective Study

Michael E. Nance, PhD[1], Ryan M. Davis, MD[2], Ambarish P. Bhat, MD[2]

[1], School of Medicine, University of Missouri, One Hospital Drive, Columbia, Missouri, USA 65212

[2], Department of Vascular and Interventional Radiology, University of Missouri, One Hospital Drive, Columbia, Missouri, USA 65212

School of Medicine
University of Missouri Health

BACKGROUND

Lung cancer is the second most common cancer in both men and women with 228,150 new cases and 142,670 deaths in 2019. 5-year relative survival remains only 19% for all stages combined **[1]**.

Lung cancer is staged according to the American Joint Committee on Cancer. Stage I (T1-T2aN0M0) lung cancer includes tumors up to size <4cm diameter and/or involving the main bronchus without evidence of nodal or metastatic disease **[2]**.

Lobectomy or sub-lobar resection are currently recommended first-line treatment for local control of stage I tumors. However, a cohort of patients are deemed medically inoperable due to pre-existing conditions and poor lung function while others may refuse surgical intervention.

Stereotactic body radiotherapy (SBRT) is the only percutaneous therapy currently recommended for inoperable early-stage lung cancer; however, complications such as radiation pneumonitis may be undesirable.

Microwave ablation (MWA) may provide an alternative treatment for patients with early stage, inoperable lung cancer not interested in SBRT. However, studies evaluating MWA are limited, demonstrating variable efficacy, inclusivity, and methodology, making meta-analysis challenging. Therefore, further study is needed to bolster the available data on outcomes in patients treated using MWA with the goal of strengthening the pool of evidence for patients and clinicians.

The primary aim of this study was to evaluate the technical success, survival outcomes and complications in patients with primary, peripheral lung cancer treated with MWA at a single, tertiary care hospital.

METHODS

Patient Selection:

Included patients had biopsy proven stage I Non-small cell lung cancer, deemed inoperable by a multidisciplinary team. The maximum axial lesion diameter was 3 cm or less, with a normal coagulation profile (international normalized ratio [INR] ≤ 1.5 and platelets ≥ 50,000/μL) and had completed at least a 3-month follow-up after the ablation.

Computed tomography guided microwave ablation:

Ablations were performed under general anesthesia using the Emprint Ablation System with Thermosphere Technology with a frequency of 2.45 GHz, and a fixed power of 100 W, delivered via an internally cooled 14-G percutaneous antenna. The microwave antenna was placed percutaneously into the target lesion using CT guidance. The duration of ablation was increased in proportion to lesion volume to achieve complete thermal necrosis. Post procedure CT and follow up radiographs were obtained to identify immediate complications that may have needed additional treatment. An initial follow up CT was obtained in the first month after ablation. This was followed by a 3-month PET and subsequently a PET every 6 months until either death /local tumor progression, or for at least 12 months post-procedure.

Statistical Analysis:

The statistical analysis was performed using the data analysis toolkit and statistical functions in Microsoft Excel 2020, Ver. 16.38, for MacOS, IBM SPSS Statistics Ver. 26.0, and SAS Ver. 9.4. Univariate analysis was with Welch's t-test or Fisher's exact test. Cox regression was performed in SPSS. Logistic regression was performed in SAS with a Firth penalized maximum likelihood to correct for small sample size. Summary statistics are expressed as geometric mean ± standard deviation. Significance was established as p <0.05.

RESULTS

Demographics

Table 1. Microwave ablation patient demographics

Parameter	Cases
Gender	n=21
Male	n=10 (47.6%)
Female	n=11 (52.4%)
Age (y)	73.8±8.2 (range:56-87)
Male	72.5±7.5
Female	74.9±9.0
BMI (kg/m^2)	30.1±11.0 (range:19-65)
Male	26.6±7.6
Female	33.4±12.9
Race	
Caucasian	n=19 (90.5%)
Black	n=1 (4.8%)
Asian	n=1 (4.8%)
Prior history of cancer	n=8 (38.1%)
NSC-US	n=1 (4.8%)
PSCC	n=2 (9.5%)
PAC	n=4 (19.0%)
HNSCC	n=1 (4.8%)
Smoking history	n=20 (95.2%)
Avg. PY	52.1±38.6 (range:1-130)
Co-morbidities	
Diabetes	n=5 (23.8%)
CHF	n=1 (4.8%)
HTN	n=15 (71.4%)
CKD	n=2 (9.5%)
HLD	n=13 (61.9%)
A.Fib	n=4 (19.0%)
Obesity	n=12 (57.1%)
Malnutrition	n=2 (9.5%)
CAD	n=6 (28.6%)
OSA	n=6 (28.6%)

Notes: y, year, BMI, body mass index, NSC-US, non-small cell unspecified, PSCC, pulmonary squamous cell carcinoma , PAC, pulmonary adenocarcinoma, HNSCC, head and neck squamous cell carcinoma, PY, pack-years, CHF, congestive heart failure, HTN, hypertension, CKD, chronic kidney disease, HLD, hyperlipidemia, A.Fib, atrial fibrillation, CAD, coronary artery disease, OSA, obstructive sleep apnea

Table 2.Tumor characteristics

Parameter	Cases
Tumor location	n=21
Rt. Apex	n=1 (4.8%)
RUL	n=6 (28.6%)
RML	n=0 (0%)
RLL	n=5 (23.8%)
LUL	n=6 (28.6%)
LLL	n=3 (14.3%)
Tumor Pathology	
PAC	n=7 (33.3%)
PSCC	n=6 (28.6%)
CG	n=1 (4.8%)
NET	n=1 (4.8%)
NSC-US	n=2 (9.5%)
No result	n=4 (19.0%)
Morphology	
Tumor longest Dimension	17.4±5.4 mm
Tumor shortest Dimension	13.1±4.0 mm
Depth from pleura	19.7±15.1 mm

Notes: Rt, right, RUL, right upper lobe, RML, right middle lobe, RLL, right lower lobe, LUL, left upper lobe, LLL, left lower lobe, PAC, pulmonary adenocarcinoma, PSCC, pulmonary squamous cell carcinoma, CG, caseating granuloma, NET, neuroendocrine tumor, NSC-US, non-small cell unspecified

This study evaluated 21 patients (10 male and 11 female; mean age 73.8±8.2 years) with primary lung tumors treated with MWA between January 2013 and August 2019. Patient (**Table 1**) and tumor (**Table 2**) characteristics are presented.

Overall & Progression Free Survival

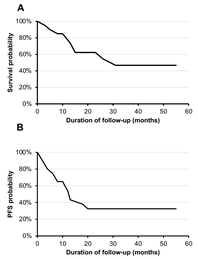

Table 3. Survival probabily post-ablation

Interval in months	OS Probability	PFS Probability
(0-5)	95.1%	95.1%
(5-10)	84.6%	80.4%
(10-15)	67.6%	54.4%
(15-20)	61.8%	33.6%
(20-25)	61.8%	20.8%
(25-30)	54.0%	11.2%
(30-35)	45.7%	5.1%
(35-40)	45.7%	2.3%
(40-45)	45.7%	1.1%
(45-50)	45.7%	0.5%
(50-55)	45.7%	0.2%
(55-60)	45.7%	0.1%

Figure 1 and Table 3: In Figure 1, Kaplan Meier survival curves for **A)** overall survival (OS) and **B)** progression free survival (PFS) are shown. Table 3 shows OS and PFS probability at different time frames post-ablation.

Complications

Table 4. Complications following microwave ablation

Complication	Surviving	Dead	*p*-value
Pneumothorax requiring pleural drain	n=3 (14.3%)	n=2 (9.5%)	0.439
Small parietal hemorrhage	n=1 (4.8%)	n=0 (0%)	

Factors affecting overall survival

Table 5. Cox regression for individual predictors

Parameter	HR (95% CI)	*p*-value
Age (y)		
55-65	ref value 1	0.114
66-75	6.8 (0.7,70.4)	0.108
>76	1.6 (0.2,16.2)	0.707
Female Gender	0.1 (0.03,0.7)	0.014
Smoking history (PY)	1.0 (0.95, 1.01)	0.121
Time to ablation	1.0 (0.99,1.01)	0.950
Tumor longest dim.	1.1 (1.0, 1.3)	0.197
Pred. FVC %	1.0 (0.95,1.04)	0.843
Pred. FEV1 %	1.0 (0.91,1.03)	0.295
FEV1:FVC ratio	0.94 (0.85,1.03)	0.178
Diabetes	1.0 (0.16,6.5)	0.997
CAD	0.7 (0.11,0.4.2)	0.663
CHF	1.8 (0.2,19.1)	0.623
HLD	4.0 (0.8,20.1)	0.091
A. Fib	1.1 (0.18,6.6)	0.937
Obesity	1.1 (0.17,6.6)	0.945
OSA	2.2 (0.5,10.5)	0.327
HTN	1.5 (0.25,9.1)	0.648
CKD	2.5 (0.18,34.8)	0.503

Table 6. Univariate analysis of parameters effects on overall survival

Parameter	Surviving	Dead	*p*-value
Age (y)	73.8±9.6	73.8±6.5	0.994
Female Gender	n=7 (63.3%)	n=4 (36.4%)	0.670
BMI (kg/m^2)	29.9±13.7	30.5±6.7	0.903
Smoking history (PY)	47.5±39.2	52.4±41.3	0.785
Tumor location			0.401
Rt. Apex	n=0 (0%)	n=1 (4.8%)	
RUL	n=4 (19.0%)	n=2 (9.5%)	
RML	n=0 (0%)	n=0 (0%)	
RLL	n=2 (9.5%)	n=3 (14.3%)	
LUL	n=3 (14.3%)	n=3 (14.3%)	
LLL	n=3 (14.3%)	n=0 (0%)	
Tumor pathology			0.226
PAC	n=6 (28.6%)	n=1 (4.8%)	
PSCC	n=3 (14.3%)	n=3 (14.3%)	
CG	n=0 (0%)	n=1 (4.8%)	
NET	n=1 (4.8%)	n=0 (0%)	
NSC-US	n=1 (4.8%)	n=1 (4.8%)	
Tumor longest dimen. (mm)	17.0±3.4	18.0±7.5	0.716
Tumor shortest dimen. (mm)	12.7±3.6	13.7±4.6	0.596
Depth from pleura (mm)	21.1±15.3	17.5±15.7	0.620
Pred. FVC %	84.7±15.2	73±21.6	0.093
Pred. FEV1 %	57.1±19.9	47.3±13.7	0.132
FVC/FEV1 ratio	53.8±19.3	50.9±14.7	0.726
Co-morbidities			0.921
Diabetes	n=1 (4.8%)	n=3 (14.3%)	
CHF	n=0 (0%)	n=1 (4.8%)	
HTN	n=7 (33.3%)	n=6 (28.6%)	
CKD	n=1 (4.8%)	n=1 (4.8%)	
HLD	n=5 (23.8%)	n=7 (33.3%)	
A.Fib	n=1 (4.8%)	n=3 (14.3%)	
Obesity	n=4 (19.0%)	n=5 (23.8%)	
Malnutrition	n=0 (0%)	n=1 (4.8%)	
CAD	n=3 (14.3%)	n=2 (9.5%)	
OSA	n=2 (9.5%)	n=3 (14.3%)	

Tables 5 and 6: Cox regression demonstrated a significant reduction in hazard with female sex. Several co-morbidities were associated with increased hazard including HLD (HR 4.0), OSA (HR 2.2) and CKD (HR 2.5). Univariate analysis (**Table 6**) showed a strong trend towards higher lung function in surviving patients.

Age and Sex adjusted effects on overall survival

Table 7. Age and gender adjusted effects on OS

Parameter	OR (95% CI)	*p*-value
Tumor histology		
Squamous cell carcinoma	ref value 1	
Adenocarcinoma	0.13 (0.005,3.6)	0.175
Non-small cell-unspecified	0.51 (0.013,19.3)	0.936
Neuro-endocrine	0.13 (0.001,32)	0.482
Tumor location		
Left upper lobe	ref value 1	
Left lower lobe	0.18 (0.01,7.0)	0.253
Right upper lobe	0.52 (0.05,5.7)	0.543
Right lower lobe	1.6 (0.13,18.6)	0.607
Pre-ablation lung function		
Pred. FVC %	0.95 (0.89,1.02)	0.155
Pred. FEV1 %	0.96 (0.89,1.03)	0.288
FEV1/FVC ratio	0.99 (0.93,1.07)	0.859
Co-morbidities		
Diabetes	3.8 (0.36,40)	0.268
Coronary artery disease	1.9 (0.20,18)	0.578
Hyperlipidemia	4.3 (0.60,31)	0.145
Atrial fibrillation	3.5 (0.31,38)	0.309
Obstructive sleep apnea	2.3 (0.28,18)	0.443
Obesity	3.1 (0.40,24)	0.279

Table 7: Age and Sex adjusted multivariate analysis did not demonstrate any statistically significant parameters affecting overall survival (OS). Adenocarcinoma and neuro-endocrine histology trended towards improved survival compared to Squamous carcinoma. Similarly, LLL tumors had survival than LUL. The presence of co-morbidities trended towards poorer survival with increased OR. Hyperlipidemia, diabetes, obesity, and atrial fibrillation had >3 fold increased odds of dying.

Table 8: Multivariate analysis was used to look at factors affecting progression free survival (PFS). No factors were statistically significant however, adenocarcinoma and neuro-endocrine histology trended toward improved PFS. Tumor morphology did not have a significant effect.

Table 8. Age and gender adjusted effects on PFS

Parameter	OR (95% CI)	*p*-value
Tumor histology		
Squamous cell carcinoma	ref value 1	
Adenocarcinoma	0.88 (0.06,12.8)	0.419
Non-small cell-unspecified	1.2 (0.03,41.2)	0.902
Neuro-endocrine	0.37 (0.002,90)	0.484
Tumor morphology		
Longest dimension	0.99 (0.82,1.2)	0.915
Depth from the pleura	0.98 (0.93,1.04)	0.522
Smoking pack years	1 (0.98,1.03)	0.631

DISCUSSION

MWA is safe with a high technical success rate. In our study, technical success was defined as complete ablation without residual tumor. The technical success rate observed in this study (85.7%) is comparable to previous studies **[3,4].**

Complications were minimal and predominantly included pneumothorax and small pleural hemorrhages.

MWA overall survival in this study was similar to previous reports of MWA in lung cancer and compares favorably to survival outcomes reported for SBRT and surgery **[5,6]**. Similarly, overall survival was influenced by patient characteristics such as sex, co-morbidities, and lung function prior to the procedure.

Even with surgical resection, Bugge et al. reported a 20% risk of dying due to co-morbidities highlighting the importance of underlying health status regardless of the intervention **[7]**. This suggests that survival may be even further improved in MWA if performed in patients deemed medically fit for surgery.

When adjusting for age and sex, our results suggests tumor histology may contribute to overall survival and progression free survival. Large cell, adenosquamous, and small cell histology typically carry a poor prognosis. There inclusion in this study may have further underestimated survival rates.

Lastly, our results did not demonstrate an effect of tumor dimensions or depth from the pleura on progression free survival. It should be noted that all treated tumors in this study were <3.0cm in size. The literature suggests that 3.0cm is a reasonable cut-off for preventing local recurrence. Unfortunately, there have not been any systematic trials comparing ablation zone margins, tumor dimensions and histology on local recurrence. Further study evaluating the interplay between these parameters may yield standardized protocols based on clinical evidence.

CONCLUSIONS

1) **Microwave ablation is safe, effective and has a high technical success rate**
2) **Complications are minor and typically involves pneumothorax or small amounts of bleeding**
3) **Survival is comparable to outcomes data with SBRT suggesting MWA may be an alterative for patients who are not surgical candidates or elect not to have surgery**
4) **Survival following MWA is impacted by underlying patient characteristics and co-morbidities**
5) **Tumor histology may play a role in survival and local progression. Studies with larger sample sizes are required to further clarify.**

REFERENCES

1. *Siegel et al. Cancer statistics, 2019. CA: A Cancer Journal for Clinicians, (2019), 7-34, 69(1)*
2. Amin MB, Edge SB, Greene FL et al (Eds), AJCC (American Joint Committee on Cancer) Cancer Staging Manual, 8th edition, Springer, Chicago 2017.
3. *Zheng et al. Local efficacy and survival after microwave ablation of lung tumors: A retrospective study in 183 patients. Journal of Vascular and Interventional Radiology, (2016), 1806-1814, 27(12)*
4. *Wolf et al. Microwave ablation of lung malignancies: Effectiveness, CT findings, and safety in 50 patients. Radiology, (2008), 871-879, 247 (3)*
5. Watson RA et al. Is microwave ablation an alternative to stereotactic ablative body radiotherapy in patients withinoperable early-stage primary lung cancer? Interact CardioVasc Thorac Surg 2019;29:539–43
6. Strand et al. Survival after resection for primary lung cancer: apopulation based study of 3211 resected patients. Thorax2006;61:710–715. doi: 10.1136/thx.2005.05648
7. Bugge A et al. Long term survival after surgical resection for non-small cell lung cancer. *European Respiratory Journal, (2017), PA4292*

Percutaneous Thermal Ablation and Cementoplasty for Painful Extra-Spinal Osseous Lesions: Case Examples and Review

Matthew Moccia, DO[a], Christian Sleeper, BA[a,b], Joseph Gerding, MD[a] and Ethan Dobrow, MD[c]

a - Maine Medical Center, Portland, Maine; b – Tufts University School of Medicine, Boston, Massachusetts; c - Veterans Affairs Maine Healthcare System, Augusta, Maine

Purpose/Introduction

As the prevalence of cancer increases along with the life expectancy of cancer patients, so too does the number of patients with painful osseous metastatic lesions. Numerous treatment strategies for extra-spinal osseous metastases exist including radiation therapy (RT), open surgery, and minimally invasive procedures. However, the effectiveness of RT may be constrained by dose limitations and radio-resistant tumors. Pain relief may also be delayed or inadequate with RT alone. Open surgical excision and fixation is often morbid or not feasible. Through a series of case examples we will discuss the minimally invasive percutaneous options available including radiofrequency ablation (RF), microwave ablation (MWA), and cryoablation when either used in isolation or in combination with cementoplasty utilizing polymethyl methacrylate (PMMA).

Methods

We include three case examples of patients with extra-spinal osseous metastatic lesions treated with combination thermal ablation and cementoplasty. Case 1: A 64 year-old male with a history of metastatic renal cell carcinoma status post right nephrectomy with a recurrence of a painful distal femoral osseous lesion at the site of prior palliative RT. Case 2: An 89 year-old male with a history of melanoma and new lung mass with a painful, lytic rib lesion and worsening pleurodynia. Case 3: A 77 year-old male with newly diagnosed esophageal adenocarcinoma and painful left iliac metastasis preventing ambulation.

Case #1 – Metastatic Renal Cell Carcinoma

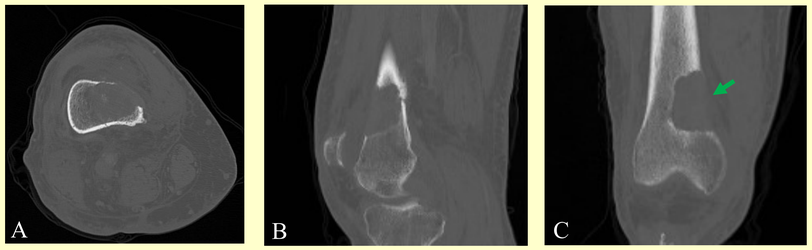

Non-contrast images of the right distal femur (***A-C***). ***A,*** Axial image of the right femur demonstrates a lytic lesion within the distal femoral diaphysis. ***B***, Sagittal reformatted image clearly demonstrates destruction of the anterior cortex of the distal femur. ***C***, Coronal reformatted image shows the lesion extending to the medial margin of the femoral diaphysis with destruction of the medial cortex (**green arrow**).

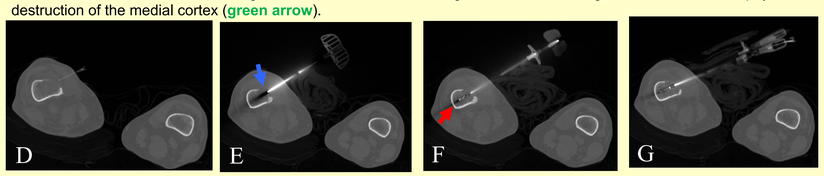

Intraprocedural CT fluoroscopic images (***D-K***) from combined radiofrequency ablation and cementopasty. ***D,*** Utilizing a 25G needle, the subcutaneous tissues were anesthetized with lidocaine. ***E***, Two 11G access trocars, were slowly advanced with the tip of each positioned at the margin of the destroyed medial cortex (**blue arrow**). ***F***, A drill was then advanced to within 0.5 cm of the lateral cortex (**red arrow**). ***G***, Two OsteoCool™ RF ablation probes were then advanced into the femoral lesion and 15 minutes of thermal ablation was performed to target temperature per IFU.

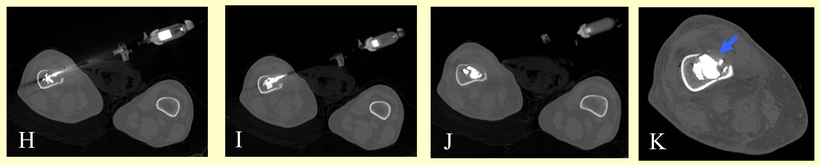

H-J, The ablation probes were then removed and PMMA was then slowly instilled through the trocars utilizing the Medtronic Kyphon® Cement Delivery System. ***K***, The trocars were then removed and a final CT fluoroscopic image revealed excellent cement fill within the right femoral lesion without extracortical extrusion (**blue arrow**).

Results

Case 1: OsteoCool™ RF ablation probes (Medtronic, Minneapolis, MN) were placed under CT fluoroscopic guidance and ablated to target temperature and time per IFU, followed by cementoplasty. Case 2: A cryoprobe (Endocare, Austin, TX) was advanced into the left sixth rib lesion using CT fluoroscopy. Three freeze cycles were performed, per IFU. Intra-procedural images demonstrating complete coverage of the ice ball. Case 3: A PR 15 NeuWave™ MWA probe (Ethicon, Somerville, NJ) was inserted into the left iliac bone under CT fluoroscopic guidance with two overlapping zones treated with 3 cycles at 40W until 105 ^{oC} achieved, followed by cementoplasty.

Case #2 – Metastatic Melanoma

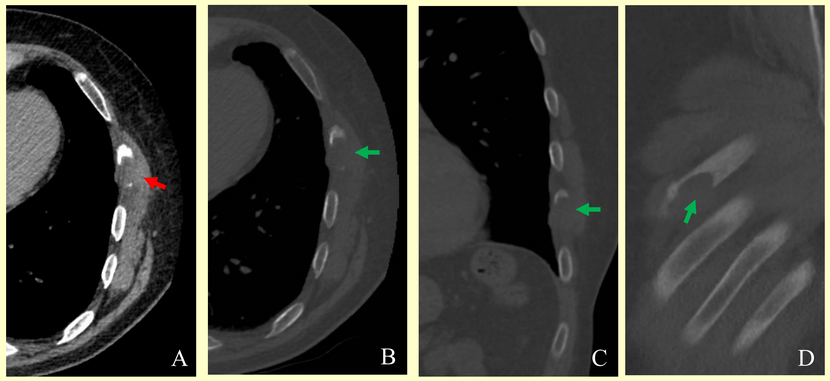

Non-contrast images of the chest (***A-D***). ***A,*** Axial image (soft tissue window) of the left chest wall reveals a lytic lesion involving the left lateral sixth rib with a prominent soft tissue component (**red arrow**). ***B-D***, Axial, coronal and sagittal images (bone window) demonstrates the lytic left lateral sixth rib lesion with near circumferential destruction of the cortical margins (**green arrows**).

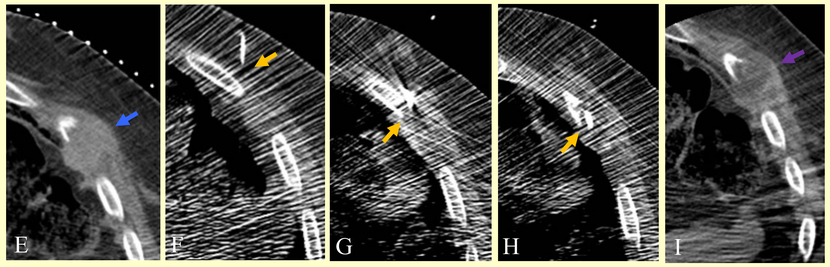

Intraprocedural CT fluoroscopic images (***E-I***) from CT-guided cryoablation. ***E,*** Initial axial image of the left chest wall demonstrates the lytic lesion involving the left lateral sixth rib (**blue arrow**). A metallic grid was used to determine the skin entry site. ***F-G***, Utilizing CT guidance, a cryoprobe was slowly advanced into the lesion. In this case, the rib is used as a cantilever to angle the cryoprobe along the long axis of the lesion in order to maximize ice ball coverage (**orange arrows**). Following three freeze cycles, post-cryoablation images were obtained and revealed complete coverage of the lesion with the ice ball (**purple arrow**).

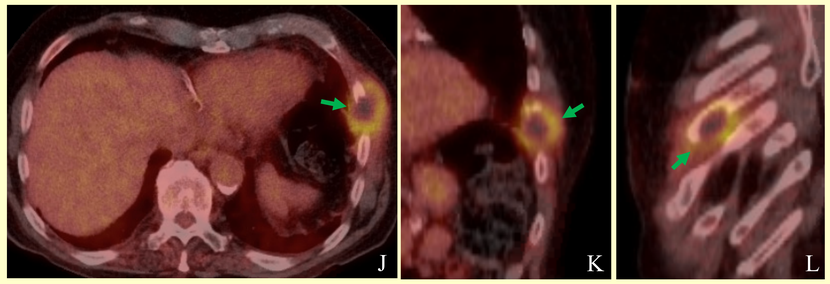

Follow-up PET-CT (***J-L***) obtained one week following CT-guided cryoablation. ***J-L***, Axial, coronal and sagittal images demonstrate post-treatment changes within the left lateral sixth rib with a photopenic center and a thin rib of increased FDG uptake surrounding the lesion (**green arrows**).

Case #3 – Metastatic Esophageal Cancer

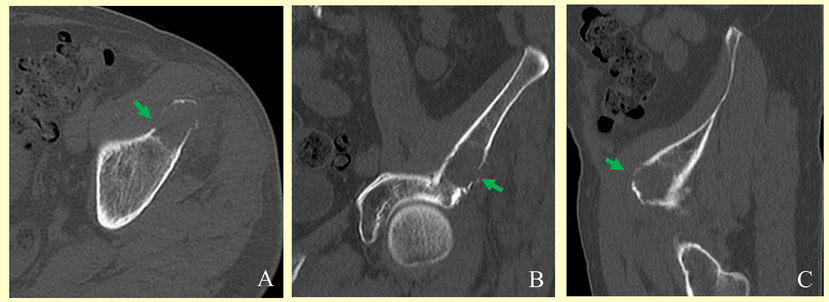

Non-contrast axial (A), coronal (B), and sagittal (C) images of the left iliac bone demonstrate a lytic bone lesion with cortical thinning and breakthrough of the anterior, medial, and lateral margins (**green arrows**).

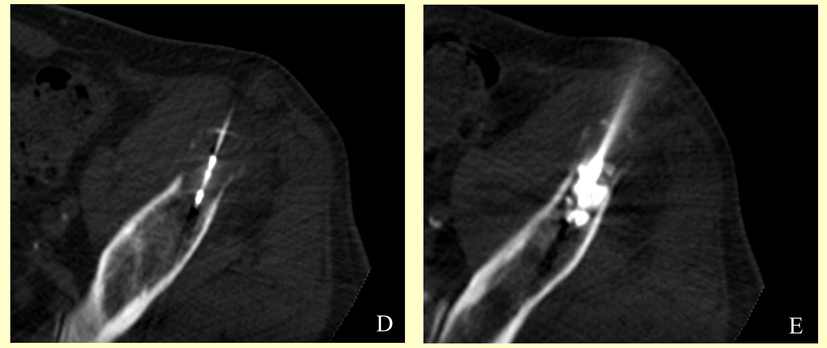

Intraprocedural CT fluoroscopic images (***D-E***) from combined microwave ablation and cementopasty. ***D,*** Given the lytic nature of the mass, the PR 15 MWA probe was easily advanced into the lytic mass without the use of any bone access needle. Ablation was performed at 40W until a temperature of 105^{oC} was achieved. Three cycles were performed with 1-minute intervals between ablations. Two overlapping ablation zones were utilized to ensure coverage of the entire metastasis. ***E***, A 13-gauge Murphy M2 needle (IZI Medical, Ownings Mills, MD) was inserted into the ablated mass and Kyphon HV-R PMMA cement (Medtronic, Minneapolis, MN) was injected with Medallion polycarbonate syringes (Merit Medical, Jordan, UT) under intermittent CT fluoroscopic guidance. The patient was pain free and completely ambulatory immediately following the procedure.

Conclusion

Painful osseous metastases represent a challenging clinical entity for which multiple treatment options are available. Percutaneous thermal ablation when used in isolation or in combination with cementoplasty offers a safe and effective alternative therapeutic modality.

References

1. Catena, V., Roubaud, G., Crombe, A., Kind, M., Palussiere, J. and Buy, X., 2018. Image-Guided Bone Consolidation in Oncology. *Seminars in Interventional Radiology*, 35(04), pp.221-228.
2. Cornelis, F., Tutton, S., Filippiadis, D. and Kelekis, A., 2017. Metastatic Osseous Pain Control: Bone Ablation and Cementoplasty. *Seminars in Interventional Radiology*, 34(04), pp.328-336.
3. Deib, G., Deldar, B., Hui, F., Barr, J. and Khan, M., 2019. Percutaneous Microwave Ablation and Cementoplasty: Clinical Utility in the Treatment of Painful Extraspinal Osseous Metastatic Disease and Myeloma. *American Journal of Roentgenology*, 212(6), pp.1377-1384.
4. Gjorgjievska, A., Thivolet, A., Bouhamama, A., Cuinet, M., Pilleul, F., Tselikas, L., de Baère, T., Deschamps, F. and Mastier, C., 2018. Musculoskeletal Metastases Management: The Interventional Radiologist's Toolbox. *Seminars in Interventional Radiology*, 35(04), pp.281-289.
5. Kurup, A., Callstrom, M. and Moynagh, M., 2018. Thermal Ablation of Bone Metastases. *Seminars in Interventional Radiology*, 35(04), pp.299-308.
6. Tomasian, A., Madaelil, T., Wallace, A., Wiesner, E. and Jennings, J., 2020. Percutaneous thermal ablation alone or in combination with cementoplasty for renal cell carcinoma osseous metastases: Pain palliation and local tumour control. *Journal of Medical Imaging and Radiation Oncology*, 64(1), pp.96-103.
7. Tselikas, L., Gravel, G., de Baère, T., Deschamps, F. and Yevich, S., 2018. Percutaneous Cement Injection for the Palliative Treatment of Osseous Metastases: A Technical Review. *Seminars in Interventional Radiology*, 35(04), pp.268-280.

Pitfalls in Interpreting Post Radioembolization Imaging – What the Interventional Radiologist Needs to Know

Eugene Bivins Jr, MD, Muhammad Noor MD, Christopher Smith MD, Grant Webber MD, Thomas J. Ward MD, Francisco Contreras MD, Barbara Manchec MD

INTRODUCTION

Over the last 20 years, transarterial radioembolization (TARE) has become increasingly used to treat hepatocellular carcinoma (HCC), cholangiocarcinoma, and hepatic metastasis from colorectal cancer or neuroendocrine tumors[1]. Unlike other transarterial or locoregional therapies, TARE induces both embolic and radiation changes which can result in more variable post-treatment imaging findings [1,2]. We review the post-TARE imaging findings with emphasis on common imaging interpretation pitfalls.

MATERIAL AND METHODS

The findings presented are based on experience of the investigators and review of the literature. A series of patients treated with TARE at a single institution were identified. Post-TARE imaging was reviewed to identify common post-treatment tumor and liver parenchymal changes.

AUTHOR INFORMATION

Contact Information

Email: Eugene.bivinsjr.md@adventhealth.com
Phone: 727-709-1730

Affiliation

Department of Radiology
Advent Health Medical Group/Central Florida Division
601 E. Rollins, Orlando, FL 32803

CASE 1

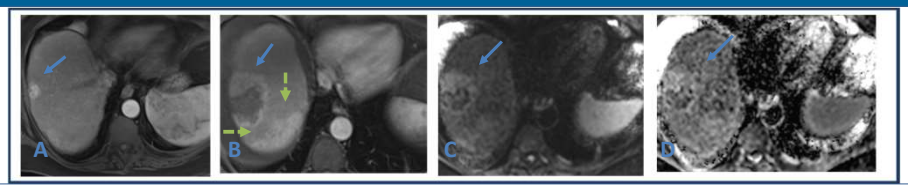

A) Axial T1+C pre-treatment HCC lesion (arrow), other segment VI lesion not shown. B) Axial T1+C 1-month post-TARE demonstrating enlarged hypoenhancing lesion zone w/ thickened perilesional enhancement (blue arrow) corresponding with surrounding edema and granulation tissue formation, increased ill-defined parenchymal enhancement representing post-treatment inflammation (green arrow) of not shown second lesion. Post-TARE 1-month diffusion imaging, C) DWI and D) ADC does not demonstrate restricted diffusion.

CASE 2

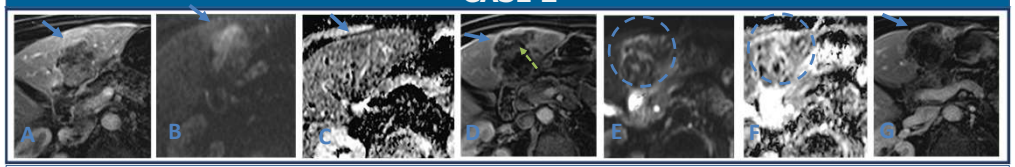

A) Axial T1+C 1-min Sub pre-treatment HCC lesion (arrows) demonstrating heterogenous washout, DWI (B)and ADC (C) imaging demonstrates mild diffusion restriction (arrow). D) Axial T1+C 1-min Sub 6 weeks post-TARE hypoenhancing lesion w/ scattered areas of nodular enhancement (green arrow) and perilesional enhancement (blue arrow), DWI (E) and ADC (F) imaging demonstrating no diffusion restriction (arrow). G) Axial T1+C 1-min Sub 3 weeks post-TARE hypoenhancing treatment zone demonstrating mild size reduction w/ associated capsular contraction and decreased perilesional enhancement (arrow).

CASE 3

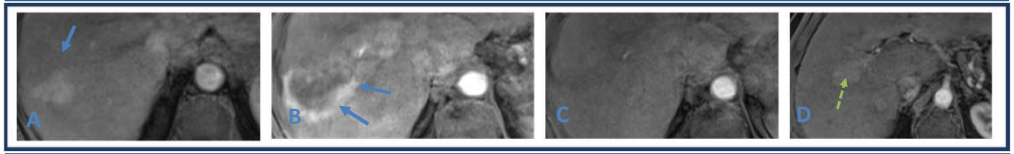

A) Axial T1+C pre-treatment HCC (arrows). B) Axial T1+C 5-weeks post-TARE shows enlarged hypoenhancing treatment zone w/ perilesional enhancement (arrow). C) Axial T1+C 5-mon post-TARE demonstrates decreased perilesional enhancement (arrow). D) Axial T1+C 16-mon post-TARE new enhancing lesion at the inferior margin of treatment zone (green arrow).

CASE 4

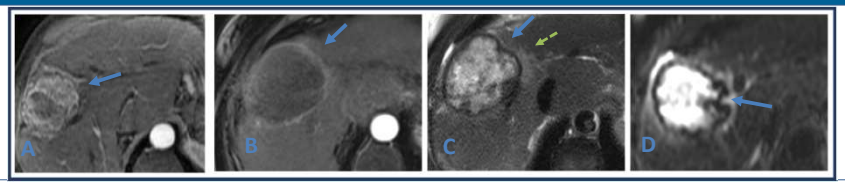

A) Axial T1+C pre-treatment HCC (arrows). B) Axial T1+C 3-months post-TARE mild enlarged hypoenhancing lesion zone w/ thin perilesional enhancement (arrow) and C) Axial T2FS 3-months post-TARE demonstrates central heterogenous T2 signal and hypointense perilesional rim (blue arrow) with adjacent edema (green arrow), corresponding to post-TARE necrosis with surrounding granulation tissue. D) Granulation tissue demonstrates absent signal on DWI (blue arrow).

DISCUSSION

The most common pitfalls in interpreting post-TARE imaging changes are a result of peritumoral edema, inflammation, ring enhancement, hemorrhage, or fibrosis. This can lead to underestimating treatment response or overestimating tumor progression (i.e. pseudoprogression) especially in the early post-treatment period[1]. Understanding the pretreatment imaging characteristics of the tumor, such as vascularity, can reduce posttreatment interpretation errors. Treatment effectiveness cannot be interpreted based on lesion size alone. Treatment response in hypervascular tumors should be interpreted based on intratumoral enhancement patterns, perilesional posttreatment inflammation or ring enhancement[3]. Treatment response of hypovascular tumors is based on lesion size and intratumoral changes in attenuation or signal intensity. Diffusion-weighted imaging (DWI) is helpful to determine early response to treatment, especially in hypovascular tumors[1].

CONCLUSION

Understanding the post-radioembolization imaging findings is crucial to avoiding interpretation errors that could potentially result in suboptimal patient outcomes.

REFERENCES

1. Spina, J. C., Hume, I., Pelaez, A., Peralta, O., Quadrelli, M., & Monaco, R. G. (2019). Expected and Unexpected Imaging Findings after 90Y Transarterial Radioembolization for Liver Tumors. RadioGraphics, 39(2), 578-595. doi:10.1148/rg.2019180095
2. Ibrahim, S. M., Nikolaidis, P., Miller, F. H., Lewandowski, R. J., Ryu, R. K., Sato, K. T., . . . Salem, R. (2008). Radiologic findings following Y90 radioembolization for primary liver malignancies. Abdominal Imaging, 34(5), 566-581. doi:10.1007/s00261-008-9454-y
3. Lencioni, R., & Llovet, J. (2010). Modified RECIST (mRECIST) Assessment for Hepatocellular Carcinoma. Seminars in Liver Disease, 30(01), 052-060. doi:10.1055/s-0030-1247132

Pitfalls of Single-Photon Emission Computed Tomography Imaging for Yttrium-90 Planning: What the Interventionalist Should Know

Jafroodifar A, Goel A, Thibodeau R, Deshmane S, Mirchia K, Jawed M
Department of Radiology, SUNY Upstate Medical University, Syracuse NY

CIOctober 2020 ONLINE
Symposium on Clinical Interventional Oncology

UPSTATE MEDICAL UNIVERSITY

PURPOSE:

To explore the importance of single-photon emission computed tomography (SPECT) imaging artifacts, including misregistration and motion, that Interventional Radiologists (IR) should be aware of to properly manage patients and minimize unnecessary radiation and procedural risks.

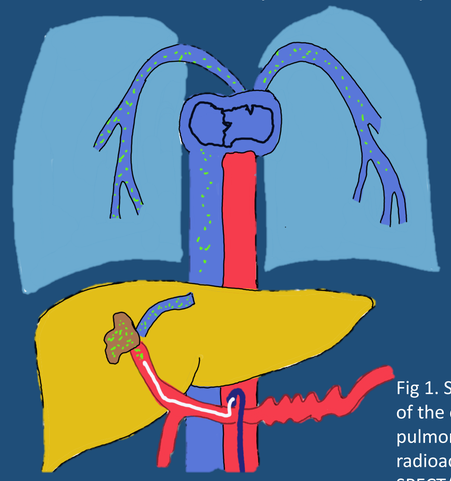

Fig 1. Schematic outline of the concept of hepatic-pulmonary shunting of radioactive particles. SPECT/CT is used to predict percentage of shunting from liver to lung. Original drawing.

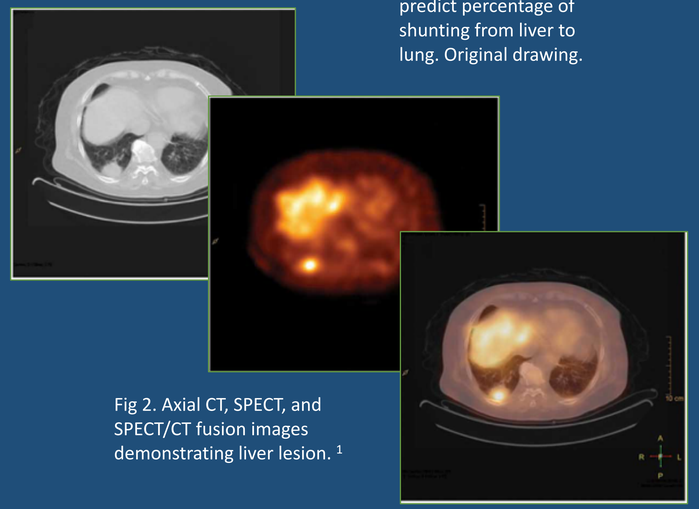

Fig 2. Axial CT, SPECT, and SPECT/CT fusion images demonstrating liver lesion. [1]

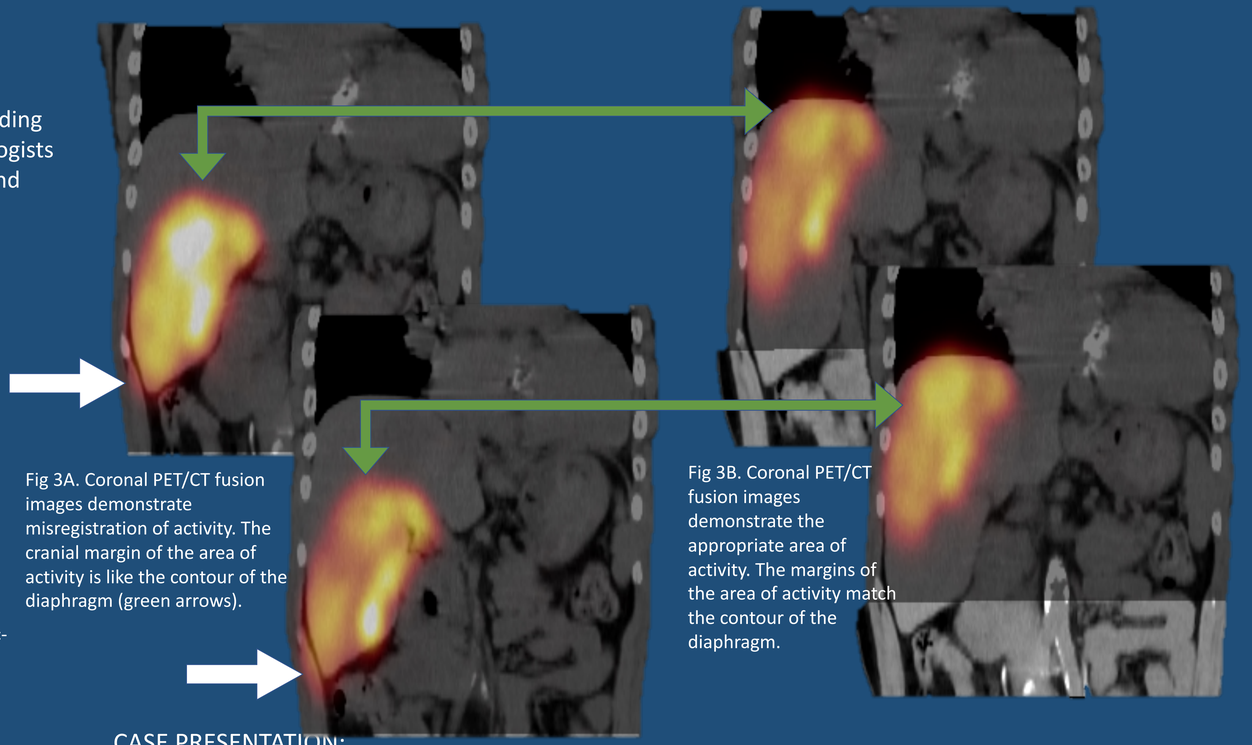

Fig 3A. Coronal PET/CT fusion images demonstrate misregistration of activity. The cranial margin of the area of activity is like the contour of the diaphragm (green arrows).

Fig 3B. Coronal PET/CT fusion images demonstrate the appropriate area of activity. The margins of the area of activity match the contour of the diaphragm.

CASE PRESENTATION:

A 56-year-old male patient who presented for Yttrium-90 (Y90) mapping procedure in preparation radioembolization for metastatic melanoma affecting segments 7 and 8 of his liver. Super-selective cannulation of segment 7 and 8 branches of the right hepatic artery and administration of 99-technetium macroaggregated albumin (tech-MAA) was performed. Post-procedural fused SPECT/CT images demonstrated tech-MAA activity within segments 5 and 6 (Fig 1A); erroneous administration and non-targeted injection of tech-MAA was feared. The patient was prepared for a second angiogram and administration of tech-MAA.

Prior to a second angiogram, further evaluation of the coronal and sagittal reformatted SPECT/CT images revealed areas of activity within the body wall adjacent to the right lateral edge of the liver (white arrows in Fig 3A). Also, the superior contour of the area of activity on coronal images showed a striking similarity to the contour of the diaphragm (green arrows in Fig 3A and 3B). The combination of findings were suggestive of a misregistration artifact leading to the relative caudal fusion of SPECT images with the CT images. It was decided to re-image the patient in order to confirm the suspicion as opposed to a second angiogram. New images demonstrated appropriate alignment of the area of activity with segment 7 and 8 of the liver.

RESULTS:

Knowledge of misregistration artifact on SPECT/CT images helped prevent further radioactive dosing of the patient during Y90 planning procedure. Furthermore, it saved the patient from further contrast and radiation exposure from a repeat angiogram, consistent with the “as low as reasonably achievable” (ALARA) principle.

CONCLUSIONS:

SPECT/CT imaging is prevalent and used frequently in Y90 planning procedures to appropriately map the area of intent for Y90 radioembolization. IR who are familiar with different SPECT artifacts will be able to appropriately make clinical decisions to save patients from inappropriate radiation. The most important artifact that IR should be aware of is misregistration, as it can mimic relevant findings if the provider is not aware of the entity.

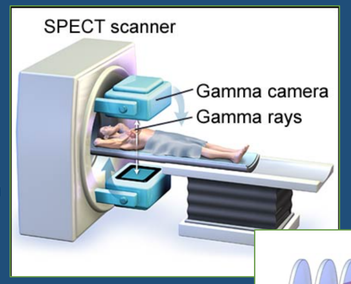

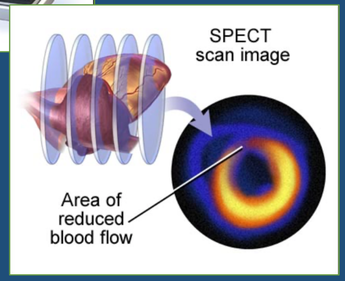

Fig 4. SPECT scanner detects gamma rays from organs and concurrent CT slices are fused to create hybdrid images. [2]

References:
1. Zhang H, Gao S, Chen B and Cheng G: Comparison of the accuracy of 99mTc-3P4-RGD2 SPECT and CT in diagnosing solitary pulmonary nodules. Oncol Lett 12: 2517-2523, 2016
2. Adapted from the Ohio Heart and Vascular Consultants SPECT Scan information page. https://medmovie.com/library_id/3090/topic/cvml_0223i/summary/

PROXIMAL FEMORAL REPLACEMENT VERSUS INTERNAL FIXATION FOR THE TREATMENT OF METASTATIC BONE DISEASE OF THE PROXIMAL FEMUR

B Clayton MD[1], C Gusho BS[1], N Mehta MD[1], W Hmeidan BS[1], M Colman MD[1], S Gitelis MD[1], A Blank, MD, MS[1]

[1]RUSH UNIVERSITY MEDICAL CENTER

Disclosures: Please see AAOS/MSTS list of disclosures.

INTRODUCTION

Proximal femoral metastases are often treated with proximal femoral replacement (PFR) or internal fixation (IF).

Previous studies have demonstrated possible benefits of PFR over IF, though the best method of reconstruction is uncertain.[1-5]

This study compared surgical outcomes of PFR versus IF for treatment of metastatic disease of the proximal femur.

METHODS

Throughout a consecutive 15-year period 126 procedures (IF n=102; PFR n=24) were performed.

Primary Tumor	Frequency	Percent
Breast	34	27.0
Kidney	31	24.6
Lung	19	15.1
Myeloma	12	9.5
Metastatic Sarcoma	9	7.1
Prostate	4	3.2
Lymphoma	2	1.6
Other	15	11.9
Total	**126**	**100.0**

Table 1. Tumor types treated.

	*PFR (n=24)	*IF (n=102)
Femoral head or neck†	7 (29.2%)	15 (14.7%)
Peri/Intertrochanteric†	5 (20.8%)	25 (24.5%)
Subtrochanteric†	7 (29.2%)	15 (14.7%)
Diaphyseal†	4 (16.7%)	40 (39.2%)
Impending Fracture†	10 (41.7%)	75 (73.5%)
Actual Fracture†	14 (58.3%)	26 (25.5%)
No Radiation	10 (41.7%)	18 (17.6%)
Neoadjuvant Radiation	4 (16.7%)	25 (24.5%)
Adjuvant Radiation	9 (37.5%)	45 (44.1%)

Table 11. Lesion characteristics and therapies. *missing data omitted. PFR, proximal femoral replacement. IF, internal fixation. † $p < 0.05$ on Chi Square Test.

RESULTS

- Preoperative risk (ASA score), age, and follow-up were no different ($p>0.05$).
- PFR had higher blood loss and longer operative duration ($p<0.001$).
- Mean PFR survival was 77 months with a 5-year survival probability of 94%.
- Mean IF survival was 90 months with a 5-year survival probability of 59%.

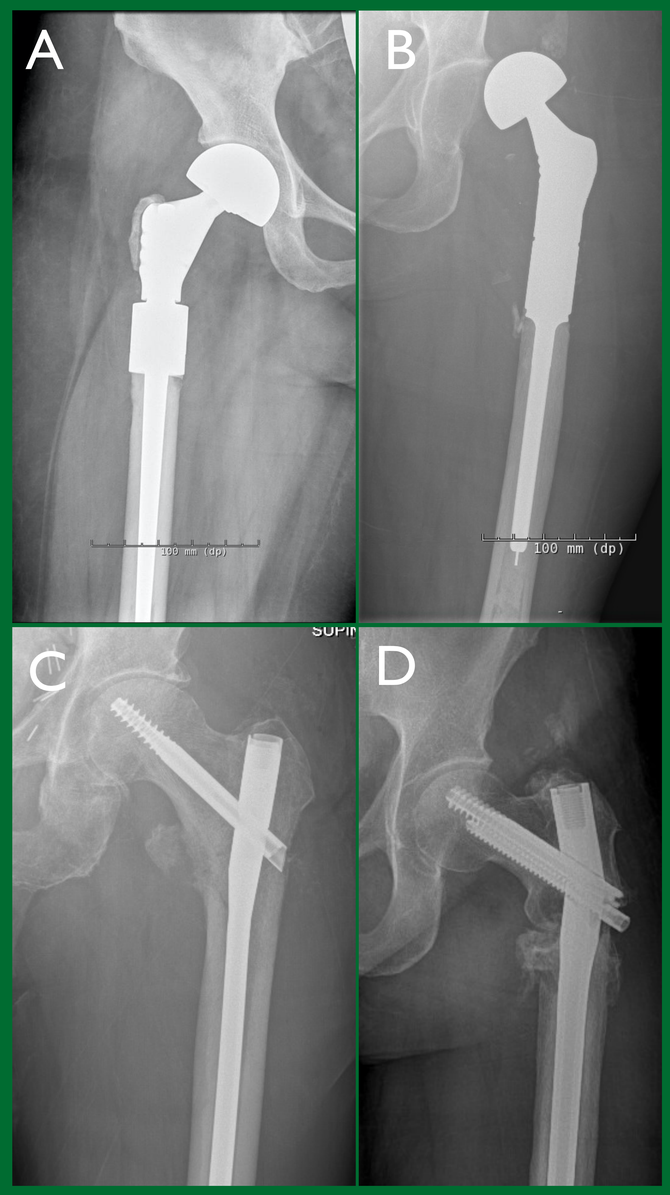

Figure 1. Uncomplicated (A) and dislocated (B) proximal femoral endoprosthetic replacement, as well as an uncomplicated (C) and failed (D) intramedullary femoral nail.

RESULTS (continued)

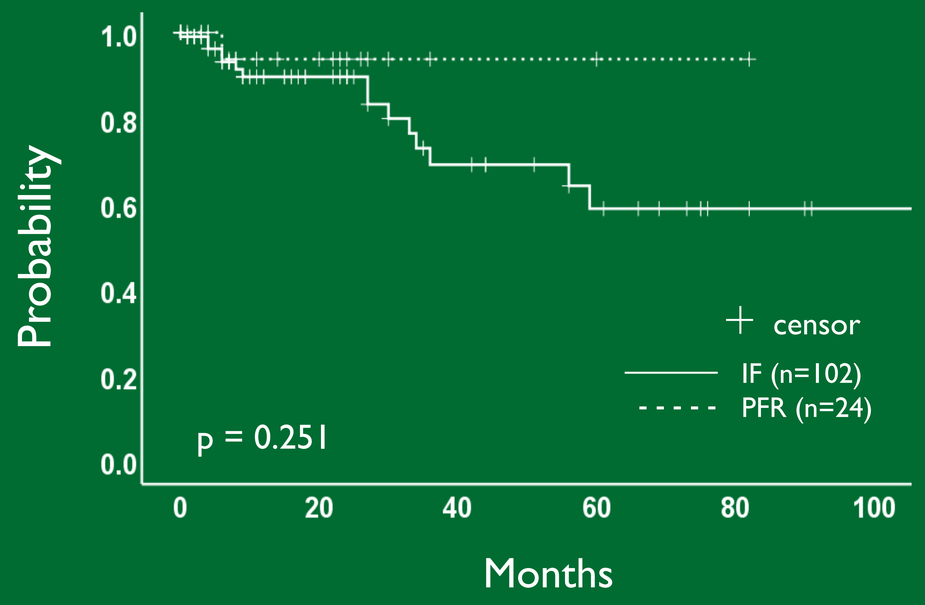

Figure 2. Implant survival. IF, internal fixation. PFR, proximal femoral replacement (n=126).

CONCLUSIONS

Metastases to the proximal femur are a challenging issue, and the advantages of IF or PFR are unclear.

For an age-matched group with similar preoperative risk there is no survival difference between IF and PFR, though PFR require longer operative times and increase blood loss.

REFERENCES

1. Khattak MJ, Ashraf U, Nawaz Z, Noordin S, Umer M. Surgical management of metastatic lesions of proximal femur and the hip. *Annals of medicine and surgery*. 2018;36:90–95.
2. Guzik G. Oncological and functional results after surgical treatment of bone metastases at the proximal femur. *BMC surgery*. 2018;18(1):1–8.
3. Di Martino A, Martinelli N, Loppini M, Piccioli A, Denaro V. Is endoprosthesis safer than internal fixation for metastatic disease of the proximal femur? A systematic review. *Injury*. 2017;48:S48–S54.
4. Tanaka T, Imanishi J, Charoenlap C, Choong PFM. Intramedullary nailing has sufficient durability for metastatic femoral fractures. *World J Surg Oncol*. 2016;14. doi:10.1186/s12957-016-0836-2
5. Harvey N, Ahlmann ER, Allison DC, Wang L, Menendez LR. Endoprostheses Last Longer Than Intramedullary Devices in Proximal Femur Metastases. *Clin Orthop Relat Res*. 2012;470(3):684-691. doi:10.1007/s11999-011-2038-0

Review of Prostate Artery Embolization and Its Emerging Utility in the Management of Prostate Cancer

Goel A, Thibodeau R, Jafroodifar A, Labella D, Jawed M, Tewari SO
Department of Radiology, SUNY Upstate Medical University, Syracuse NY

CIOctober Symposium on Clinical Interventional Oncology 2020 ONLINE

UPSTATE MEDICAL UNIVERSITY

Introduction:

- Patients >40 years of age with BPH who do not respond to medical treatment or cannot undergo surgery should be considered for prostatic artery embolization (PAE). Indications and contraindications for PAE are shown in Table 1.
- Primarily used for benign prostatic hyperplasia with good outcomes on prostatic volume reduction and improvement in IPSS (Figure 2)
- PAE may be used to treat prostatic cancer in patients who are not suitable for surgery and/or radiation therapy
  - Reduction in prostatic volume
  - Reduce/eliminate prostatic bleeding from localized prostate cancer
  - Special consideration for patient

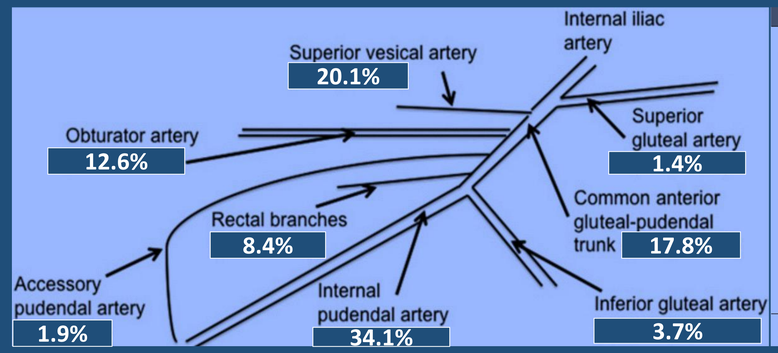

Table 1. PA Origin and Arterial Anastomosis Type

Finding	Incidence
PA origin	214 (100)
Internal pudendal artery	73 (34.1)
Superior vesical artery	43 (20.1)
Anterior common gluteal-pudendal trunk	38 (17.8)
Obturator artery	27 (12.6)
Prostatorectal trunk	18 (8.4)
Inferior gluteal artery	8 (3.7)
Accessory pudendal artery	4 (1.9)
Superior gluteal artery	3 (1.4)
Type of anastomosis	
Internal pudendal arteries	42 (43.3)
Contralateral PAs	17 (17.6)
Ipsilateral PAs	13 (13.4)
Rectal arteries	14 (14.4)
Vesical arteries	11 (11.3)
Lateral accessory pudendal arteries	30 (20)

PA = prostatic artery.
Values in parentheses are percentages.

Figure 1: Prostatic Origin and Arterial Anastomosis[5]

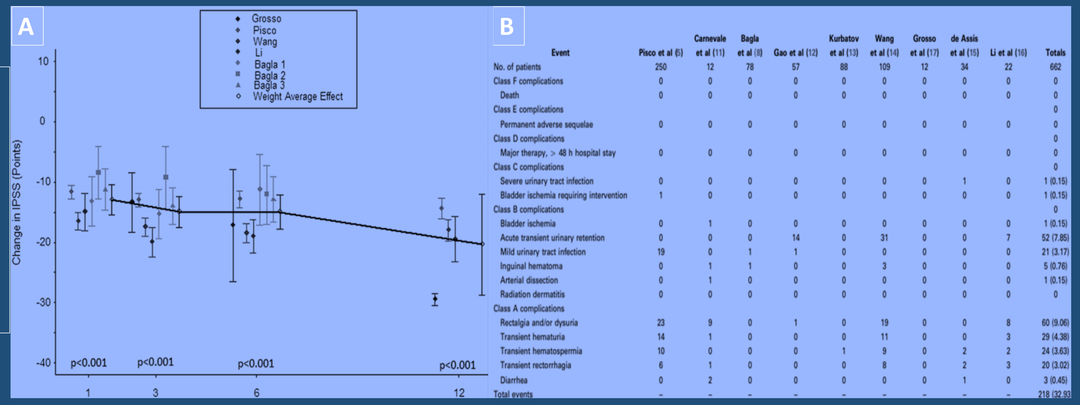

B

Event	Pisco et al (6)	Carnevale et al (11)	Bagla et al (8)	Gao et al (12)	Kurbatov et al (13)	Wang et al (14)	Grosso et al (17)	de Assis et al (15)	Li et al (16)	Totals
No. of patients	250	12	78	57	88	109	12	34	22	662
Class F complications	0	0	0	0	0	0	0	0	0	0
Death	0	0	0	0	0	0	0	0	0	0
Class E complications										0
Permanent adverse sequelae	0	0	0	0	0	0	0	0	0	0
Class D complications										0
Major therapy, > 48 h hospital stay	0	0	0	0	0	0	0	0	0	0
Class C complications										0
Severe urinary tract infection	0	0	0	0	0	0	0	1	0	1 (0.15)
Bladder ischemia requiring intervention	1	0	0	0	0	0	0	0	0	1 (0.15)
Class B complications										0
Bladder ischemia	0	1	0	0	0	0	0	0	0	1 (0.15)
Acute transient urinary retention	0	0	0	14	0	31	0	0	7	52 (7.85)
Mild urinary tract infection	19	0	1	1	0	0	0	0	0	21 (3.17)
Inguinal hematoma	0	1	1	0	0	3	0	0	0	5 (0.76)
Arterial dissection	0	1	0	0	0	0	0	0	0	1 (0.15)
Radiation dermatitis	0	0	0	0	0	0	0	0	0	0
Class A complications										
Rectalgia and/or dysuria	23	9	0	1	0	19	0	0	8	60 (9.06)
Transient hematuria	14	1	0	0	0	11	0	0	3	29 (4.38)
Transient hematospermia	10	0	0	0	1	9	0	2	2	24 (3.63)
Transient rectorrhagia	6	1	0	0	0	8	0	2	3	20 (3.02)
Diarrhea	0	2	0	0	0	0	0	1	0	3 (0.45)
Total events	–	–	–	–	–	–	–	–	–	218 (32.93)

Figure 2: Meta-Analysis of Improvements of I-PSS (A)[6] and Table of Adverse Events (B)[6]

Table 1: Indications, Contraindications, Work Up

Work up	HPI (prostate symptoms, sexual health, current prostate meds), I-PSS, UA, PSA, PVR, DRE, uroflowmetry, imaging (TRUS, MRI, or CTA)
Candidacy	I-PSS ≥13, failed medical therapy for at ≥3 months, uroflow <10 mL/sec, PVR >100 mL, prostate size >50 g. median lobe <3 cm
Contraindications	Active UTI or prostatitis, prostate or bladder cancer, chronic renal failure, bladder dysfunction, bladder stones, excessive vessel tortuosity or severe atherosclerosis, I-PSS ≤12, high PVR, asymptomatic patient, prostate <50g, medial lobe >3 cm

UA = urinalysis, PSA = prostate specific antigen, PVR = post void residual, DRE = digital rectal exam, TRUS = transrectal ultrasound, MRI = magnetic resonance imaging, CTA = computed tomography angiography

Table 2: Anatomical Variations of the Prostate Artery[4]

Classification	Incidence of Variant	Description
Type I	28.7%	IVA originates from anterior division of IIA with a common trunk with SVA
Type II	14.7%	IVA originates from anterior division of IIA and inferior to SVA
Type III	18.9%	IVA originates from obturator artery
Type IV	31.1%	IVA originates from IPA
Type V	5.6%	Less common origins

IVA = inferior vesical artery, SVA = superior vesical artery, IIA = internal iliac artery

Pre-, Peri-, and Post-procedural Care

- *Pre-procedure*: two Dulcolax for two nights prior to procedure to prevent constipation, insert Foley catheter
- *Periprocedure*: one-time dose of intravenous ciprofloxacin/levofloxacin, nitroglycerin immediately after catheterization of prostatic artery and before injecting embolic, conscious sedation (versed and fentanyl), and anticoagulation (intravenous heparin)
- *Post-procedure*
  - Remove foley
  - Medications: ibuprofen 800mg TID x 7 days, ciprofloxacin 500mg BID x 7 days, Pyridium 100-200mg TID, Vesicare 5mg daily, Dulcolax 20mg OD
  - Intravenous fluids, restrict physicial activity x 2-3 days, and follow-up (4-6 weeks s/p PAE)

Technique

1) Radial access with tumescent anesthesia (100mcg nitroglycerine, 9mL 1% lidocaine)
   - Recommend anti-spasmodic radial cocktail (e.g. 200mcg nitroglycerine, 2000 IU heparin, 2.5mg verapamil)
2) Hypogastric angiogram: identify prostatic artery and origin,
3) Catheterization of prostatic artery: materials include ≤2.4F shapable tip wire 0.014 inch
4) Selective injection of prostatic artery
5) Cone beam protocols
6) Embolization of prostatic artery: slow injection, identify potential non-targets, and embolize with coils if necessary
7) Hemostasis

Figure 3: International Prostate Symptom Score (I-PSS)[7]

In the past month	Not at all	Less than 1 in 5 times	Less than half the time	About half the time	More than half the time	Almost always	Patient Score
Incomplete Emptying	0	1	2	3	4	5	
Frequency	0	1	2	3	4	5	
Intermittency	0	1	2	3	4	5	
Urgency	0	1	2	3	4	5	
Weak Stream	0	1	2	3	4	5	
Straining	0	1	2	3	4	5	
Nocturia	None	1 Time	2 Times	3 Times	4 Times	5 Times	
Total I-PSS Score							
Scoring	*1-7: Mild*		*8-19: Moderate*			*20-35: Severe*	

References
1) McWilliams JP, Kuo MD, Rose SC, et al. Society of Interventional Radiology Position Statement: Prostate Artery Embolization for Treatment of Benign Disease of the Prostate. J Vasc Interv Radiol 2014; 25:1349-1351.
2) Gao YA, Huang Y, Zhang R,et al. Benign prostatic hyperplasia: prostatic arterial embolization versus transurethral resection of the prostate—a prospective, randomized, and controlled clinical trial. Radiology 2014; 270:920–928.
3) S. Golzarian J, Antunes AA, Bilhim T, et al. Prostatic artery embolization to treat lower urinary tract symptoms related to benign prostatic hyperplasia and bleeding in patients with prostate cancer: proceedings from a multidisciplinary research consensus panel. J Vasc Interv Radiol 2014; 25:665–674.
4) Carnevale FC, Soares GR, de Asses AM, et al. Anatomical Variants in PRostate Artery Embolization: A Pictorial Essay. Cardiovasc Intervent Radiol 2017 Sep;40(9):1321-1337.
5) Bilhim T, Pisco JM, Rio Tinto H, et al. Prostatic arterial supply: anatomic and imaging findings relevant for selective arterial embolization. *J Vasc Interv Radiol*. 2012;23(11):1403-1415. doi:10.1016/j.jvir.2012.07.028
6) Uflacker A, Haskal ZJ, Bilhim T, Patrie J, Huber T, Pisco JM. Meta-Analysis of Prostatic Artery Embolization for Benign Prostatic Hyperplasia. *J Vasc Interv Radiol*. 2016;27(11):1686-1697.e8. doi:10.1016/j.jvir.2016.08.004
7) Barry MJ, Fowler FJ Jr, O'Leary MP, Bruskewitz RC, Holtgrewe HL, Mebust WK, Cockett AT. The American Urological Association symptom index for benign prostatic hyperplasia. The Measurement Committee of the American Urological Association. J Urol. 1992; 148(5):1549-57; discussion 1564.

Splenic Artery Embolization in the Setting of Splenic Malignancies: What Do I Need to Know?

Goel A, Jafroodifar A, Siddique Z, Thibodeau R, Pinter D
Department of Radiology, SUNY Upstate Medical University, Syracuse NY

INDICATIONS

Splenic arterial embolization (SAE) is a procedure that has classically been used in the setting of stable post-traumatic splenic laceration hemorrhage. However, given the rise of more advanced techniques in arterial intervention, the procedure has emerged as a valuable tool in many other disease etiologies., including in the treatment of splenic neoplasia The overall indications for SAE can be divided into two overarching categories: traumatic and nontraumatic [1,3]. Table 1 summarizes the further breakdown of these categories (it should be noted this list is not exhaustive but covers the most common indications).

TECHNIQUE

All technique begins with ultrasound-guided access to the femoral artery, and selection of the celiac trunk with a curved catheter (4-5 French) [1] – such as Cobra C2 or RC2 (Cook Medical). Alternatively, a reversed-curve catheter may also be used – such as Simmons 1 or VS1 (Cook Medical) [1]. Angiogram of the celiac trunk helps determine the origin of the splenic artery and demonstrates the surrounding collateral vasculature. These collaterals include the left gastric artery, gastroepiploic arteries, and pancreatic artery branches [1-5].

Splenic Neoplasms

- The concept of splenic irradiation can be used in a variety of pathologies
- Transarterial transplenic irradiation considered in the setting of inoperable transplenic neoplasms
- Additional conjunctive therapy can also be considered via radiofrequency ablation

Other instances of splenic embolization use:

Hypersplenism (and other similar pathologies related to increased destruction of red blood cells)

- Partial embolization is preferred in order to preserve the spleens normal function, typically 60-70% of total visceral mass [1]
  - Selective vs nonselective method
    - Selective method requires more distal branch catheterization with embolization performed, using 300-500 µm or 500-700 µm particles [3], until the desired splenic volume persists on parenchymal angiogram
    - Nonselective method uses a more proximal method with random injection of embolic particles (polyvinyl alcohol particles [1]) until the desired splenic volume persists on parenchyma angiogram
- Typically proximal embolization will not be successful due to the collateral vessels that will remain intact
- Used more commonly in patients preparing for surgical splenectomy

Portal hypertension

- Reduction of spleen volume results in less venous drainage into the portal vein, leading to decreased portal pressures, and theoretically alleviating symptoms
- Classically treated with partial embolization, although data is limited

Blunt splenic trauma

- Microcoils [1], gelatin, or particles (300-500 µm) [3] placed as distally as possible in the region of active vascular damage using a micro-selective catheter
- Try to spare as much of the normal spleen as possible
- in case of re-rupture, place more proximally – just distal to the pancreatic branches [1] – to decrease overall pressure in splenic vasculature

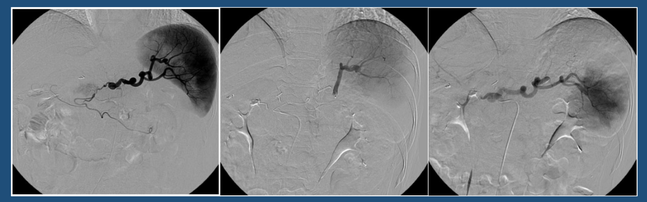

Fig 5 Splenic arteriogram demonstrating normal parenchymal blush, followed by upper pole embolization, followed by normal lower pole blush in the absence of upper pole flow. Originally by Ahuja et al. [3]

Origin	Course	Terminus	
Celiac axis (90.6%)	Suprapancreatic (74.1%)	Divided prior to hilum (97%)	Two (63.1%)
Aorta (8.1%)	Enteropancreatic (18.5%)		Four (18.8%)
Other (1.3%)	Intrapancreatic (4.6%)		Six (9.7%)
	Retropancreatic (2.8%)		Greater than six (5.6%)
		Passed through hilum without division (3%)	

Table 3 Origin, course, and terminus of the splenic artery variants and their incidences examined from cadavers. Adapted from Pandey et al. [2]

Fig 1. Axial CT images demonstrating A) Hemangioma. B) B-cell lymphoma of the spleen. C) Mantle cell lymphoma. [1]

Materials Used
Yttrium-90
Radiofrequency Ablation
Gelatin sponge pledgets (for embolization)
Polyvinyl alcohol particles (PVA) (for embolization)
Coils (for embolization)

Table 2 Most commonly used treatment materials.

COMPLICATIONS

- Persistent hemorrhage
- Infarction
- Splenic abscess
- Splenic rupture
- Sepsis
- Splenic vein thrombosis
- Unremitting bronchopneumonia [1,3]

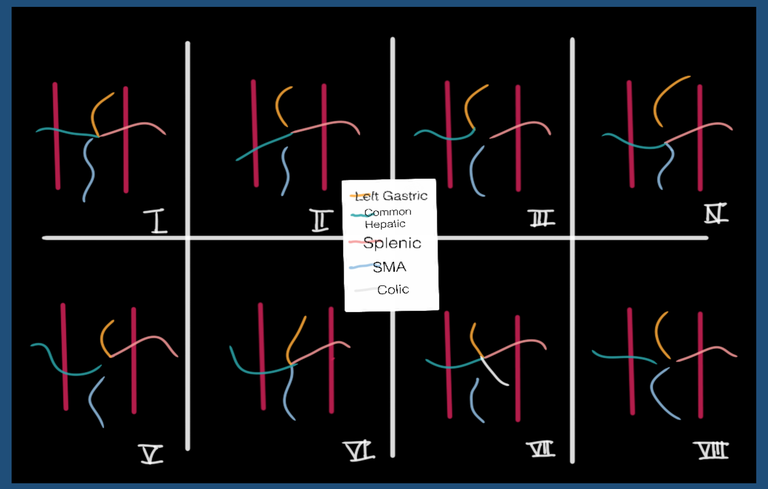

Fig 4 Variation of celiac trunk and origin of the splenic artery according to the Uflacker's classification. Adapted from Yash et al. [7]. Original drawing.

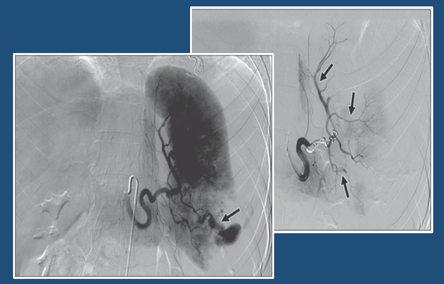

Fig 6 Splenic arteriogram demonstrating active hemorrhage in the lower pole of the spleen. After coiling of the splenic artery, distal to the pancreatic branches, there is decreased flow into the spleen with no active extravasation present. Originally by Madoff et al. [1]

REFERENCES

1. Case contributed by Dr Schubert to Radiopaedia. URL: https://radiopaedia.org/cases/b-cell-lymphoma-involving-the-spleen
2. Pandey SK, Bhattacharya S, Mishra RN, Shukla VK. Anatomical variations of the splenic artery and its clinical implications. Clin Anat. 2004;17(6):497-502. doi:10.1002/ca.10220
3. Ahuja C, Farsad K, Chadha M. An Overview of Splenic Embolization. AJR Am J Roentgenol. 2015;205(4):720-725. doi:10.2214/AJR.15.14637
4. Prasanna LC, Alva R, Sneha GK, Bhat KM. Rare variations in the Origin, Branching Pattern and Course of the Celiac Trunk: Report of Two Cases. Malays J Med Sci. 2016;23(1):77-81.
5. Moore EE, Cogbill TH, Jurkovich GJ, Shackford SR, Malangoni MA, Champion HR. Organ injury scaling: spleen and liver (1994 revision). J Trauma 1995;38:323–324.
6. Demetriades D. (2012) Spleen Injury Grading. In: Vincent JL., Hall J.B. (eds) Encyclopedia of Intensive Care Medicine. Springer, Berlin, Heidelberg. https://doi.org/10.1007/978-3-642-00418-6_517
7. Yash KA, Purushothama RN, Ramesh KR. Variants of Coeliac Trunk, Hepatic Artery and Renal Arteries in Puducherry Population. International Journal of Anatomy, Radiology and Surgery. 2018 Jan, Vol-7(1): RO38-RO43
8. Case contributed by Dr Al-Deeb to Radiopaedia. URL: https://radiopaedia.org/cases/splenic-injury-aast-grade-iii-2?lang=us

Technical Considerations of Adrenal Ablation

Barbara Manchec[1], M.D., Yilun Koethe[2], M.D., Constantino Pena[2,3], M.D., Brian Schiro[2,3], M.D., Ripal Gandhi[2,3], M.D.

[1] Advent Health
[2] Miami Cardiac and Vascular Institute
[3] Miami Cancer Institute

Miami Cancer Institute
BAPTIST HEALTH SOUTH FLORIDA

Miami Cardiac & Vascular Institute
BAPTIST HEALTH SOUTH FLORIDA

AdventHealth

Learning Objectives

Review indications and contraindications for percutaneous adrenal ablation, procedural planning, technical considerations, post-procedural care, and expected outcomes.

Background

Most adrenal lesions can be diagnosed with clinical history, biochemical evaluation, and diagnostic imaging. Current guidelines recommend surgical removal of several adrenal lesions, including pheochromocytomas, adrenocortical carcinomas (ACC), unilateral functional adenomas, and nonfunctional adenomas ≥ 4 cm [1, 2]. As more studies are published on adrenal ablations, procedural details have been refined.

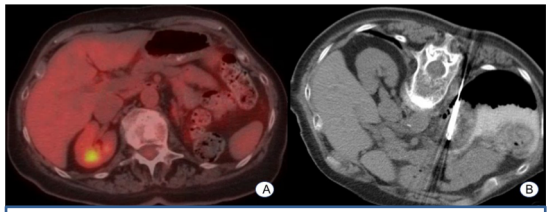

Figure 1. 81-year-old female with 1.8 cm biopsy-proven left adrenal metastasis (squamous cell carcinoma) demonstrating mild hypermetabolism on PET/CT (A). Patient underwent CT-guided cryoablation (Galil IceRod) which required preablation hydropneumodissection (2% contrast:saline solution) to displaced the diaphragm and lung (B).

Periprocedural and Procedural Details

Optimal candidates for image-guided adrenal ablation will have lesions < 4 cm. Absolute contraindications include inability to safely access the target despite protective maneuvers (Figure 1), uncorrectable coagulopathy (INR >1.5, platelet <50K/uL), and inability to tolerate sedation.

The risk of hypertensive crisis during adrenal ablation is not limited to pheochromocytoma, therefore premedication with an α-adrenergic inhibitor is recommended (Table 1). β-blocker can subsequently be added if the patient has persistent tachycardia. Additional procedural considerations include having an anesthesiologist with experience in managing catecholamine-induced complications, establishing an arterial line, and alerting the anesthesiologist prior to manipulation of the probe or applying thermal energy. Hemodynamic changes typically occur during ablation for RFA/MWA or thawing for cryoablation.

Most adrenal ablations are performed with the patient in prone or ipsilateral decubitus position (Figure 2). Transhepatic approach can be performed if necessary.

Post-procedural management of medications can be complex, requires multidisciplinary cooperation, and varies by the type of adrenal mass being ablated. For example, stress dose glucocorticoids should be initiated on post-ablation day 1 after ablation of a cortisol-secreting adenoma due to persistent suppression of the HPA axis.

Outcomes

The outcomes for ablation of functional adenomas have yielded promising results (Table 2). Adrenal ablation has been shown to be non-inferior to laparoscopic adrenalectomy for aldosteronomas [3, 4]. Furthermore, the ablation groups had shorter operations, less blood loss, less post-procedural pain, and shorter hospital stays [3, 4]. The outcomes for pheochromocytoma and ACC are limited, thus adrenal ablation should be limited to patients who are not surgical candidates or refuse surgery.

Teaching Points

Management of adrenal lesions with percutaneous ablation requires multidisciplinary collaboration. Procedural preparation to avoid complication from hypertensive crisis should include: 1. premedication regimen, 2. anesthesiologist experienced in managing catecholamine-induced complications, 3. establishing an arterial line, and 4. alerting the anesthesiologist prior to manipulation of the probe or applying thermal energy. Additionally, adrenal ablation is comparable or better than surgery in select patients.

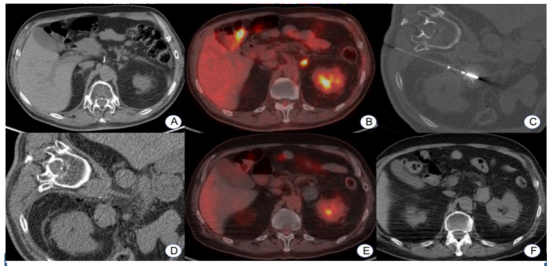

Figure 2. 67-year-old male with esophageal adenocarcinoma status post esophagectomy and gastric pull-through surgery found to have a new 1 cm left adrenal lesion on CT scan (A). Hypermetabolism on PET/CT (B) and an adrenal biopsy (not shown) confirmed metastasis. The patient underwent CT-guided RFA (Angiodynamics) 2 months later (C) when the lesion measured 4 cm. Immediate post-ablation CT (D) is without acute complication. Four months after ablation, the PET/CT (E and F) demonstrates no significant FDG uptake or enlargement.

Table 1. Common Preprocedural Medications

Class	Initiation	Treatment Target	Medication	Starting Dose	Titration
α-adrenergic inhibitor	1-3 weeks before ablation	Until BP 130/85 mm Hg or patient develops orthostatic hypotension	Phenoxy-benzamine	10 mg BID	May increase by 10 mg/day every other day, maximum dose 300-400 mg daily
			doxazosin	1 mg QD	May double dose every week, maximum dose 16 mg/day
Nonselective β-adrenergic inhibitor	After adequate α blockade	Resolution of tachycardia	propranolol	10-40 mg TID	May increase every 3-7 days
			atenolol	12.5 mg QD or BID	May increase dose every 7 days, maximum dose 200 mg/day

Table 2. Aldosterone-Secreting Adenomas

Study	Ablation Modality	Patient Number	Mean Tumor Size (cm)	Mean Follow-up (months)	Technical Success (%) (single/second session)	Biochemical Markers (% normalization, SS improvement)	Mean Blood Pressure (mm Hg) (before, after, SS improvement)	Mean Number of Antihypertensives (before/after, SS improvement)	Potassium (% normokalemia, SS improvement)
Liu et al.	RFA	36	1.6	74.4	92%/100%	92%, SS	158/94, 128/76, SS	1.8/1.2, NA	100%[±], SS
Yang et al.	RFA	7	1.8	6	100%	100%, SS	153/92, 122/72, SS	3.4/1.4, SS	NA, SS
Szejnfeld et al.	RFA	9	1.8	3	100%	89%[‡], SS	166/105, 133/92, SS	3.2/1.3, SS	NA, NA
Ren et al.	MWA	3	NA	NA	100%	100%, NA	NA, NA, NA	NA, NA	100%, NA
Sarwar et al.	RFA	12	1.6	15.2	NA	NA, NA	145/94, 129/81, SS	3.0/1.8, SS	100%, SS
Mendiratta-Lala et al.	RFA	10	NA[ω]	21.2 (biochemical) & 41.4 (clinical)[Φ]	100%	100%[℄], NA	149/90, 124/76, SS	3.1/1.3, SS	100%[α], NA
Abbas et al.	Cryoablation (4) & RFA (1)	5	1.8	12	100%	60%, NA	164/95, 131/73, NA	3.4/1.6, NA	80%, NA
Xiao et al.	Chemical ablation	7 (9 adenomas)	2.8	24	2-5 treatments	100%	155/107, 135/88	NA	100%

SS – Statistically significant
[±] 2 patients remained on spironolactone
[‡] One patient without normalization of biochemical markers had an adrenal nodule in close proximity to IVC and was incompletely treated
[ω] All adenomas were < 3.2 cm.
[Φ] Follow-up means include 3 patients with other functional adrenal masses.
[℄] Post-ablation aldosterone available for 9 (out of 10) patients.
[α] Post-ablation potassium available for 7 (out of 10) patients.

Contact Information

Barbara Manchec
Barbara.Manchec.MD@adventhealth.com
Twitter: @Manchec_MD
Phone: 954-851-2543

References

1. Fassnacht, M., et al., *Management of adrenal incidentalomas: European Society of Endocrinology Clinical Practice Guideline in collaboration with the European Network for the Study of Adrenal Tumors.* Eur J Endocrinol, 2016. **175**(2): p. G1-G34.
2. Zeiger, M.A., et al., *American Association of Clinical Endocrinologists and American Association of Endocrine Surgeons Medical Guidelines for the Management of Adrenal Incidentalomas: executive summary of recommendations.* Endocr Pract, 2009. **15**(5): p. 450-3.
3. Yang, M.H., et al., *Comparison of radiofrequency ablation versus laparoscopic adrenalectomy for benign aldosterone-producing adenoma.* Radiol Med, 2016. **121**(10): p. 811-9.
4. Sarwar, A., et al., *Clinical Outcomes following Percutaneous Radiofrequency Ablation of Unilateral Aldosterone-Producing Adenoma: Comparison with Adrenalectomy.* J Vasc Interv Radiol, 2016. **27**(7): p. 961-7.

Transarterial Chemoembolization and Adjuvant Stereotactic Radiotherapy in patients with Non-resectable Hepatocellular Carcinoma

Abhijit L. Salaskar, MD, MPH ; Philip Blumenfeld, MD; Michael H. Hamblin, MD [1]

Amita Saint Francis Hospital, Evanston, IL

PURPOSE

To report outcomes of transarterial chemoembolization (TACE) and adjuvant stereotactic body radiotherapy (SBRT) for the treatment of nonresectable hepatocellular carcinoma (HCC).

CASE PRESENTATION

Case 1: 72 year old female with past medical history of diabetes, idiopathic thrombocytopenic purpura (ITP) and cirrhosis (Child Pugh Score of 6 = Class A) underwent MR abdomen which revealed a 3.3 x 3.6 cm mass within segment 6 of liver. The mass demonstrated arterial phase enhancement and washout **(Fig 1 A & B)**. In the setting of cirrhosis, mass was consistent with HCC. Presence of ITP precluded biopsy of this mass.

Case 2: 88 year old male with past medical history of ESRD on hemodialysis, atrial fibrillation, thrombocytopenia and cirrhosis (Child Pughs Score of 7 = Class B) was admitted to our institution with fever and altered mental status. CT revealed a 3.8 cm hypodense mass in the lateral aspect of segment 7 of the liver. The mass demonstrated relative washout on the venous phase **(Fig 2 A & B)**. CT guided core biopsy of the mass reveled moderately differentiated HCC.

TREATMENT

As per BCLC staging system, TACE of the right hepatic mass (BCLC intermediate stage B) was planned in both cases. The afferent third order branch of right hepatic artery was selected with 2.8 Fr Maestro microcatheter and 0.016 Headliner microwire. The TACE was achieved by initially administering a mixture of 75 mg of Doxorubicin, 10 ml of lipiodol and 10 ml of 61% isovue-300 followed by administration of a vial of Embosphere 500-700 µm microspheres mixed with 10 ml of 61% isovue-300. The subsequent DSA demonstrated decreased tumor blush and stasis of contrast within the mass (Fig 1C, 1D, 2C). Three to four months later, each of these patients underwent SBRT (5000 cGy in 5 fractions) to liver segment 7 for local control.

CASE 1

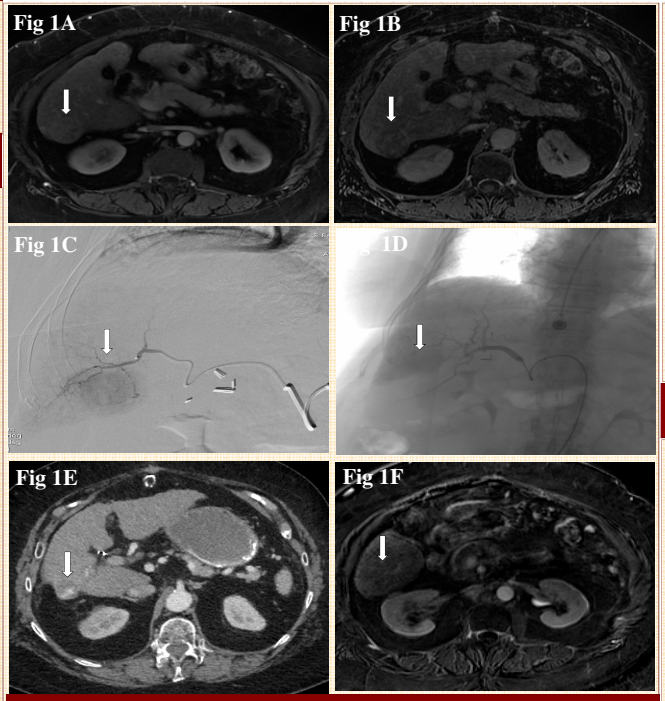

CASE 2

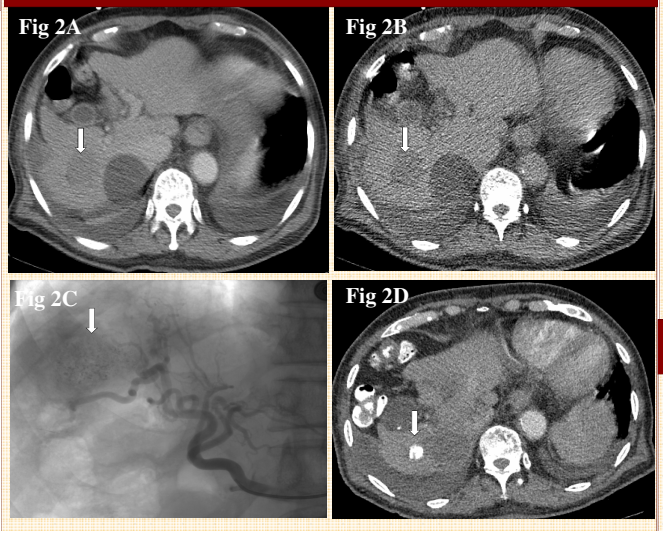

OUTCOME

Case 1: CT scan obtained 27 months (Fig 1 E) after TACE and SBRT showed reduction in the size of the hepatic mass (2.4 x 2.2 cm) and Dynamic contrast MR demonstrated absence of enhancement on subtraction sequence (Fig 1F). The AFP levels were within normal limits. No other evidence of recurrence or metastatic disease was identified.

Case 2: CT scan obtained 18 months after TACE and SBRT demonstrated a 1.5 cm hyperdensity at the site of prior mass (Fig 2D) and AFP levels were within normal limits. No other evidence of recurrence or metastatic disease was identified.

DISCUSSION

The optimal treatment for HCC of size ≥ 3 cm is less clear. According to BCLC treatment algorithm, AASLD & NCCN guidelines, TACE is a recommended treatment for intermediate stage HCC in patients who are not candidates for surgical resection or tumor ablation. However TACE alone rarely achieves complete control of HCC tumor and it has been considered a palliative treatment. SBRT is another effective therapeutic option for inoperable HCC. SBRT allows focused dose of radiation to the tumor using less number of fractions. NCCN has recommended SBRT as a possible alternative to TACE for unresectable tumors. A prior retrospective study has suggested improved outcomes of combined treatment with TACE + SBRT versus TACE alone in patients with HCC tumors ≥ 3 cm. These results are being evaluated in a prospective clinical trial. Recently published pilot trial found that single-dose SBRT followed by TACE within 24 hours is tolerable and MRI revealed favourable acute changes in tumor permeability/perfusion after SBRT. As per our limited experience, combined treatment with TACE+ SBRT has shown improved tumor response.

REFERENCES

1. Mu Jacob R, Turley F, Redden DT, Saddekni S, Aal AK, Keene K, Yang E, Zarzour J, Bolus D, Smith JK, Gray S, White J, Eckhoff DE, DuBay DA. Adjuvant stereotactic body radiotherapy following transarterial chemoembolization in patients with non-resectable hepatocellular carcinoma tumours of ≥ 3 cm. HPB (Oxford). 2015 Feb;17(2):140-9. doi: 10.1111/hpb.12331. Epub 2014 Sep 4. PMID: 25186290

2. Tse RV, Hawkins M, Lockwood G, Kim JJ, Cummings B, Knox J, Sherman M, Dawson LA. Phase I study of individualized stereotactic body radiotherapy for hepatocellular carcinoma and intrahepatic cholangiocarcinoma. J Clin Oncol. 2008 Feb 1;26(4):657-64. doi: 10.1200/JCO.2007.14.3529. Epub 2008 Jan 2. Erratum in: J Clin Oncol. 2008 Aug 10;26(23):3911-2. PMID: 18172187.

3. Clinical trial: https://clinicaltrials.gov/ct2/show/NCT01247298

4. Sebastian NT, Miller ED, Yang X, Diaz DA, Tan Y, Dowell J, Spain J, Rikabi A, Elliott E, Knopp M, Williams TM. A Pilot Trial Evaluating Stereotactic Body Radiation Therapy to Induce Hyperemia in Combination With Transarterial Chemoembolization for Hepatocellular Carcinoma. Int J Radiat Oncol Biol Phys. 2020 Jul 23:S0360-3016(20)31452-8. doi: 10.1016/j.ijrobp.2020.07.033. Epub ahead of print. PMID: 32712254.

Disclosure : No financial support or assistance